THE ROLE OF P130CAS SIGNALING DOMAINS IN CELL MIGRATION

By

Leslie M. Meenderink

Dissertation

Submitted to the Faculty of the

Graduate School of Vanderbilt University

in partial fulfillment of the requirements

for the degree of

DOCTOR OF PHILOSOPHY

in

Cell and Developmental Biology

December, 2010

Nashville, Tennessee

Approved:

Kathleen L. Gould, Ph.D.

Steven K. Hanks, Ph.D.

Irina Kaverina, Ph.D.

Ethan Lee, Ph.D.

Donna J. Webb, Ph.D.

DEDICATION

This dissertation is dedicated to my husband Daniel Gochberg and my family who have always encouraged me in the pursuit of my education.

ACKNOWLEDGMENTS

This work would not have been possible without the financial support of the National Institutes of Health (RO1 GM049882), the Vanderbilt MSTP (training grant T32-GM07347), the American Heart Association (Predoctoral Fellowship 0815136E), and Vanderbilt University (Dissertation Enhancement Grant).

First, I want to thank my mentor Steve Hanks who welcomed me into his lab and has taught me so much in my time here. I want to thank him for his patience, his help, and his friendship. I am grateful to those with whom I have worked especially the current and former members of the Hanks Lab: Larisa Ryzhova, Dominique Donato, Weifeng Luo, Jan Brabek, Anna Edmondson, Huiling Liu, Sabata Lund, Nah-Young Shin, and Priscila Siesser. In particular I want to thank Larisa who has been a constant help in the lab both for her skills and knowledge as well as her daily encouragement and warm smile. I also want to thank Dominique and Sabata, my fellow Hanks Lab graduate students who have been great friends and colleagues. I also want to thank all my fellow MSTP students who have welcomed me into their class and have become great friends.

I want to thank the members of my committee Kathy Gould, Irina Kaverina, Donna Webb, and Ethan Lee for all their help and encouragement. Kathy has always found the right words to encourage me when I needed. Irina has been a second mentor to me in my Ph.D. studies and a good friend. I also want to thank my MSTP advisors Jim Goldenring and Maureen Gannon and the numerous Vanderbilt faculty and students who have made Vanderbilt such a great working and learning environment including: the

Microtubules and Motors group, the laboratories of both Ethan and Laurie Lee, the Kaverina lab, the Tyska lab, and Alyssa Weaver.

I would like to thank additional collaborators. Within the lab, Larisa Ryzhova helped with numerous biochemical assays and IP experiments, Dominique Donato generated the mCherry-actin and mCherry-paxillin constructs that were essential to my studies, and Sabata Lund assisted with sequencing. Daniel Gochberg assisted with modeling adhesion rate calculations. Irina Kaverina leant her insights and microscopes to my studies. Ethan Lee and his student Chris Cseleyni helped me make *Xenopus* egg extracts for *in vitro* actin experiments. Yuli Wang and his student Andy Rape hosted me at Carnegie Mellon University to evaluate cellular traction forces. I want to thank Catherine Alford in the core for cell sorting. I would like to thank the following people for key reagents: Hisamaru Hirai provided Cas -/- MEFs, Gary Nolan for Phoenix E cells, Maria Nemethova for the mCherry-C1 vector, and Al Reynolds for the LZRS-MS-IRES-GFP vector.

I want to thank Paul Forscher who was my first mentor and introduced me to scientific research, microscopy, and the cytoskeleton. Paul always reminded me that science is fun as well as hard work. I also must thank Daniel Suter from the Forscher lab, who first had the patience to teach me how to do things in a lab.

I thank my parents and family for their support and encourage throughout my educational exploits. Finally, I thank my husband Daniel and daughter Madeline Rose for making me smile every day.

TABLE OF CONTENTS

Page

LIST OF TABLES

LIST OF FIGURES

LIST OF ABBREVIATIONS

15F p130Cas signaling variant with all 15 YxxP tyrosines changed to phenylalanine

15F/mPR p130Cas signaling variant with the SD tyrosines changed to phenylalanine and the SBD proline motif changed to alanines

aa amino acid

Abl v-abl Abelson murine leukemia viral oncogene homolog

Akt serine/threonine kinase named for its discovering in mice developing spontaneous thymic lymphomas; **Ak**, mouse strain classification and **t**, transforming

ANOVA analysis of variance

Arg abl-related gene

Arp actin-related protein

BCAR1 breast cancer anti-estrogen 1 gene, a.k.a. p130Cas

BCAR3 breast cancer anti-estrogen 2 gene, a.k.a. AND-34

C3G a Ras-family guanine nucleotide exchange factor

Cas Crk-asociated substrate

Cas-L lymphocyte type Cas, a.k.a. HEF-1

CCH Cas-family C-terminal homology

Cdc42 cell division control protein 42 homolog

CMS Cas ligand with multiple SH3 domains

Csk c-src tyrosine kinase

DCas *Drosophila melanogaster* p130Cas, a.k.a. *DmCas*

DIC differential interference contrast

DmCas *Drosophila melanogaster* p130Cas

DNS did not spread

DPSS diode-pumped solid-state (laser)

ECM extracellular matrix

EDTA ethylene diamine tetraacetic acid, chelating agent

Efs embryonic Fyn substrate, a.k.a. Efs/Sin

EGFR epidermal growth factor receptor

EGTA ethylene glycol tetraacetic acid, chelating agent

EM-CCD electron multiplying charge coupled device

ER estrogen receptor

ER+ estrogen receptor positive

ER- estrogen receptor negative

ERK extracellular-signal-regulated kinase

FA focal adhesion

FACS fluorescence-activated cell sorting

FAK focal adhesion kinase

FAK56D *Drosophila melanogaster* FAK

FAT focal adhesion targeting

FBA fibrillar adhesion

FRAP fluorescence recovery after photobleaching

FRET fluorescence resonance energy transfer

FRNK FAK-related non-kinase

GEF guanine nucleotide exchange factor

GFP green fluorescent protein

Grb2 growth factor receptor bound protein 2

HEF-1 human enhancer of filamentation 1, a.k.a. Cas-L

HEPES 4-(2-hydroxyethyl)-1-piperazineethanesulfonic acid

HEPL HEF1/Efs/p130Cas-like

HER2-Neu human epidermal growth factor receptor 2-

IB immunoblot

ILK integrin-linked kinase

IP immunoprecipitation

IR insulin receptor tyrosine kinase

JNK c-Jun N-terminal kinase

LD leucine-aspartic acid (repeat)

LIM Lin11, Isl-1, Mec-3 (-like domain)

LIMK LIM domain kinase

mDia1 Diaphanous-related formin-1

MEFs mouse embryo fibroblasts

MLCK myosin light-chain kinase

mPR p130Cas signaling variant with the SBD proline motif RPLPSPP changed to RAAASPP

n.s. not significant

NA numerical aperture

NMR nuclear magnetic resonance

NSP novel Src homology 2-containing protein

NSP1 novel Src homology 2-containing protein 1

NSP2 novel Src homology 2-containing protein 2, a.k.a. AND-34

NSP3 novel Src homology 2-containing protein 3, a.k.a. Chat

p p-value (probability of the null hypothesis being true)

PAK1 p21 protein-activated kinase 1

PALM photoactivated light microscopy

PBS phosphate buffered saline

PDK1 phosphoinositide-dependent kinase-1

PI3K phosphoinositide 3-kinase

PIPES piperazine-N,N'-bis(2-ethanesulfonic acid)

PKA protein kinase A

PKC protein kinase C

Plan Apo Plan Apochromat

PMSF phenylmethylsulfonyl fluoride, serine protease inhibitor

PR-39 anti-microbial peptide

PTP-1B protein tyrosine phosphatase 1B

PTP-PEST protein tyrosine phosphatase with P (proline) E (glutamic acid) S (serine) T (threonine) sequence

PxxP proline-x-x-proline motif, where x is any amino acid

pY phosphotyrosine

PYK2 protein tyrosine kinase 2

R-Ras Ras-related protein

Rac1 Ras-related C3 botulinum toxin substrate 1

Rap1 Ras-related protein 1

RhoA Ras homolog gene family, member A

ROCK Rho-associated protein kinase

RPLPSPP arginine-proline-leucine-proline-serine-proline-proline, proline-rich motif

s.d. standard deviation

s.e.m. standard error of the mean

SBD Src-binding domain

SD substrate domain

SDS sodium dodecyl sulfate

SDS-PAGE sodium dodecyl sulfate-polyacrylamide gel electrophoresis

SER serine-rich domain

SFKs Src family kinases

SH2 Src-homology 2

SH3 Src-homology 3

Shep-1 SH2 domain-containing Eph receptor-binding protein 1, a.k.a. Chat

SHIP-2 Src-homology 2 containing inositol phosphatase-2

Sin Src interacting protein, a.k.a. Efs/Sin

STAT5b signal transducer and activator of transcription 5b

Syk spleen tyrosine kinase

TBS Tris-buffered saline

TESK1 testis-specific protein kinase 1

TIRF total internal reflection fluorscence

uPAR urokinase (uPA) receptor

WASP Wiskott-Aldrich syndrome protein

WAVE WASP family Verprolin-homologous protein

WT wild type

Y397 tyrosine at amino acid position 397

YDYV tyrosine-aspartic acid-tyrosine-valine motif

YDxP tyrosine-aspartic acid-x-proline motif, where x is any amino acid

YopH *Yersinia* tyrosine phosphatase

YxxP tyrosine-x-x-proline motif, where x is any amino acid

CHAPTER I

INTRODUCTION TO CELL MOTILITY AND P130CAS SIGNALING

Cell Motility

Cell migration is a fundamental biological process that is important in normal physiological processes including embryonic development, tissue homeostasis, wound healing, and immune surveillance (Horwitz and Webb, 2003, Lauffenburger and Horwitz, 1996, Ridley et al., 2003). However, when cell migration becomes dysregulated it contributes to disease pathology including mental retardation, osteoporosis, atherosclerosis, chronic inflammation, and cancer (Horwitz and Webb, 2003, Lauffenburger and Horwitz, 1996, Ridley et al., 2003, Hall, 2009). Cell migration is a highly dynamic process during which numerous signals must be integrated to generate a coordinated cellular response. This process depends on several key structures including the actin and microtubule cytoskeleton networks and focal adhesion sites. These structures are spatially and temporally coordinated by Rho family GTPases, in particular Cdc42, Rac1 and RhoA (Wittmann and Waterman-Storer, 2001, Nobes and Hall, 1999). The result is a cyclical process that can be broken down into several key steps including: an initial polarized morphology, followed by protrusion of the leading edge, adhesion to the substratum, contraction to pull the cell forward, and release of the cell rear (reviewed in (Etienne-Manneville, 2004, Le Clainche and Carlier, 2008, Ridley et al., 2003).

Key Structures in Cell Motility

Actin and microtubule interactions are fundamental to establish and maintain dynamic cellular asymmetries in numerous processes including migration (Rodriguez et al., 2003). Focal adhesion (FA) sites provide the structural link between the actin cytoskeleton and the extracellular matrix (ECM) and through integrin engagement regulate enzymes and adapter proteins to control cell behavior (Miranti and Brugge, 2002). Focal adhesion sites and the cytoskeleton are intimately coupled, with actin- and microtubule-mediated interactions regulating FA dynamics (Wehrle-Haller and Imhof, 2003) and integrin-mediated signaling directing cytoskeleton rearrangements (Miranti and Brugge, 2002).

Microtubule Cytoskeleton

Microtubules are not required for migration per se, but rather modulate the migratory machinery by establishing and maintaining cellular polarity (Siegrist and Doe, 2007, Wehrle-Haller and Imhof, 2003). It was noted in 1970 that intact microtubules are required to maintain the polarized distribution of actin protrusions at the leading edge of migrating fibroblasts (Vasiliev et al., 1970). Microtubules are polymers with inherent directionality that form a polarized network for protein and vesicle movement throughout the cell (Etienne-Manneville, 2004). In migrating cells, microtubules are nucleated from two central structures, the centrosome (Bettencourt-Dias and Glover, 2007) and the Golgi complex (Efimov et al., 2007). In migrating cells, these structures are often linked with the centrosome situated in front of the nucleus and the Golgi positioned around the centrosome in an extended ribbon-like array (Sutterlin and Colanzi, 2010). Microtubule minus-ends are anchored at the centrosome and Golgi while polymerization extends

microtubule plus-ends to the cell edges (Sutterlin and Colanzi, 2010). However, the geometries of these two networks differ, the centrosome produces a symmetric, radial array while the Golgi produces a polarized array that extends primarily toward the leading edge (Efimov et al., 2007).

In migrating cells, numerous microtubule-dependent processes are directed toward the leading edge, including Cdc42-dependent centrosome and Golgi reorientation, vesicular trafficking, and the presence of stable detyrosinated microtubules (Wittmann and Waterman-Storer, 2001, Sutterlin and Colanzi, 2010). In addition, microtubule dynamics both self-regulate and alter local actin and focal adhesion dynamics (Rodriguez et al., 2003). Microtubule growth stimulates actin assembly at the leading edge (through Rac1 activation) and drives a positive feedback loop to stimulate additional microtubule growth (through Rac1/Pak-mediated inhibition of Op18) (Rodriguez et al., 2003). Conversely, microtubule shortening drives actomyosin contraction (through RhoA activation) and microtubule stabilization (through RhoA/mDia) (Rodriguez et al., 2003). Finally, microtubule-targeting of focal adhesion sites as a result of repeated cycles of growth and catastrophe results in focal adhesion disassembly (Kaverina et al., 1999, Ezratty et al., 2005). Polarized vesicular trafficking and directed migration both specifically require the asymmetric Golgi-derived microtubule array (Miller et al., 2009). While a potential relationship has not yet been evaluated, this may also be true for other polarized MT-dependent functions (as hypothesized in (Efimov et al., 2007)).

Actin Cytoskeleton

Despite the essential role that microtubules play in establishing polarity in many cell types, some cells are able to migrate in the complete absence of microtubules

(including keratocytes, neutrophils, and lymphocytes (Scliwa and Honer, 1993). In the simplest case using lamellar fish keratocyte fragments, either an existing gradient of actin assembly and myosin contractility or perturbation of a symmetric cell fragment to create an asymmetry in contractility was sufficient to drive migration (Euteneuer and Schliwa, 1984, Verkhovsky et al., 1999b). Extending this work to intact cells, an externally enforced contractility gradient stimulated protrusion in fibroblasts lacking microtubules (Kaverina et al., 2000). This data helped establish the consensus that the actin cytoskeleton provides the primary driving force behind protrusion and migration (Small et al., 2002).

Actin monomers polymerize into filamentous-actin (F-actin), a polymer that can be used to generate diverse cellular structures (Le Clainche and Carlier, 2008). Like microtubules, actin polymers have an inherent directionality, which is reinforced by differential polymerization kinetics. Actin assembles preferentially at the "barbed" end and disassembles at the "pointed" end (Bugyi and Carlier, 2010). Three principal actin structures are prominent in migrating cells: filopodia and lamellipodia at the leading edge, and stress fibers that cross the cell body and connect adhesion sites (Le Clainche and Carlier, 2008). The lamellipodium consists of a thin sheet of densely-packed branched actin filaments (Borisy and Svitkina, 2000) (although, a recent report indicated that lamellipodial actin is a dense meshwork of overlapping, unbranched filaments (Urban et al., 2010)), while both filopodia and stress fibers are composed of parallel bundled actin filaments (Le Clainche and Carlier, 2008).

Lamellipodium

The lamellipodium polarizes in the direction of migration and provides the driving force for protrusion (Etienne-Manneville, 2004, Small et al., 2002). Actin assembly in the lamellipodium is mediated by Rac1/WAVE activation of the Arp2/3 complex and occurs primarily at the leading edge (Pollard and Borisy, 2003, Lai et al., 2008, Borisy and Svitkina, 2000). Constant polymerization coupled with membrane resistance and/or myosin II contractility generates retrograde flow of the lamellipodial actin meshwork away from the leading edge (Vicente-Manzanares et al., 2009, Wittmann and Waterman-Storer, 2001) where actin filaments are severed and depolymerized (Pollard and Borisy, 2003). This process of treadmilling (Lai et al., 2008, Wang, 1985) is converted into forward movement as actin filaments couple to nascent adhesion sites (Wehrle-Haller and Imhof, 2003, Alexandrova et al., 2008). The rate of formation of nascent adhesion sites within the lamellipodium is proportional to the rate of protrusion (Choi et al., 2008).

Filopodia

Similar to the lamellipodium, filopodia are polarized toward the leading edge with actin assembly at their tips driving protrusion and retrograde flow (Mellor, 2010, Faix et al., 2009). Activation of Cdc42 drives the formation of filopodia (Nobes and Hall, 1995), but the mechanism of formation remains controversial. There are currently three models, convergent elongation, tip nucleation, and the cascade pathway (Mellor, 2010). The convergent elongation model proposes branched filaments from the lamellipodium nucleated by Arp2/3 activity converge and form a bundled filopodium that avoids capping by association with the filopodia "tip complex" enabling continued elongation (Svitkina et al., 2003). The tip nucleation model proposes filopodial protrusion is driven

by formins, rather than by the Arp2/3 complex, and that filopodial and lamellipodial nucleation arise from distinct signaling pathways with separable core machineries (Faix et al., 2009). Finally, the cascade pathway model proposes a hybrid mechanism whereby dendritic Arp2/3-nucleated lamellipdial actin filaments receive additional signals (including processive elongation by formins) and become bundled filopodia, but that lamellipodial formation is a key step in filopodia formation (Biyasheva et al., 2004, Gupton and Gertler, 2007). This controversy is further complicated by recent data on the structure of the lamellipodium (Urban et al., 2010), which differs from the prevailing branched dendritic network model of lamellipodium structure; however, this newly proposed unbranched lamellipodium structure could bypass the need to transform a dendritic lamellipodial actin network into filaments with processive elongation. In addition to their protrusive role, filopodia extending in front of and embedded within the lamellipodium serve a sensory role (Mellor, 2010, Faix et al., 2009). The plus-end directed motor, Myosin-X is concentrated at filopodial tips (Berg et al., 2000) where it transports cargo, including β-integrins (Zhang et al., 2004) and other receptors (Mellor, 2010). Consistent with this concentration of receptors at their tips, filopodia are implicated in the formation of nascent adhesion sites at the leading edge (Nobes Hall 1995, Faix Rottner 2006).

Stress Fibers

Stress fibers, the actin structures that classically connect adhesion sites, have been organized into three classes: ventral stress fibers (anchored to FAs at both ends), dorsal stress fibers (one end anchored to an FA with the other end extending dorsally into a loose actin network), and transverse arcs (form at the base of the lamella, not connected

to FAs at either end) (Small et al., 1998). In migrating cells, stress fibers have uniform polarity at the interface with adhesion sites, barbed ends point toward the adhesion, while the central regions of fibers have graded polarity with mixed filament directionality (Cramer et al., 1997). Stress fibers form through nascent actin assembly from adhesion sites (Hotulainen and Lappalainen, 2006), with purified integrin adhesions exhibiting actin assembly potential (Butler et al., 2006). In addition stress fibers form by end-to-end joining of short actin and myosin bundles, with end-to-end joining of these sub-structures with adhesion-anchored fibers resulting in ventral stress fibers anchored to focal adhesions at both ends (Hotulainen and Lappalainen, 2006). An alternate hypothesis for the formation of the graded polarity filaments includes the incorporation of existing actin filaments in the lamella through retrograde flow and myosin contraction (Verkhovsky et al., 1995, Verkhovsky et al., 1999a, Anderson et al., 2008). Both modes of assembly are consistent with the observed filament polarity. The cooperative reorganization of actin into stress fibers is regulated by RhoA signaling to mDia1 and ROCK, which stimulate actin assembly and contractility respectively (Watanabe et al., 1999, Hotulainen and Lappalainen, 2006, Pellegrin and Mellor, 2007). Mature stress fibers display periodic banding of alpha-actinin and myosin (Pellegrin and Mellor, 2007). It is the presence of myosin that imparts contractility to stress fibers, which are the major mediators of cellular contraction (Kumar et al., 2006, Peterson et al., 2004, Katoh et al., 2001, Pellegrin and Mellor, 2007). In addition, the cross-linking of actin by alpha-actinin and myosin II promotes FA maturation (Choi et al., 2008, Vicente-Manzanares et al., 2009).

Adhesion Sites

Migration requires the transmission of cellular forces to the ECM through adhesion to the substrate. Cell adhesion to the ECM is mediated by integrins, transmembrane receptors that link the ECM to the actin cytoskeleton. These integrin contact sites, commonly called focal adhesions, not only mediate adhesion, but also form a large protein signaling network that regulates cell migration (Miranti and Brugge, 2002). An analysis of the molecular interactions within adhesion sites revealed more than 150 proteins in the "integrin adhesome" including both integral adhesion components and transiently interacting proteins (Zaidel-Bar et al., 2007a). These dynamic structures both transduce cellular traction forces and in turn respond to changes in force by remodeling and coordinating cytoskeletal rearrangements (Lock et al., 2008). Although adhesion sites clearly exist on a continuum of size and molecular composition, they have been grouped into several classes: nascent adhesions/focal complexes at the leading edge, mature/classic focal adhesions connected to stress fibers, and fibrillar adhesions that align with ECM fibers (Dubash et al., 2009). Due to the large number of focal adhesion proteins, only a few key aspects of integral structural and signaling molecules will be discussed in this chapter.

Adhesion Nanoparticles and Focal Complexes

The molecular organization of the earliest adhesive complexes is not clear, but a plausible primary adhesive subunit is speculated to consist of at least two α/β integrin heterodimers connected to actin filaments by a talin dimer (Geiger et al., 2009). This hypothetical complex could account for the talin-dependent 2 pN 'slip bonds' detected between fibronectin-coated beads and the cytoskeleton (Jiang et al., 2003). ECM-

cytoskeleton connections were evaluated by restraining fibronectin-coated beads on the cell surface using laser tweezers and measuring the smallest force required to break connections, 'slip bonds', between the actin cytoskeleton and matrix on the bead surface (Jiang et al., 2003). Underscoring its essential role, cells lacking both talin isoforms initiate spreading, but fail to form adhesions (Zhang et al., 2008). Subsequent recruitment of vinculin to talin initiates clustering of activated integrins (via the head domain) and further reinforces the link to the actin cytoskeleton (via the tail domain) (Humphries et al., 2007). The addition of vinculin is a key step in the ability of early adhesion sites to transduce force (Galbraith et al., 2002).

The earliest adhesion sites detectable by standard microscopy techniques are focal complexes, with diameters of approximately 100 nm (Geiger et al., 2009). However, smaller structures (30-40 nm) containing integrins and some integral FA proteins have been detected using PALM (photoactivated light microscopy) (Shroff et al., 2007, Shroff et al., 2008, Geiger et al., 2009). Focal complexes form under the lamellipodium lasting on the order of seconds until they either turn over or mature into focal adhesions, typically at the base of the lamellipodium (Ponti et al., 2004, Alexandrova et al., 2008, Choi et al., 2008, Geiger et al., 2009). The fast retrograde actin flow in the lamellipodium is required for the formation of nascent adhesions, and their maturation at the base of the lamellipodium correlates with a transition to slower retrograde actin flow in the lamella (Alexandrova et al., 2008). Thus, Rac1 and Cdc42 drive not only lamellipodial protrusion but also formation of nascent adhesion complexes (Nobes and Hall, 1995). In addition to integrins, talin, and low levels of vinculin, focal complexes have also been reported to contain paxillin, p130Cas, Arp2/3 complex, low levels of FAK

(focal adhesion kinase) and alpha-actinin, and high levels of tyrosine phosphorylation (Donato et al., 2010, Nobes and Hall, 1995, Zaidel-Bar et al., 2003, DeMali et al., 2002). Paxillin, p130Cas, and FAK all contribute to the tyrosine phosphorylation signal in focal complexes, as detected by phospho-specifc antibody staining in fixed cells and a tandem Src-SH2 FRET (fluorescence resonance energy transfer) probe in live cells (Fonseca et al., 2004, Webb et al., 2004, Ballestrem et al., 2006).

Focal Adhesions

As they mature into focal adhesions, focal complexes elongate centripetally and become coupled to stress fibers (Geiger et al., 2009, Wolfenson et al., 2009a). This maturation zone typically defines the transition from the lamellipodium to the lamella. Once the process of maturation is complete, adhesion sites become stationary (tens of minutes), then as the cell moves forward, the focal adhesions disassemble as they near the rear of the lamella due to forward translocation of the cell (Rid et al., 2005, Wolfenson et al., 2009a). Coupled to its role in driving contractility and the formation of stress fibers, RhoA also drives the formation of mature focal adhesions (Nobes and Hall, 1995), which require myosin activity for their maturation and physically elongate along actin fibers (Geiger et al., 2009, Vicente-Manzanares et al., 2009).

The molecular composition of focal adhesions differs from focal complexes. Several proteins including vinculin and FAK while clearly present in focal complexes are significantly enriched in mature focal adhesions (Zaidel-Bar et al., 2003). Other reported components of focal complexes such as alpha-actinin are more controversial. While low-levels of alpha-actinin have been reported in focal complexes (Zaidel-Bar et al., 2003), other groups (Laukaitis et al., 2001, Webb et al., 2004) report that alpha-actinin is not

present in focal complexes, and that it serves as a marker of adhesion maturation. However, from both data sets, it is clear that alpha-actinin displays a higher relative abundance in mature focal adhesions relative to focal complexes. Finally, zyxin has been identified as a definitive marker of mature adhesions that is absent from focal complexes (Zaidel-Bar et al., 2003). Like focal complexes, focal adhesions maintain high levels of tyrosine phosphorylation.

In addition to differences in molecular composition, adhesion sites develop a clear asymmetry with maturation. The connection to a stress fiber results in a break in adhesion symmetry (Wolfenson et al., 2009a). The adhesion grows centripetally along the stress fiber and undergoes differential internal dynamics within the proximal (near the stress fiber) and distal (away from the stress fiber) ends of the adhesion (Wolfenson et al., 2009b), with the proximal adhesion being more dynamic than the distal adhesion. A molecular polarity is also seen as sequential focal adhesion protein signatures from the distal to proximal ends of focal adhesions (Zamir et al., 2008). In addition to a general break in symmetry, focal adhesions have been shown to have molecular sub-domains or hotspots of activity (Zamir et al., 2008, Shroff et al., 2008, Shroff et al., 2007, Ballestrem et al., 2006). This recent work has shed light on the molecular nature of adhesions as well as their non-uniformity, has highlighted their complexity, and underscores the need for advanced imaging techniques to dissect the spatial and temporal dynamics of these structures.

Fibrillar Adhesions

Focal adhesions can mature into fibrillar adhesions (FBAs), which are specialized to participate in fibrillogenesis, fibronectin matrix assembly. The maturation of focal

adhesions to FBAs requires translocation of the adhesion, the removal of a subset of integrins, paxillin dephosphorylation, and the incorporation of tensin (Zaidel-Bar et al., 2007b, Dubash et al., 2009, Pankov et al., 2000). This maturation process as well as fibrillogenesis is dependent on Rho signaling (Dubash et al., 2009). FBAs are more centrally located than focal adhesions and can be up to 20 μm in length (Dubash et al., 2009), with the presence of tensin serving as the hallmark of FBAs (Zamir et al., 1999). While FBAs share some components with both focal complexes and focal adhesions, they do not contain most of the enzymatic signaling proteins present in focal complexes and focal adhesions, have low levels of tyrosine phosphorylation, and are not thought to play a role in signal transduction (Zamir et al., 1999, Dubash et al., 2009). Rather their primary role appears to be assembling matrix components (Dubash et al., 2009, Pankov et al., 2000).

Integrin-mediated Adhesion Signaling

Integrin clustering rapidly recruits a diverse set of signaling and adapter proteins that collect around the integrin cytoplasmic tails and associated actin filaments (Lock et al., 2008). The unique position of integrins at the cell surface allows them to integrate information bi-directionally, classically termed "outside-in" and "inside-out" signaling (Pozzi and Zent, 2003, Lock et al., 2008). Outside-in signaling entails activating integrins via their ECM ligands, then integrins signal through their cytoplasmic tails to the associated adhesion proteins. Conversely, inside-out signaling modulates both the affinity of integrins for their ECM ligands and integrin clustering ability through interactions with the cytoplasmic tail that change integrin conformation. Through these pathways integrins regulate the actin cytoskeleton, cell growth, differentiation, and

survival, as well as their own activity (Wolfenson et al., 2009a, Reddig and Juliano, 2005, Assoian and Klein, 2008, LaFlamme et al., 2008, Legate et al., 2009).

The proteins in the adhesome form a highly-interconnected signaling network (Zaidel-Bar et al., 2007a). Within adhesion sites, the adhesion components/signaling nodes often interact with numerous other adhesion proteins (sometimes more than ten potential interacting partners), either binding to, or directly activating or inactivating other components (Zamir and Geiger, 2001, Zaidel-Bar et al., 2007a). Tyrosine phosphorylation is one of the key signaling events at adhesions sites, which are often defined by their high levels of tyrosine phosphorylation (Wozniak et al., 2004). The tyrosine kinases FAK and Src are two of the major kinases at adhesion sites (Wozniak et al., 2004). While additional tyrosine kinases (Abl, Csk, Fyn, IR, Lyn, Pyk2, Syk, TESK1) as well as serine-threonine kinases (Akt, ERK, ILK, JNK, LIMK, PAK1, PDK1, PKA, PKC, ROCK) are found at adhesion sites (Zaidel-Bar 2007), they will not be discussed in detail.

FAK and Src function together as a complex to facilitate substrate phosphorylation. FAK targeting to adhesions is likely mediated, in part, by interactions between the FAK focal adhesion targeting (FAT) domain and the LD2 and LD4 motifs at the N-terminus of paxillin, a scaffold protein present in focal complexes (Tachibana et al., 1995, Bertolucci et al., 2005). *In vitro* studies suggest that FAK may also bind talin (Chen et al., 1995) and the cytoplasmic tail of β_1 integrins (Schaller et al., 1995). Upon integrin engagement and clustering, FAK autophosphorylates tyrosine 397, creating a high-affinity binding site for Src (Schaller et al., 1994). Src binding to the phosphorylated-Y397 releases Src autoinhibitory interactions resulting in a transient

FAK/Src signaling complex. Autophosphorylation is the best-characterized FAK phosphorylation event, after which despite its intrinsic kinase activity, it functions primarily as a scaffold (Schaller et al., 1999, Lock et al., 2008). After FAK/Src complex formation, Src further phosphorylates FAK and other adhesion targets and linking integrin signaling to the activation of the RhoGTPases (Huveneers and Danen, 2009). The two main Src substrates at adhesion sites are the scaffold proteins, p130Cas and paxillin (Hanks et al., 2003, Mitra and Schlaepfer, 2006). The ultimate focus of this chapter is on the former and its role in the FAK/Src/p130Cas signaling module within focal adhesions, which is discussed in more detail in subsequent sections.

Adhesion Mechano-sensing

Interactions between the actin cytoskeleton and adhesion sites coordinate protrusion and the generation of cellular traction forces (Geiger et al., 2009). The adhesion itself is a mechanically responsive structure (Wolfenson et al., 2009a). Direct application of forces to cells drives adhesion formation (Riveline et al., 2001, Kaverina et al., 2002, Sniadecki et al., 2007). Even application of force to Triton X100-extracted cytoskeletons resulted in incorporation of new adhesion components (Sawada and Sheetz, 2002). Furthermore, individual adhesion components have been shown to be mechanically responsive. Simulations indicate mechanical force may facilitate the transition of β-integrin into an active conformation (Puklin-Faucher et al., 2006). Substantial unfolding of talin is required to unmask vinculin binding sites buried in the talin rod domain (Gingras et al., 2006, Papagrigoriou et al., 2004). Stretching of p130Cas increases its susceptibility to Src phosphorylation (Sawada et al., 2006), likely by revealing cryptic tyrosine phosphorylation sites.

Adhesion Disassembly

Four main pathways have been shown to regulate focal adhesion disassembly: inhibition of myosin contractility, FAK/Src-mediated signaling, calpain-mediated proteolysis, and microtubule-mediated endocytosis (Dubash 2009 and Wolfenson 2009), but how these various pathways are coordinated is still unknown.

Just as focal adhesions grow and undergo maturation in response to stress fiber tension, they disassemble upon its release (Wolfenson et al., 2009a). Interference with myosin contractility initiates adhesion disassembly both in the presence and absence of microtubules (known regulators of adhesion disassembly) (Wolfenson et al., 2009a, Helfman et al., 1999, Bershadsky et al., 1996). Thus, one hypothesis for the mechanism of adhesion disassembly is that it entails local down-regulation of myosin-mediated forces (Wolfenson et al., 2009a). This local myosin inhibition may be facilitated by microtubules through a pathway that includes Rho inhibition mediated by the tyrosine kinase, Arg (Broussard et al., 2008, Peacock et al., 2007).

Tyrosine phosphorylation has also been shown to play a role in adhesion disassembly (Crowley and Horwitz, 1995). Cells deficient in FAK or Src family kinases have defects in migration (Ilic et al., 1995, Klinghoffer et al., 1999). An analysis of the rates of adhesion disassembly in cells deficient for major focal adhesion signaling proteins revealed Src, FAK (Y397 phosphorylation), p130Cas, and paxillin (tyrosine phosphorylation) are required for efficient focal adhesion disassembly (Webb et al., 2004). In addition inhibitors of ERK and MLCK, known effectors of FAK/Src signaling, decreased the rates of adhesion disassembly (Webb et al., 2004).

Calpain was first localized at adhesion sites in 1987 and it was hypothesized that cells may regulate adhesion through selective proteolysis (Beckerle et al., 1987). Since that time calpain has been shown to regulate adhesion sites, and deletion of a calpain subunit or inhibition of calpain results in defects in adhesion disassembly (Huttenlocher et al., 1997, Palecek et al., 1998, Dourdin et al., 2001). Numerous prominent adhesion components have been identified as potential calpain targets including: talin, α-actinin, vinculin, integrins, FAK, Src, paxillin (Perrin and Huttenlocher, 2002, Dubash et al., 2009). Talin has been verified as a calpain target in cells, and a protease resistant point mutant yields defects similar to calpain inhibition (Franco et al., 2004). Calpain proteolysis is also implicated downstream of microtubule targeting of adhesions (Bhatt et al., 2002).

In migrating cells, repeated microtubule targeting of individual adhesions preceded adhesion disassembly (Kaverina et al., 1999). A robust assay was developed to study this phenomenon; initial nocodazole treatment disrupts microtubules and stimulates focal adhesion formation, which is followed by nocodazole washout to facilitate microtubule regrowth and coordinated adhesion disassembly (Ezratty et al., 2005). In this coordinated assay, microtubule-mediated adhesion disassembly depends on FAK and dynamin, which have ultimately been shown to regulate clathrin-mediated endocytosis of integrins (Ezratty et al., 2005, Chao and Kunz, 2009, Ezratty et al., 2009).

How these various adhesion disassembly pathways function together is still not understood. However, microtubules have been implicated in several of the disassembly mechanisms and disruption of the microtubule cytoskeleton results in robust adhesion

assembly (Bershadsky et al., 1996). Thus, microtubules may play a role as master regulators of adhesion disassembly (Broussard et al., 2008).

Discovery of p130Cas

P130Cas (Crk-associated substrate) is a prominent substrate of the Src tyrosine kinase in the integrin adhesome that has been implicated in the control of cell migration, the cell cycle, survival, apoptosis, cancer transformation and metastasis, development, and bacterial pathogenesis (Chodniewicz and Klemke, 2004, Bouton et al., 2001, Defilippi et al., 2006, O'Neill et al., 2000, Tikhmyanova et al., 2010a). P130Cas was first identified twenty years ago as a highly tyrosine phosphorylated protein in *v-Crk* and *v-Src* transformed cells (Mayer et al., 1988, Reynolds et al., 1989, Matsuda et al., 1990). P130Cas was affinity purified from *v-crk* transformed cells and peptide sequences were obtained (Sakai et al., 1994). Subsequent molecular cloning of the cDNA revealed conserved protein-protein interaction domains including an N-terminal SH3 domain and a large "substrate domain" (SD) containing fifteen putative SH2-binding motifs (Sakai et al., 1994). With this unique structure, p130Cas was hypothesized to function as a docking protein. This hypothesis has largely been confirmed over time with the identification of numerous interacting proteins. Thus, while lacking intrinsic enzymatic activity, p130Cas is able to exert spatiotemporal control over signaling pathways by recruiting and activating downstream effectors (Bouton et al., 2001, Defilippi et al., 2006).

Domain Structure

P130Cas contains multiple conserved protein-protein interaction domains, but no domains indicative of intrinsic enzymatic activity. In addition to the N-terminal SH3 domain and the central SD already noted, p130Cas contains a Serine-rich (SER) domain, a "Src-binding domain" (SBD) near the C-terminus, and a conserved "Cas-family C-terminal homology" (CCH) domain (Bouton et al., 2001, Defilippi et al., 2006, O'Neill et al., 2000, Donato et al., 2010), see Figure 1. The function of these principal domains will be discussed in more detail below. P130Cas is conserved from flies (*Drosophila melanogaster*) to humans, but is not present in *Caenorhabditis elegans* or *Saccharomyces cerevisiae* (Zaidel-Bar, 2009, Singh et al., 2008).

Cas-family Members

P130Cas is the founding member of the Cas family, which consists of four proteins in mammals: p130Cas/BCAR1, HEF-1/Cas-L/NEDD9, Efs/Sin, and HEPL/CASS4 (Singh et al., 2008, Tikhmyanova et al., 2010a), see Figure 1. Only one Cas family member is present in lower vertebrates, chordates, and insects, corresponding to p130Cas (Singh et al., 2008). The most highly conserved regions within the Cas family are the N-terminal SH3 domain and the C-terminal CCH domain (Alexandropoulos et al., 2003, Donato et al., 2010, Tikhmyanova et al., 2010a), see Figure 2. Another highly conserved motif is the YDYV sequence in the SBD, which is invariant in three of the four mammalian protein family members and the single *Drosophila melanogaster* family member. Only p130Cas and Efs/Sin contain the proline-rich motif of the SBD.

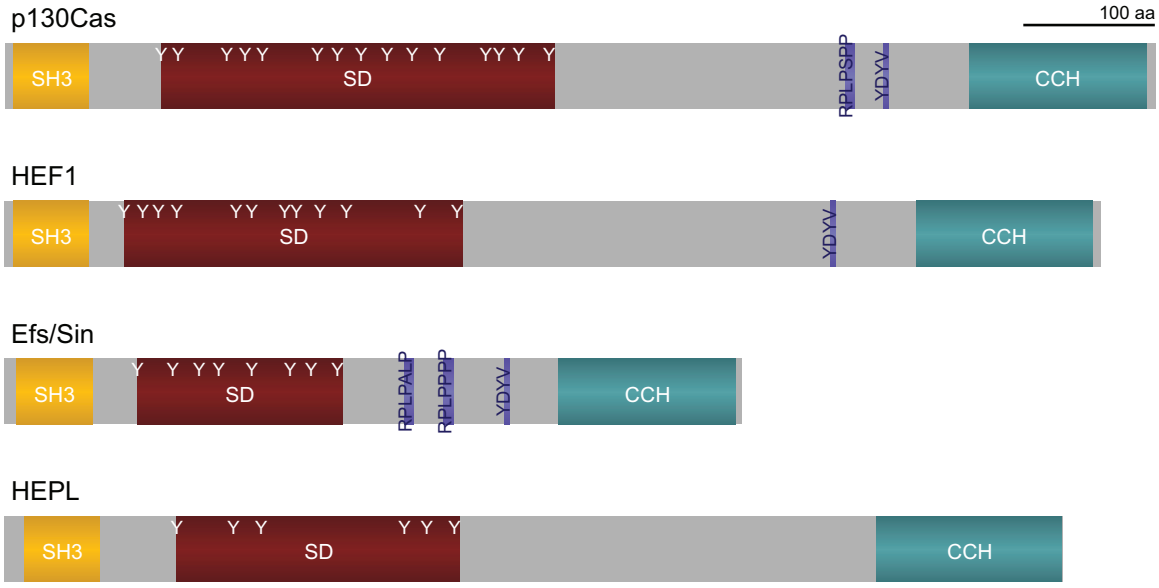

Figure 1. Diagram of Cas family member domain structures. The primary structure of the four mouse Cas family members is represented to scale from the N-terminus to the C-terminus with the major interaction domains indicated. Scale bar is 100 amino acids (aa). P130Cas is 874 amino acids and contains an SH3 domain aa 7-63; a substrate domain (SD) aa 119-417 with YxxP tyrosines at residues 119, 132, 169, 183, 196, 238, 253, 271, 291, 310, 331, 366, 376, 391, and 414; a bipartite Src-binding domain (SBD) with a proline-rich motif RPLPSPP aa 639-645, and a YDYV SH2 domain binding motif aa 668-671; and a Cas-family C-terminal homology (CCH) domain aa 734-869. HEF1 is 833 amino acids and contains an SH3 domain aa 7-63; an SD aa 91-347 with YxxP tyrosines at residues 91, 105, 117, 131, 176, 188, 213, 222, 240, 260, 316, and 344; a partial SBD with only the YDYV SH2 domain binding motif aa 628-631; and a CCH domain aa 693-826. Efs/Sin is 560 amino acids and contains an SH3 domain aa 9-66; an SD aa 101-256 with YxxP tyrosines at residues 101, 128, 148, 163, 188, 217, 233, and 253; an SBD with two proline-rich motifs RPLPALP aa 304-310 and RPLPPPP aa 334-340, and a YDYV SH2 domain binding motif aa 380-383; and a CCH domain aa 421-555. HEPL is 804 amino acids and contains an SH3 domain aa 15-71; an SD aa 131-345 with YxxP tyrosines at residues 131, 174, 195, 304, 321, and 342; and a CCH domain aa 673-803. HEPL does not contain either part of the SBD.

Figure 2. Cas family protein sequence alignment. Protein sequence alignments were performed using p130Cas, Mouse Uniprot ID Q61140; HEF1, Mouse Uniprot ID O35177; EFS, Mouse Uniprot ID Q64355; DmCAS, Drosophila Uniprot ID Q7KVE5; and HEPL, Mouse Uniprot ID Q08EC4. Conserved motifs are indicated by color: the SH3 domain (orange), YxxP motifs in the SD (dark red), SBD motifs (dark purple), and the CCH domain (cyan). Within the domains (SH3, SBD YDYV motif, and CCH) sequence identity is indicated by white text on black, sequence similarity is indicated by white text on grey. The two most highly conserved domains are the N-terminal SH3 domain and the C-terminal CCH domain. The SH3 has 34% sequence identity and 36% sequence similarity while the CCH has 16% sequence identity and 15% sequence similarity.

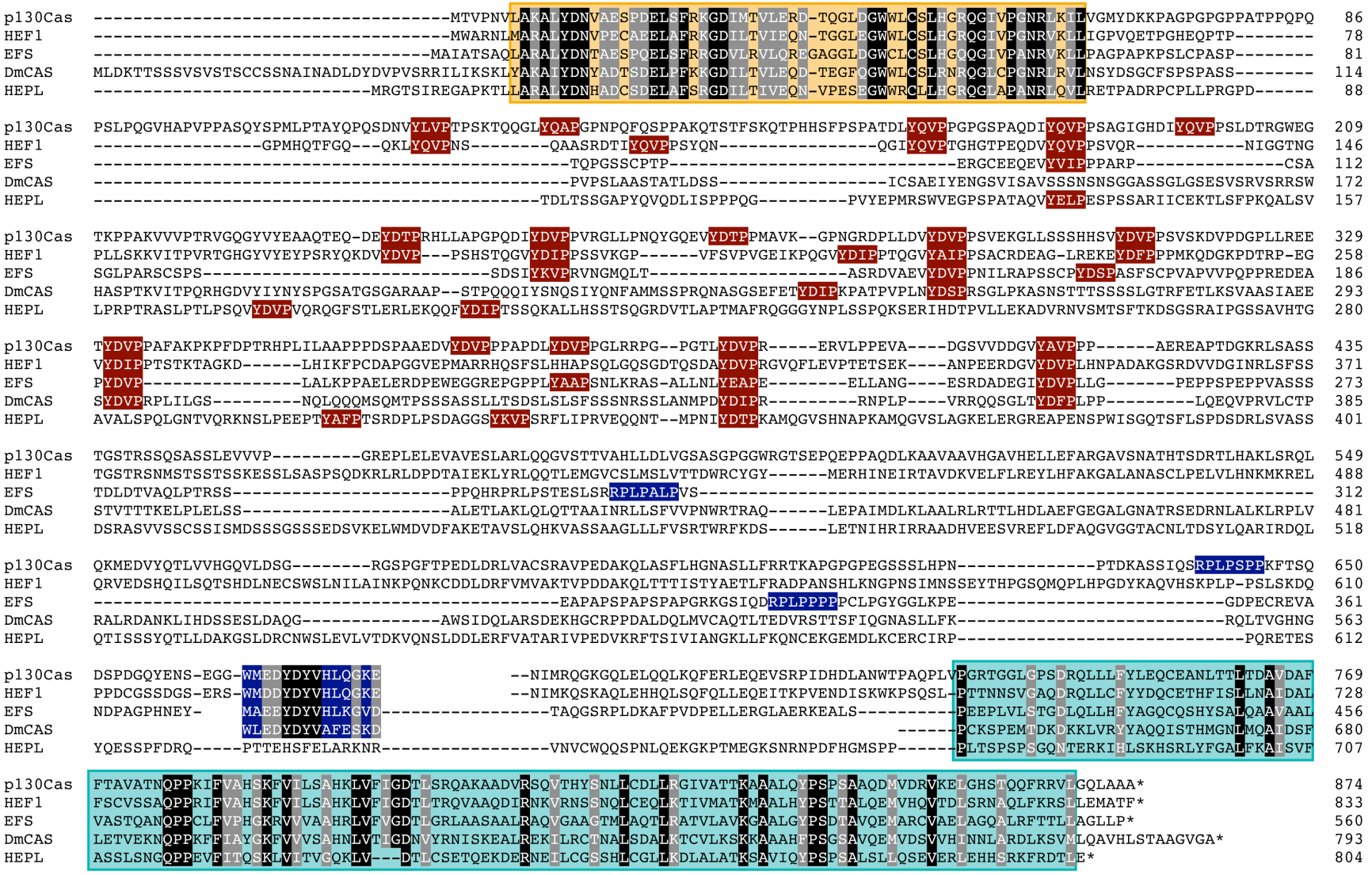
p130Cas ----------MTVPNVLAKALYDNVAESPDELSFRKGDIMTVLERD-TQGLDGWWLCSLHGRQGIVPGNRLKILVGMYDKKPAGPGPGPPATPPQPQ 86
HEF1 ----------MWARNLMARALYDNVPECAEELAFRKGDILTVIEQN-TGGLEGWWLCSLHGRQGIVPGNRVKLLIGPVQETPGHEQPTP-------- 78
EFS ----------MAIATSAQLARALYDNTAESPQELSFRRGDVLRVLQRE-GAGGLDGWCLCSLHGQQGIVPANRVKLLPAGPAPKPSLCPASP-------- 81
DmCAS MLDKTTSSSVSVSTSCCSSNAINADLDYDVPVSRRILIKSKLYAKAIYDNYADTSDELPFKKGDILTVLEQD-TEGFQGWWLCSLRNRQGLCPGNRLRVLNSYDSGCFSPSPASS-------- 114
HEPL ----------MRGTSIREGAPKTLLARALYDNHADCSDELAFSRGDILTIVEQN-VPESEGWWRCLLHGRQGLAPANRLQVLRETPADRPCPLLPRGPD------ 88
p130Cas PSLPQGVHAPVPPASQYSPMLPTAYQPQSDNVYLVPTPSKTQQGLYQAPGPNPQFQSPPAKQTSTFSKQTPHHSFPSPATDLYQVPPGPGSPAQDIYQVPPSAGIGHDIYQVPPSLDTRGWEG 209
HEF1 ----------GPMHQTFGQ---QKLYQVPNS--------QAASRDTIYQVPPSYQN----------QGIYQVPTGHGTPEQDVYQVPPSVQR----------NIGGTNG 146
EFS ----------TQPGSSCPTP----------ERGCEEQEVYVIPPPARP----------CSA 112
DmCAS ----------PVPSLAASTATLDSS----------ICSAEIYENGSVISAVSSSNSNSGGASSGLGSESVSRVSRRSW 172
HEPL ----------TDLTSSGAPYQVQDLISPPPQG---------PVYEPMRSWVEGPSPATAQVYELPESPSSARIICEKTLSFPKQALSV 157
p130Cas TKPPAKVVVPTRVGQGYVYEAAQTEQ-DEYDTPRHLLAPGPQDIYDVPPVRGLLPNQYGQEVYDTPPMAVK--GPNGRDPLLDVYDVPPSVEKGLLSSSHHSVYDVPPSVSKDVPDGPLLREE 329
HEF1 PLLSKKVITPVRTGHGYVYEYPSRYQKDVYDVP---PSHSTQGVYDIPPSSVKGP------VFSVPVGEIKPQGVYDIPPTQGVYAIPPSACRDEAG-LREKEYDFPPPMKQDGKPDTRP-EG 258
EFS SGLPARSCSPS----------SDSIYKVPRVNGMQLT----------ASRDVAEVYDVPPNILRAPSSCPYDSPASFSCPVAPVVPQPPREDEA 186
DmCAS HASPTKVITPQRHGDVYIYNYSPGSATGSGARAAP--STPQQQIYSNQSIYQNFAMMSSPRQNASGSEFETYDIPKPATPVPLNYDSPRSGLPKASNSTTTSSSSLGTRFETLKSVAASIAEE 293
HEPL LPRPTRASLPTLPSQVYDVPVQRQGFSTLERLEKQQFYDIPTSSQKALLHSSTSQGRDVTLAPTMAFRQGGGYNPLSSPQKSERIHDTPVLLEKADVRNVSMTSFTKDSGSRAIPGSSAVHTG 280
p130Cas TYDVPPAFAKPKPFDPTRHPLILAAPPPDSPAAEDVYDVPPPAPDLYDVPPGLRRPG--PGTLYDVPR-----ERVLPPEVA----DGSVVDDGVYAVPPP------AEREAPTDGKRLSASS 435
HEF1 VYDIPPTSTKTAGKD------LHIKFPCDAPGGVEPMARRHQSFSLHHAPSQLGQSGDTQSDAYDVPRGVQFLEVPTETSEK----ANPEERDGVYDVPLHNPADAKGSRDVVDGINRLSFSS 371
EFS PYDVP----------LALKPPAELERDPEWEGGREPGPPLYAAPSNLKRAS-ALLNLYEAPE--------ELLANG----ESRDADEGIYDVPLLG-------PEPPSPEPPVASSS 273
DmCAS SYDVPRPLILGS---------NQLQQQMSQMTPSSSASSLLTSDSLSLSFSSSNRSSLANMPDYDIPR---------RNPLP----VRRQQSGLTYDFPLPP---------LQEQVPRVLCTP 385
HEPL AVALSPQLGNTVQRKNSLPEEPTYAFPTSRDPLPSDAGGSYKVPSRFLIPRVEQQNT--MPNIYDTPKAMQGVSHNAPKAMQGVSLAGKELERGREAPENSPWISGQTSFLSPDSDRLSVASS 401
p130Cas TGSTRSSQSASSLEVVVP---------GREPLELEVAVESLARLQQGVSTTVAHLLDLVGSASGPGGWRGTSEPQEPPAQDLKAAVAAVHGAVHELLEFARGAVSNATHTSDRTLHAKLSRQL 549
HEF1 TGSTRSNMSTSSTSSKESSLSASPSQDKRLRLDPDTAIEKLYRLQQTLEMGVCSLMSLVTTDWRCYGY------MERHINEIRTAVDKVELFLREYLHFAKGALANASCLPELVLHNKMKREL 488
EFS TDLDTVAQLPTRSS----------PPQHRPRLPSTESLSRRPLPALPVS---------- 312
DmCAS STVTTTKELPLELSS----------ALETLAKLQLQTTAAINRLLSFVVPNWRTRAQ------LEPAIMDLKLAALRLRTTLHDLAEFGEGALGNATRSEDRNLALKLRPLV 481
HEPL DSRASVVSSCSSISMDSSSGSSSEDSVKELWMDVDFAKETAVSLQHKVASSAAGLLLFVSRTWRFKDS------LETNIHRIRRAADHVEESVREFLDFAQGVGGTACNLTDSYLQARIRDQL 518
p130Cas QKMEDVYQTLVVHGQVLDSG--------RGSPGFTPEDLDRLVACSRAVPEDAKQLASFLHGNASLLFRRTKAPGPGPEGSSSLHPN----------PTDKASSIQSRPLPSPPKFTSQ 650
HEF1 QRVEDSHQILSQTSHDLNECSWSLNILAINKPQNKCDDLDRFVMVAKTVPDDAKQLTTTISTYAETLFRADPANSHLKNGPNSIMNSSEYTHPGSQMQPLHPGDYKAQVHSKPLP-PSLSKDQ 610
EFS ----------EAPAPSPAPSPAPGRKGSIQDRPLPPPPPCLPGYGGLKPE---------- 361
DmCAS RALRDANKLIHDSSESLDAQG----------AWSIDQLARSDEKHGCRPPDALDQLMVCAQTLTEDVRSTTSFIQGNASLLFK----------RQLTVGHNG 563
HEPL QTISSSYQTLLDAKGSLDRCNWSLEVLVTDKVQNSLDDLERFVATARIVPEDVKRFTSIVIANGKLLFKQNCEKGEMDLKCERCIRP----------PQRETES 612
p130Cas DSPDGQYENS-EGG-WMEDYDYVHLQGKE --NIMRQGKGQLELQQLKQFERLEQEVSRPIDHDLANWTPAQPLVPGRTGGLGPSDRQLLLFYLEQCEANLTTLTDAVDAF 769
HEF1 PPDCGSSDGS-ERS-WMDDYDYVHLQGKE --NIMKQSKAQLEHHQLSQFQLLEQEITKPVENDISKWKPSQSL-PTTNNSVGAQDRQLLCFYYDQCETHFISLLNAIDAL 728
EFS NDPAGPHNEY- MAEEYDYVHLKGVD----------TAQGSRPLDKAFPVDPELLERGLAERKEALS----------PEEPLVLSTGDLQLLHFYAGQCQSHYSALQAAVAAL 456
DmCAS WLEDYDYVAFESKD------PCKSPEMTDKDKKLVRYYAQQISTHMGNLMQAIDSF 680
HEPL YQESSPFDRQ-----PTTEHSFELARKNR----------VNVCWQQSPNLQEKGKPTMEGKSNRNPDFHGMSPP------PLTSPSPSGQNTERKIHLSKHSRLYFGALFKALSVF 707
p130Cas FTAVATNQPPKIFVAHSKFVILSAHKLVFIGDTLSRQAKAADVRSQVTHYSNLLCDLLRGIVATTKAAALQYPSPSAAQDMVDRVKELGHSTQQFRRVLGQLAAA* 874
HEF1 FSCVSSAQPPRIFVAHSKFVILSAHKLVFIGDTLTRQVAAQDIRNKVRNSSNQLCEQLKTIVMATKMAALHYPSTTALQEMVHQVTDLSRNAQLFKRSLLEMATF* 833
EFS VASTQANQPPCLFVPHGKRVVVAAHRLVFVGDTLGRLAASAALRAQVGAAGTMLAQTLRATVLAVKGAALGYPSDTAVQEMARCVAELAGQALRFTTLLAGLLP* 560
DmCAS LETVEKNQPPKFFIAYGKFVVVSAHNLVTIGDNVYRNISKEALREKILRCTNALSDALKTCVLKSKKAAAHFPSGSAVQEMVDSVVHINNLARDLKSVMLQAVHLSTAAGVGA* 793
HEPL ASSLSNGQPPEVFITQSKLVITVCQKLV---DTLCSETQEKDERNEILCGSSHLCGLLKDLALATKSAVIQYPSPSALSLLQSEVERLEHHSRKFRDTLE* 804

P130Cas is ubiquitously expressed with elevated levels in the brain, lung, intestine, kidney, and testes of mice (Sakai et al., 1994). Despite having significant shared structural and sequence homology, other Cas family members are unable to compensate for p130Cas in a homozygous knockout mouse (Honda et al., 1998), resulting in embryonic lethality at E12.5. The resulting Cas -/- mouse embryonic fibroblasts (MEFs) have disorganized actin stress fibers and defects in cell migration (Honda et al., 1998, Honda et al., 1999).

P130Cas as a Docking Protein: targeting, signaling, and functional roles

P130Cas provides spatial and temporal control of signaling through its localization, activation (through tyrosine phosphorylation), and recruitment of effector proteins at adhesion sites. Because of its numerous protein-protein interaction domains, p130Cas is generally thought of as a docking protein, providing numerous binding sites for potential effectors (Bouton et al., 2001, Defilippi et al., 2006). The SH3 and CCH domains function primarily in targeting p130Cas to adhesion sites (Donato et al., 2010). After localization, p130Cas is activated and both the SD (Cho and Klemke, 2002, Klemke et al., 1998, Shin et al., 2004) and SBD (Burnham et al., 2000) have direct functions in initiating signaling events. The known p130Cas binding partners and their interacting domains are summarized in Table 1 and additional details are discussed below.

Table 1. p130Cas binding partners and characterized interacting domains.

p130Cas Domain	Binding Partner	Interacting Domain	References
SH3	FAK PYK2 FRNK PTP-1B PTP-PEST C3G CMS PR-39	proline-rich motif	(Polte and Hanks, 1995, 1997) (Astier et al., 1997) (Harte et al., 1996) (Liu et al., 1996) (Garton et al., 1997) (Kirsch et al., 1998) (Kirsch et al., 1999) (Chan and Gallo 1998)
SD	Crk Nck SHIP-2	SH2	(Sakai et al., 1994) (Schlaepfer et al., 1997) (Prasad et al., 2001)
SER	14-3-3	lysine 49	(Garcia-Guzman et al., 1999)
SBD	SFKs Nephrocystin PI3K	SH2, SH3 SH3 SH3	(Nakamoto et al., 1995, 1997) (Donaldson et al., 2000) (Li et al., 2000)
CCH	AND-34 Chat Ajuba	GEF GEF Pre-LIM	(Gotoh et al., 2000) (Sakakibara and Hattori, 2000) (Pratt et al., 2005)

P130Cas Targeting

P130Cas exists in a large cytoplasmic pool (Donato et al., 2010). In response to integrin-mediated adhesion, p130Cas localizes to adhesions and becomes tyrosine phosphorylated (Nojima et al., 1995, Petch et al., 1995, Vuori et al., 1996). Activation of p130Cas in adhesion sites was later confirmed by immunostaining for p130Cas SD tyrosines with phospho-specific antibodies (Fonseca et al., 2004, Ballestrem et al., 2006). Thus adhesion localization correlates with p130Cas activation. However, a p130Cas mutant with phenylalanine substitutions of all fifteen SD YxxP tyrosines still localized to adhesions (Cunningham-Edmondson and Hanks, 2009), indicating localization does not require p130Cas SD tyrosine phosphorylation. P130Cas rapidly localizes to focal complexes and persists in adhesions throughout their lifetimes (Donato et al., 2010). In addition, p130Cas has a high mobile fraction and rapid exchange rate relative to paxillin, another early adhesion protein, emphasizing its dynamic interaction at adhesion sites (Donato et al., 2010).

Two previous studies evaluated adhesion targeting of epitope-tagged p130Cas mutants with conflicting results (Nakamoto et al., 1997, Harte et al., 2000). Hirai and colleagues evaluated an SH3 deletion mutant and a C-terminal deletion mutant lacking the SBD and large portion of the C-terminal region and concluded that the SH3 domain and SBD were both required for targeting (Nakamoto et al., 1997). Bouton and colleagues saw no p130Cas targeting defects with mutation of the SH3 domain, but noted that the SH3 domain by itself was sufficient to target adhesions (Harte et al., 2000). In addition, Bouton and colleagues saw p130Cas targeting defects in a C-terminal deletion that did not interfere with the SBD and concluded that the C-terminus, not the SBD, was

the targeting domain in the C-terminal region of p130Cas (Harte et al., 2000). A recent study (Donato et al., 2010) provides clear quantitative evidence that clarifies the p130Cas targeting domains. Hanks and colleagues confirmed the importance of the SH3 domain for targeting and clarified that the C-terminal region required for targeting is in fact the highly conserved CCH domain (Donato et al., 2010). Deletion of either the SH3 or CCH domain caused defects in p130Cas targeting and phosphorylation that was blocked completely only when both the SH3 and CCH domains were deleted. Furthermore, similar to what has previously been shown for the SH3 domain (Harte et al., 2000), the CCH alone is sufficient to target adhesions sites (Donato et al., 2010).

The targeting mechanism has important implications for the p130Cas mechano-sensing function (Sawada et al., 2006). The model proposed that mechanical extension was mediated by the presence of two adhesion targeting domains, with tension on the adhesion resulting in extension and phosphorylation of the SD through exposure of cryptic tyrosine residues. Rather than SH3 and SBD anchor points as previously proposed (Sawada et al., 2006), the SH3 and CCH domains are likely to anchor p130Cas at the N- and C-termini respectively to facilitate extension (Donato et al., 2010).

FAK is a prominent adhesion protein that interacts with the p130Cas SH3 domain. A yeast-two-hybrid screen looking for FAK interacting proteins independently identified p130Cas (Polte and Hanks, 1995), which binds the FAK proline rich regions, PR1 and PR2 (Polte and Hanks, 1995, Harte et al., 1996, Polte and Hanks, 1997). Using an inducible FAK expression system, FAK was shown to be required for the SH3 domain to target p130Cas to adhesion sites (Donato et al., 2010). Although the p130Cas CCH domain has been hypothesized to take on a conformation similar to the FAK FAT domain

(Arold et al., 2002), unlike FAK, p130Cas does not appear to target through paxillin (Donato et al., 2010). While the CCH has known binding partners, the adhesion targeting protein is not known.

SH3 Domain: additional binding partners

In addition to binding FAK (Polte and Hanks, 1995, Polte and Hanks, 1997), p130Cas also binds the FAK family member PYK2 (Astier et al., 1997) and FRNK (FAK-related non-kinase) (Harte et al., 1996). The p130Cas SH3 domain also binds two phosphatases PTP-1B (Liu et al., 1996) and PTP-PEST (Garton et al., 1997), which have also been implicated in the dephosphorylation of p130Cas (Liu et al., 1996, Garton et al., 1996). In addition to adhesion targeting, through these interactions, the SH3 domain may function as a switch regulating the tyrosine phosphorylation state of p130Cas. The SH3 domain binds the guanine nucleotide exchange factor C3G (Kirsch et al., 1998), forming a possible link between p130Cas and Rap1 (Gotoh et al., 1995) and R-Ras (Gotoh et al., 1997) activation. The SH3 also binds CMS (Cas ligand with multiple SH3 domains) (Kirsch et al., 1999), and the anti-microbial peptide PR-39 (Chan and Gallo, 1998).

Cas-family C-terminal Homology (CCH) Domain: binding partners

While the conservation of the p130Cas C-terminal region has been recognized (Arold et al., 2002, Alexandropoulos et al., 2003), designation of the C-terminal 141 amino acids as a distinct conserved domain called the CCH is relatively recent (Donato et al., 2010). Two NSP (novel Src homology 2-containing protein) family member guanine nucleotide exchange factors (GEFs) interact with the CCH domain, AND-34/BCAR3/NSP2 (Gotoh et al., 2000) and Chat/NSP3/Shep-1 (Sakakibara and Hattori,

2000). AND-34 localizes to the lamellipodium and membrane ruffles (Riggins et al., 2003), while Chat co-localized with p130Cas in actin filaments and membrane ruffles (Sakakibara and Hattori, 2000). A third NSP-family member, NSP1, is known to associate with p130Cas (Lu et al., 1999). It is anticipated that NSP1 also interacts with the p130Cas CCH because of the significant conservation between NSP family members in the interacting GEF domain (Alexandropoulos and Regelmann, 2009), but direct interaction mapping studies have not confirmed this interaction. The CCH also binds Ajuba (Pratt et al., 2005), which is implicated in recruiting p130Cas to the lamellipodium and membrane ruffles, but is not integral for p130Cas localization to adhesions. Ajuba -/- MEFs form adhesions containing p130Cas, but have decreased lamellipodial protrusion (Pratt et al., 2005).

P130Cas Signaling

The p130Cas SD signals by recruiting downstream effectors in response to tyrosine phosphorylation. The SD is characterized by fifteen YxxP motifs, ten of which can be efficiently phosphorylated by Src (Shin et al., 2004). Of these ten motifs, nine are YDxP motifs and thus conform to the optimal binding motif for Crk and Nck adaptors (Songyang and Cantley, 1995), the two best characterized p130Cas SD binding proteins (Sakai et al., 1994, Schlaepfer et al., 1997). Tyrosine phosphorylation of these sites *in vivo* has largely been confirmed through mass spectrometry phospho-proteomics (Rush et al., 2005, Luo et al., 2008). A summary of the p130Cas phosphotyrosine sites detected by mass spectrometry is presented in Table 2.

Table 2. Phosphosite.org summary of p130Cas phosphotyrosines detected by mass spectrometry. Tyrosine residues are numbered according to the human p130Cas protein. LTP is low-throughput, and HTP is high-throughput.

Detection Method		Tyrosine Residue	Peptide Sequence	p130Cas Domain
LTP	HTP			
3	>25	Y128-p	SKAQQGLyQVPGPsP	YxxP #2
4	0	Y165-p	PSPATDLyQVPPGPG	YxxP #3
1	0	Y179	GGPAQDIyQVPPSAG	YxxP #4
1	1	Y192-p	AGMGHDIyQVPPSMD	YxxP #5
1	3	Y222-p	PTRVGQGyVyEAAQP	not YxxP
1	>25	Y224-p	RVGQGyVyEAAQPEQ	not YxxP
2	>25	Y234-p	AQPEQDEyDIPRHLL	YxxP #6
8	>25	Y249-p	APGPQDIyDVPPVRG	YxxP #7
1	>25	Y267-p	SQYGQEVyDtPPMAV	YxxP #8
1	>25	Y287-p	RDPLLEVyDVPPsVE	YxxP #9
3	23	Y306-p	PSNHHAVyDVPPSVS	YxxP #10
3	>25	Y327-p	PLLREEtyDVPPAFA	YxxP #11
1	>25	Y362-p	SPPAEDVyDVPPPAP	YxxP #12
0	>25	Y372-p	PPPAPDLyDVPPGLR	YxxP #13
5	>25	Y387-p	RPGPGtLyDVPRERV	YxxP #14
6	>25	Y410-p	GVVDSGVyAVPPPAE	YxxP #15
5	11	Y664-p	EGGWMEDyDyVHLQG	YDYV SBD
2	8	Y666-p	GWMEDyDyVHLQGKE	YDYV SBD

Although FAK binds p130Cas and recruits it to adhesion sites, FAK shows no tyrosine kinase activity toward p130Cas (Ruest et al., 2001). Rather FAK serves as a scaffold to recruit and activate Src to phosphorylate p130Cas through Src SH2 domain binding to the phosphorylated FAK Y397 (Ruest et al., 2001), see Figure 3. Direct binding of the Src SH3 domain to a proline-rich binding motif in the p130Cas SBD (Burnham et al., 2000, Ruest et al., 2001) also recruits and activates Src to phosphorylate the p130Cas SD, see Figure 3.

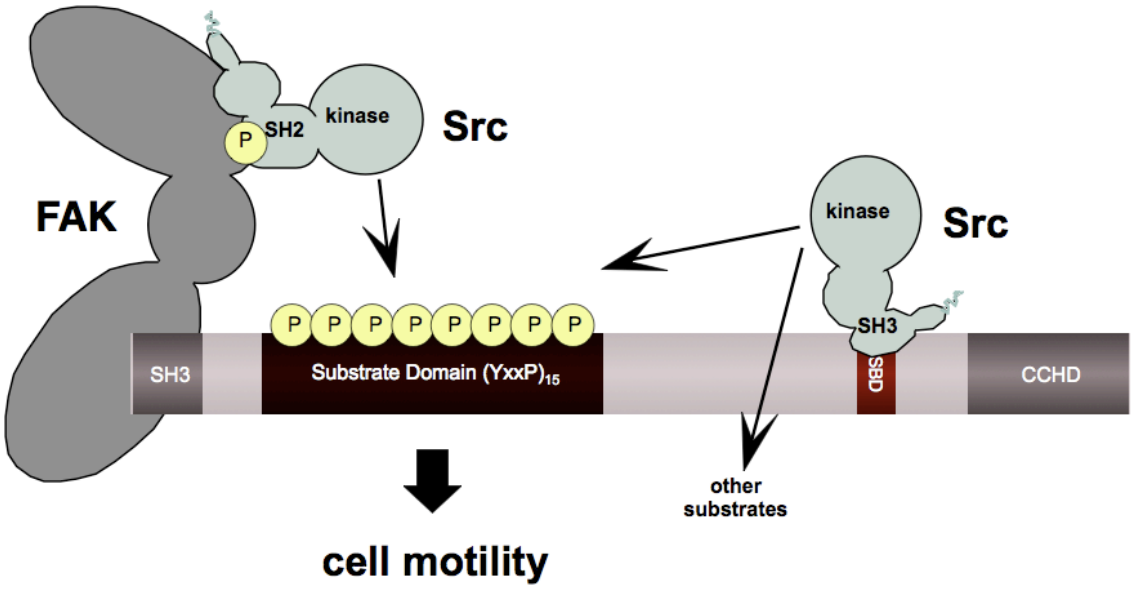

Figure 3. Diagram of the FAK/Src/p130Cas signaling complex. P130Cas interacts with FAK through its N-terminal SH3 domain. FAK autophosphorylates at Y397 and acts as a scaffold to recruit and activate Src by binding the Src SH2 domain. Src is also activated by binding the p130Cas SBD directly with its SH3 domain. Src activated through both of these mechanisms can phosphorylate the p130Cas SD YxxP tyrosines. In addition Src activated by bind the SBD can also phosphorylate other substrates. The phosphorylated Y397 and SD YxxP residues are indicated by yellow circles.

Src can bind both the proline-rich and the YDYV motifs in the SBD, via its SH3 and SH2 domains respectively (Nakamoto et al., 1995). Hirai and colleagues further demonstrated that mutation of the p130Cas proline-motif effectively blocks p130Cas/Src binding while mutation of the YDYV motif only partially blocked p13Cas/Src binding (Nakamoto et al., 1995). Subsequent studies confirmed the primary role of the proline-rich motif for p130Cas/Src binding, but found that mutation of the SH2 domain had no effect on p130Cas/Src binding (Burnham et al., 1999). This is consistent with data demonstrating disruption of the proline-motif, but not the YDYV motif significantly reduces SD phosphorylation (Fonseca et al., 2004, Brabek et al., 2005). *In vitro* studies with purified components also demonstrated that only the proline-rich motif in the SBD was required to release Src autoinhibitory interactions and facilitate processive phosphorylation of the SD (Pellicena and Miller, 2001). As mentioned above, the ability of Src to phosphorylate the SD is enhanced by physical extension of the SD, implicating p130Cas as a mechanosensor (Sawada et al., 2006). P130Cas SD phosphorylation has been detected predominantly at FAs and at the cell periphery in nascent integrin adhesion sites (Fonseca et al., 2004, Ballestrem et al., 2006).

After activation by tyrosine phosphorylation, the SD is able to recruit downstream effectors, notably the SH2/SH3 adaptors Crk and Nck that can act to promote protrusion of the plasma membrane (Chodniewicz and Klemke, 2004, Rivera et al., 2006). While the recruitment and activation of Src to phosphorylate the SD is the best-characterized signaling function of the SBD, Src activated by binding to the SBD has the potential to phosphorylate other proteins (Burnham et al., 2000), which could represent a distinct signaling function of the SBD.

Substrate Domain (SD): binding partners

As mentioned above, the SH2-SH3 adapter proteins Crk and Nck are major p130Cas binding partners that interact with SD phosphotyrosine motifs via their SH2 domains (Sakai et al., 1994, Schlaepfer et al., 1997). Both adapters are known to promote downstream signaling and have been implicated in cell motility and invasion (Feller, 2001, Buday et al., 2002). The SH2 domain of SHIP-2 (Src-homology 2 containing inositol phosphatase-2) also binds the phosphorylated SD and is regulated by adhesion (Prasad et al., 2001). Finally another SH2-SH3 adapter, Grb2 binds p130Cas in phospho-tyrosine dependent manner (Wang et al., 2000).

Src-binding Domain (SBD): additional binding partners

The SBD consists of two motifs, a Class I PxxP proline-rich motif (RPLPSPP) and an SH2-binding motif (YDYV) (Nakamoto et al., 1995) and interacts with Src family kinases (Src, SFKs) (Nakamoto et al., 1995, Nakamoto et al., 1997). The SBD proline motif has two additional known SH3-mediated binding partners Nephrocystin which interacts and colocalizes with p130Cas at cell-cell junctions in epithelial kidney cells (Donaldson et al., 2000), and PI3K which mediates adenovirus entry into cells (Li et al., 2000).

Serine-rich Domain (SER): structure, phosphorylation, and binding partners

In addition to tyrosine phosphorylation, p130Cas is serine-phosphorylated (Schlaepfer et al., 1997), but significantly less is known about the function of the SER domain in p130Cas. NMR spectroscopy studies revealed that the SER domain folds into a four helix bundle similar to the FAK FAT domain, but an invariant patch of residues

near the C-terminus of the bundle may represent a novel protein interaction domain (Briknarova et al., 2005). Significant serine phosphorylation of p130Cas was detected 3 hours after replating on fibronectin (Schlaepfer et al., 1997). Interaction of Band 14-3-3 with p130Cas is dependent on this integrin-mediated serine phosphorylation (Garcia-Guzman et al., 1999). Interestingly, p130Cas, FAK and paxillin are serine phosphorylated during mitosis, and correlates with concomitant tyrosine dephosphorylation and disruption of the FAK/Src/p130Cas signaling module (Yamakita et al., 1999).

More recently, a role for AND-34/BCAR3/NSP2 was shown in regulating serine phosphorylation of p130Cas and in the induction of anti-estrogen resistance in human breast cancer cell lines (Makkinje et al., 2009). Over-expression of AND-34, a known interacting partner of CCH domain (Gotoh et al., 2000), induces p130Cas serine phosphorylation and anti-estrogen resistance in breast cancer cell lines through an actin- and adhesion-dependent process (Makkinje et al., 2009). Conversely, knockdown of AND-34 in mesenchymal breast cancer cells decreases levels of phosphorylated p130Cas and cells reverted to a more epithelial-like morphology (Makkinje et al., 2009). These functions depend on the proline-rich domain of AND-34 (Makkinje et al., 2009), not the domain that interacts with p130Cas. The kinase responsible for the enhanced serine phosphorylation of p130Cas has not been identified.

Functional roles for p130Cas signaling

Owing to its role as a docking protein, p130Cas has a role in regulating numerous signaling pathways including migration, cancer progression and metastasis, and bacterial pathogenesis, reviewed in (Bouton et al., 2001, Defilippi et al., 2006, Tikhmyanova et al.,

2010a). The main signaling function of p130Cas is to undergo tyrosine phosphorylation of the substrate domain, described in the previous section. The SD is phosphorylated in response to numerous stimuli including integrin engagement, growth factor stimulation, antigen stimulation, neuropeptides, glucose stimulation in β cells, and uPAR (Nojima et al., 1995, Petch et al., 1995, Vuori and Ruoslahti, 1995, Casamassima and Rozengurt, 1997, Casamassima and Rozengurt, 1998, Petruzzelli et al., 1996, Rozengurt, 1998, Lee et al., 2004, Smith et al., 2008). P130Cas /Crk coupling (Chodniewicz and Klemke, 2004) is the central step in many p130Cas signaling pathways.

Cell Motility

Regulation of cell migration is the best described cellular function of p130Cas. Early studies demonstrated a role for p130Cas in cell migration (Cary et al., 1998, Honda et al., 1999). Subsequent work demonstrated that all of the main p130Cas signaling domains (SH3, SD, SBD, and CCH) are required for efficient p130Cas signaling and migration (Huang et al., 2002, Shin et al., 2004, Donato et al., 2010). P130Cas adhesion localization via the SH3 and CCH domains is required for activation (Donato et al., 2010). The SBD is involved in Src binding and is required for p130Cas SD tyrosine phosphorylation (Burnham et al., 1999), and the SD is required for p130Cas/Crk and p130Cas/Nck coupling and subsequent activation of Rac1 (Chodniewicz and Klemke, 2004, Rivera et al., 2006). Purification of leading edge pseudopodia connects p130Cas/Crk coupling with Rac1 activation specifically at the leading edge (Cho and Klemke, 2002). P130Cas is also implicated in regulating adhesion disassembly (Webb et al., 2004), which is required for efficient migration.

Cancer

Since its discovery in cells transformed by oncogene produces, *v-Src* and *v-Crk* (Mayer et al., 1988, Reynolds et al., 1989, Matsuda et al., 1990), p130Cas has been implicated in cancer signaling. P130Cas expression and/or tyrosine phosphorylation is elevated in numerous cancers and this dysregulated signaling contributes to increased migration, invasion, cell survival, and drug resistance (Tikhmyanova et al., 2010a). Studies in Src-transformed fibroblasts clearly implicate p130Cas SD signaling in driving migration and formation of invasive adhesive structures *in vitro*, and in promoting metastasis *in vivo* (Brabek et al., 2005). Furthermore, p130Cas/Crk coupling leading to Rac1 activation has been implicated in membrane protrusion, invasion, and survival (Chodniewicz and Klemke, 2004).

Particular attention has been placed on the role of p130Cas in breast cancer where high levels of p130Cas in patients are associated with a poor response to tamoxifen treatment, early recurrence, and lower rates of long-term survival (van der Flier et al., 2000, Dorssers et al., 2001). Knowledge of tissue-specific p130Cas signaling is limited due to the embryonic lethality of the p130Cas knockout mice. However, transgenic studies in mice over-expressing p130Cas in the mammary gland show epithelial hyperplasia, and double transgenic mice, expressing p130Cas in combination with HER2-Neu, have shorter tumor latency (Cabodi et al., 2006).

The human gene BCAR1 (breast cancer anti-estrogen resistance 1) that encodes p130Cas was independently identified in a screen for genes that conferred resistance to anti-estrogen drugs (e.g. tamoxifen) in breast cancer cells (Brinkman et al., 2000). Breast cancers are often classified as estrogen-receptor positive (ER+) and thus sensitive to

tamoxifen therapy, or estrogen-receptor negative (ER-) and resistant to tamoxifen therapy. However, patients that are initially susceptible to tamoxifen treatment often develop resistance. P130Cas-mediated tamoxifen resistance is apparently independent of the normal ER-mediated gene transcription profile (Dorssers et al., 2005), and has instead been linked to several Src-mediated proliferation and survival pathways (Defilippi et al., 2006, Tikhmyanova et al., 2010a). P130Cas/Src complexes can interact with the ER to stimulate ERK activation of cyclin D1 (Cabodi et al., 2004, Cabodi et al., 2006), or can act independently through an EGFR/STAT5b pathway (Riggins et al., 2006). In addition, p130Cas tamoxifen resistance has been implicated in an adhesion-dependent survival pathway through PI3K/Akt (Cowell et al., 2006).

Finally, in addition to conferring tamoxifen resistance in ER+ breast cancer cells, p130Cas expression levels are elevated in ER- breast cancer cell lines where p130Cas signaling promotes enhanced migration, invasion, and survival (Cunningham-Edmondson and Hanks, 2009).

Development

P130Cas is the most ubiquitously expressed Cas family member (Sakai et al., 1994). Other Cas family members are not able to compensate for p130Cas deficiency, resulting in embryonic lethality (Honda et al., 1998). Mice deficient in p130Cas die *in utero* at E12.5 having retarded growth and heart defects (Honda et al., 1998).

In *Drosophila*, deletion of the p130Cas homolog had a limited effect on development, but showed genetic interactions with *Drosophila* homologs of integrins, FAK, Src, and E-cadherin (Tikhmyanova et al., 2010b). In particular, the *DCas/FAK56D* double mutant (corresponding to p130Cas/FAK) was embryonic lethal with widespread

polarity defects, and reduced expression and mislocalizaton of E-cadherin (Tikhmyanova et al., 2010b). These studies implicate a role for p130Cas in regulating cell-cell adhesion signaling in development.

P130Cas signaling in the Heart and Vasculature

Mice deficient in p130Cas have poorly developed hearts with a thin myocardium and dilated blood vessels (Honda et al., 1998). Electron microscopy revealed disorganized myofibrils and disrupted Z-disks in the heart (Honda et al., 1998). FAK and p130Cas were subsequently shown to localize to Z-disks where they organize the sarcomere and cytoskeleton, and are required for the gene expression pattern associated with myocyte hypertrophy (Kovacic-Milivojevic et al., 2001, Kovacic-Milivojevic et al., 2002). P130Cas is also a key regulator of vascular smooth muscle cells with a role in regulating not only hypertrophy, but also contractility, migration, and growth, reviewed in (Tang, 2009).

P130Cas signaling in the Brain

In addition to heart defects, p130Cas deficient mice show overall growth retardation including smaller brains (Honda et al., 1998). P130Cas is expressed in the brain in both the embryo and postnatally, and is particularly high in the cerebellum (Huang et al., 2006). In individual cerebellar granule cells, p130Cas is highly tyrosine phosphorylated, concentrated in neurite growth cones, and the SD is required for axonal extension (Huang et al., 2006). The *Drosophila* p130Cas homolog, *DmCas*, was also shown to function in integrin-dependent growth cone guidance during development (Huang et al., 2007), indicating a conserved role in neuronal signaling for p130Cas.

Bacterial pathogenesis

Consistent with its role in regulating adhesion and the cytoskeleton, p130Cas has been implicated in the pathogenesis of several bacteria. In order to avoid phagocytosis, *Yersinia pseuotuberculosis* uses the phosphatase YopH to dephosphorylate p130Cas and block Rac activation, and the actin reorganization required for endocytosis (Viboud and Bliska, 2005, Weidow et al., 2000, Black and Bliska, 1997, Persson et al., 1997, Hamid et al., 1999).

Rationale of the current study and presentation of the hypothesis

P130Cas has been implicated in regulating two cellular processes essential to motility: protrusion of the leading edge and FA disassembly. Recruitment of Crk and Nck to the tyrosine-phosphorylated p130Cas SD is implicated in promoting protrusion (Klemke et al., 1998, Cho and Klemke, 2002, Rivera et al., 2006), although direct quantitative measurements of leading edge actin dynamics stimulated by SD tyrosine phosphorylation are still lacking. A study evaluating the turnover of adhesion components in randomly migrating cells implicated p130Cas in regulating FA disassembly, with the apparent rate constant for FA disassembly ~19-fold lower in Cas -/- MEFs as compared to cells expressing wild type (WT) p130Cas (Webb et al., 2004). No studies have addressed the mechanism by which p130Cas promotes FA disassembly.

Here, we utilized Cas -/- MEFs expressing p130Cas signaling variants and live cell imaging to carry out a detailed investigation of the roles of the p130Cas signaling domains in mediating cell migration and the key physical steps of leading edge actin dynamics and FA assembly/disassembly. Our results show that p130Cas SD tyrosine

phosphorylation sites are required to stimulate leading edge actin assembly and plasma membrane protrusion and to enhance the rates of both FA assembly and disassembly. Furthermore, we show that the SD and SBD make distinct additive contributions to ensure that FA disassembly proceeds without interruption.

CHAPTER II

THE ROLE OF P130CAS SIGNALING IN MIGRATION AND LEADING EDGE ACTIN DYNAMICS

Introduction

P130Cas has been implicated in regulating the dynamics of two structures essential to cell migration: the lamellipodium and adhesion sites. Understanding how p130Cas regulates cell migration and the potential contribution of individual signaling domains requires a detailed analysis of these structures. Previous studies have implicated the p130Cas/Crk/Rac1 pathway in driving not only migration, but also leading edge protrusion. However, no quantitative measurements of protrusion rate or actin dynamics downstream of p130Cas have been made. To determine the contributions of the p130Cas SD and SBD signaling to these processes, I used live-cell imaging techniques to quantify migration rates and the rates of cytoskeleton dynamics in the presence of either wild type p130Cas protein or signaling variants. The data support distinct roles for the p130Cas SD and SBD in cell migration, but a cooperative role in driving protrusion and leading edge actin dynamics.

Materials and Methods

Cells and cell culture

Cas -/- and Cas +/+ MEFs (Honda et al., 1998) were kindly provided by Hisamaru Hirai (University of Tokyo). MEFs were maintained in Dulbecco's Modified Eagle's Medium (Mediatech, Manassas, VA) supplemented with 10% fetal bovine serum (Atlanta Biologicals, Lawrenceville, GA), 1% antibiotic/antimicotic (Mediatech, Manassas, VA), and 1% non-essential amino acids (Invitrogen, Carlsbad, CA). The retroviral packaging cell line Phoenix Ectotropic (E) kindly provided by Gary Nolan (Stanford University), was maintained as previously described (Brabek et al., 2004).

Plasmids and protein expression

The LZRS-MS-IRES-GFP retroviral vector (Ireton et al., 2002) was used to express p130Cas variants in conjunction with cytoplasmic GFP from a bicistronic transcript. The cell populations used for these studies were obtained by three sequential rounds of viral infection of Cas -/- MEFs followed by one round of fluorescence-activated cell sorting (FACS) to select cells with low levels of GFP expression. P130Cas wild type (WT) and mutational variants 15F, mPR, and 15F/mPR were expressed in Cas -/- MEFs. The expression constructs for p130Cas WT and 15F (Shin et al., 2004) and mPR (Fonseca et al., 2004) have been previously described. The 15F/mPR variant was generated for this study using standard molecular biology techniques. All p130Cas variants were verified by sequencing.

The mCherry-Actin plasmid was used for transient expression. Actin was subcloned from Clontech pEGFP-actin using NheI and BglII restriction sites into the

mCherry-C1 plasmid (provided by Maria Nemethova, Vienna, Austria). The resulting product is expressed with an N-terminal mCherry tag. Cells were transfected for transient expression using Lipofectamine 2000 (Invitrogen, Carlsbad, CA).

Antibodies

Monoclonal antibody against total p130Cas (CAS-TL) was obtained from BD Transduction Laboratories (San Jose, CA). Mouse monoclonal antibody against actin was obtained from Sigma (St. Louis, MO). The polyclonal phosphospecific pCas antibodies raised against p130Cas SD tyrosines 165, 249, and 410 were from Cell Signaling Technology (Beverly, MA). Horseradish peroxidase conjugated goat-anti-mouse IgG and goat-anti-rabbit secondary antibodies were obtained from Jackson ImmunoResearch Laboratories, Inc. (West Grove, PA).

Immunoprecipitation

Subconfluent cell cultures were washed with PBS and lysed in 1% SDS boiling buffer; NP-40 buffer (50 mM This-Cl, pH 7.4, 150 mM NaCl, 5 mM EDTA, 50 mM NaF, 1% Nonidet P-40, 1 µg/ml Aprotinin, 100 µM Leupeptin, 1 mM Benzamidine, 100 µM sodium orthovanadate, 50 µg/ml PMSF) plus 1% SDS. Samples were heated to 100˚C for 5 minutes, then diluted with NP-40 buffer to 0.1% SDS. For immunoprecipitation, 1000 µg of total protein in 800 µl of lysis buffer was incubated with 2 µg CAS-TL antibody, and protein was recovered on protein G-Sepharose 4B (Sigma-Aldrich, St Louis, MO). Immunoprecipitates were then immunoblotted as described.

Immunoblotting

Subconfluent cell cultures were washed with phosphate buffered saline (PBS) and lysed in modified RIPA buffer (Brabek et al., 2004). Whole cell lysates were separated on 7% SDS-polyacrylamide gels and transferred onto nitrocellulose membrane. Nonspecific activity was blocked by incubating 1 hour at room temperature in Tris-buffered saline (TBS) containing 3% nonfat dry milk. Membranes were incubated overnight at 4˚C in primary antibody, washed extensively with TBS-T (0.05% Tween-20), and then incubated 1 hour at room temperature with secondary antibody. Immunoblots were visualized by enhanced chemiluminescence.

Wound healing migration assay

Cells were grown to confluence on glass coverslips coated with 1 µg/ml fibronectin (from human plasma, Sigma-Aldrich, St Louis, MO or Calbiochem, San Diego, CA). A pipette tip was used to make a scratch wound, then the cells were transferred to media supplemented with 10 mM HEPES (Mediatech, Manassas, VA) and mounted in a heated chamber (Warner Instruments, Hamden, CT) to maintain cells at 37˚C. Cells migrating into the denuded area were visualized on a Nikon Eclipse TE2000-E2 inverted microscope equipped with a Perfect Focus System using a 20x Plan Apo DIC objective lens. Using IPlab software (Scanalytics, Fairfax, VA), frames were captured on a CoolSnapHQ camera (Photometrics, Tucson, AZ) every five minutes for 8 hours. To determine total migration distance for each cell population, nuclei of seventy-five cells (25 each from three independent experiments) migrating at the wound edge were tracked using the ImageJ (National Institutes of Health, Bethesda, MD) Manual Tracking plugin. The mean velocity (microns/hour) was calculated for each cell population over six hours

(two to eight hours post wounding). Any cells that divided during the movie were excluded from the analysis.

Cell spreading assay

Subconfluent cells were plated onto coverslips coated with 1 µg/ml fibronectin and immediately mounted in a heated chamber (Warner Instruments, Hamden, CT) to maintain cells at 37˚C and imaged as they attached and spread. Images were captured every 5 minutes for 2 hours using a 20x Plan Apo DIC objective lens. Cells were scored as having initiated spreading after obvious protrusions had emanated from the cell periphery. Cells that divided during the analysis were not scored. Cells that attached, but neither initiated spreading nor divided during the 2-hour period were scored as DNS (did not spread). Spread cell area was quantified by analyzing cells that fully spread, and then measuring the cell area at 2-hours after plating. Cells that were still rounded or had just initiated spreading were not included in the cell area analysis.

Leading edge DIC kymography

Cells were prepared as in the wound healing migration assay and DIC images were captured using a 60x Plan Apo 1.4 NA oil-immersion DIC objective lens. Frames were captured every 3 seconds for 15 minutes starting at an average of 4.6 hours (s.d. +/- 0.5 hours) post wounding for all cells. Three kymographs were generated for each cell. The time and distance of all protrusions that were parallel to the line of analysis during the 15-minute period were used to calculate the mean protrusion velocity. The total protrusion distance and time for all three kymographs were summed to generate a mean

protrusion velocity for each cell. 60-90 cells (15 each from 4-6 separate wound assays) were analyzed for each cell type.

Live cell fluorescence imaging and photobleaching

Cells were transiently transfected with mCherry-C1-actin using Lipofectamine 2000, then grown to confluence (48 hours) on 1 μg/ml fibronectin-coated coverslips. Wounds were generated and cells mounted as in the wound healing migration assay. Cells migrating at the wound edge and expressing a low, but detectable level of fluorescently-tagged Actin were selected for imaging. Cells expressing mCherry-tagged protein were visualized using a Pinkel triple filter set (Semrock, Rochester, NY) and a TIRF 100x 1.49 NA oil-immersion lens. Images were captured on a back-illuminated EM-CCD camera, Cascade 512B (Photometrics).

Photobleaching of leading edge mCherry-actin was achieved using a 10 mW DPSS laser 85YCA010 (Melles Griot, Albuquerque, NM) and a custom-made lens (Nikon) in the position of the filter cube to focus the laser in the focal plane. A pre-bleach image was captured, the leading edge actin was photobleached for 15 seconds, then images were captured every second for 60-90 seconds. Cells expressing mCherry-actin were imaged at an average of 5.1 hours post wounding (s.d. +/- 0.9 hours) for all cells.

Leading edge wide field fluorescence kymography

Actin dynamics were quantified from mCherry-actin kymographs (see Figure 9A, right column). A photobleached region of mCherry-actin at the leading edge was used as a reference point (similar to (Wang, 1985, Lai et al., 2008)). All three rates were

calculated over the same time period immediately after photobleaching. The rate of leading edge protrusion was determined by tracking the forward movement of the newly incorporated fluorescent actin. The rate of retrograde flow was determined by tracking the rearward movement of the sharp boundary of newly incorporated fluorescent actin after bleaching (Wang, 1985, Lai et al., 2008). The rate of actin assembly was calculated as the sum of the absolute values of the retrograde flow and leading edge protrusion rates. The calculation is illustrated in a schematic in Figure 9C.

Statistical analysis

To compare the means of the numerous groups, one-way analysis of variance (ANOVA) followed by the Tukey-Kramer post hoc test was used to determine significance for pair-wise comparisons of all samples. Values were considered not significant (n.s.) when $p \geq 0.05$. Significance levels are indicated as: $*p < 0.05$, $**p < 0.01$, $***p<0.001$.

Results

P130Cas SD and SBD signaling domains have distinct roles in stimulating cell migration

Cas -/- MEFs stably expressing WT p130Cas versus mutational variants (Figure 4) were generated in order to evaluate the contribution of p130Cas signaling domains to cell migration. Three p130Cas mutants were expressed: an SD mutant (15F) in which all fifteen YxxP motif tyrosines were changed to phenylalanines, an SBD mutant (mPR) in

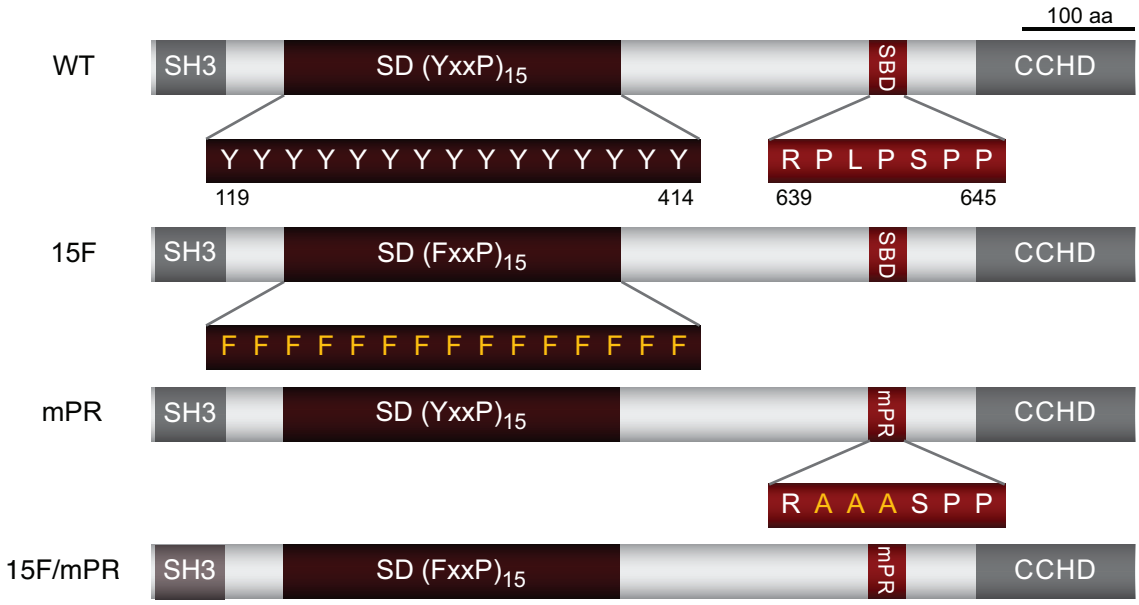

Figure 4. Diagram of the p130Cas signaling variants used in this study. Diagram indicates the SH3 domain, substrate domain (SD), Src-binding domain (SBD), and C-terminal Cas-family Homology (CCH) Domain. Shown in addition to p130Cas WT are three full-length signaling variants with amino acid substitutions indicated; 15F, all fifteen YxxP tyrosines in the SD changed to phenylalanine; mPR, proline-rich motif RPLPSPP in the SBD mutated to RAAASPP; and 15F/mPR double mutant.

which prolines in the SH3-binding motif are changed to alanines, and a double mutant (15F/mPR) in which both the SD and SBD are changed. All p130Cas variants were stably expressed in Cas -/- MEFs using a bicistronic retroviral vector that co-expresses GFP. Empty vector cells, which express only GFP, were also prepared as a control. Sorting the cells for low GFP levels yielded populations where the p130Cas variants were expressed to levels similar to endogenous p130Cas in Cas +/+ MEFs (Figure 5A). Moreover, all expressed variants gave rise to the electrophoretic mobility isoforms characteristic of p130Cas and the expected SD tyrosine phosphorylation pattern (Figure 5B). p130Cas WT cells have robust SD tyrosine phosphorylation similar to Cas +/+ cells, mPR cells have a reduced but detectable level of SD tyrosine phosphorylation, and no SD tyrosine phosphorylation is detected in Vector, 15F, and 15F/mPR cells as expected due to the absence p130Cas protein or SD phosphoacceptor tyrosines.

These cell populations (WT, 15F, mPR, 15F/mPR, and Vector) were employed to determine the contributions of the two p130Cas signaling domains to cell migration. A monolayer scratch wound assay was used to stimulate migration, and then cells migrating into the wound were imaged over 8 hours using differential interference contrast (DIC) microscopy. Figure 6A shows representative wound edges at 2, 5, and 8 hours post wounding. Tracking the movement of individual cell nuclei over the 2-8 hour period showed that WT cells migrated into the wound at a mean rate significantly faster (1.9 fold) than Vector control cells (Figure 6B). The 15F and mPR cells migrated at an intermediate rate, but still significantly faster than Vector cells (1.4 and 1.6 fold, respectively). Only the 15F/mPR cells failed to migrate into the wound faster than the Vector cells. This additive defect indicates that the SBD plays a role in driving cell

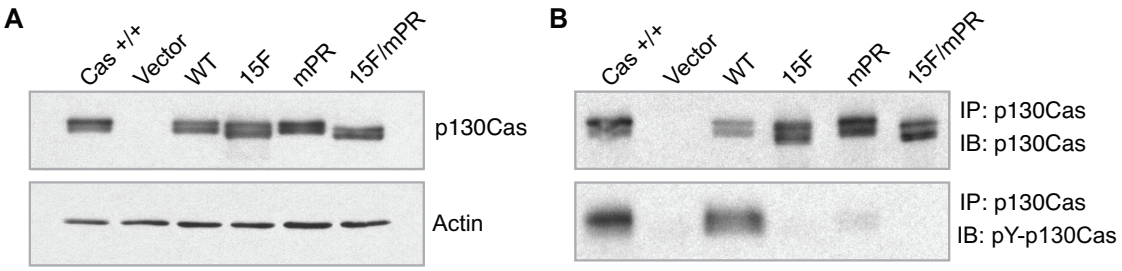

Figure 5. Expression and signaling of p130Cas variants in Cas -/- MEFs. (A) Immunoblot analysis of whole cell lysates of Cas-/- MEFs reconstituted with p130Cas variants. Cas +/+ MEFs were included as a control. Equal amounts of total protein were loaded, 15 µg per lane. WT, 15F, mPR, and 15F/mPR variants are expressed at levels similar to endogenous p130Cas in Cas +/+ MEFs. Actin immunoblot is included as a loading control. (B) Analysis of p130Cas SD tyrosine phosphorylation. Immunoprecipitates (IP) of p130Cas variants were prepared and assessed by immunoblotting (IB). Cas +/+ MEFs were included as a control. Near equal amounts of p130Cas total protein were loaded for each sample and assessed using the same antibody used for immunoprecipitation, top panel. SD tyrosine phosphorlation (SD-pY) was assessed from the same immunoprecipitates using a mixture of phosphospecific antibodies that recognize SD YxxP sites, lower panel.

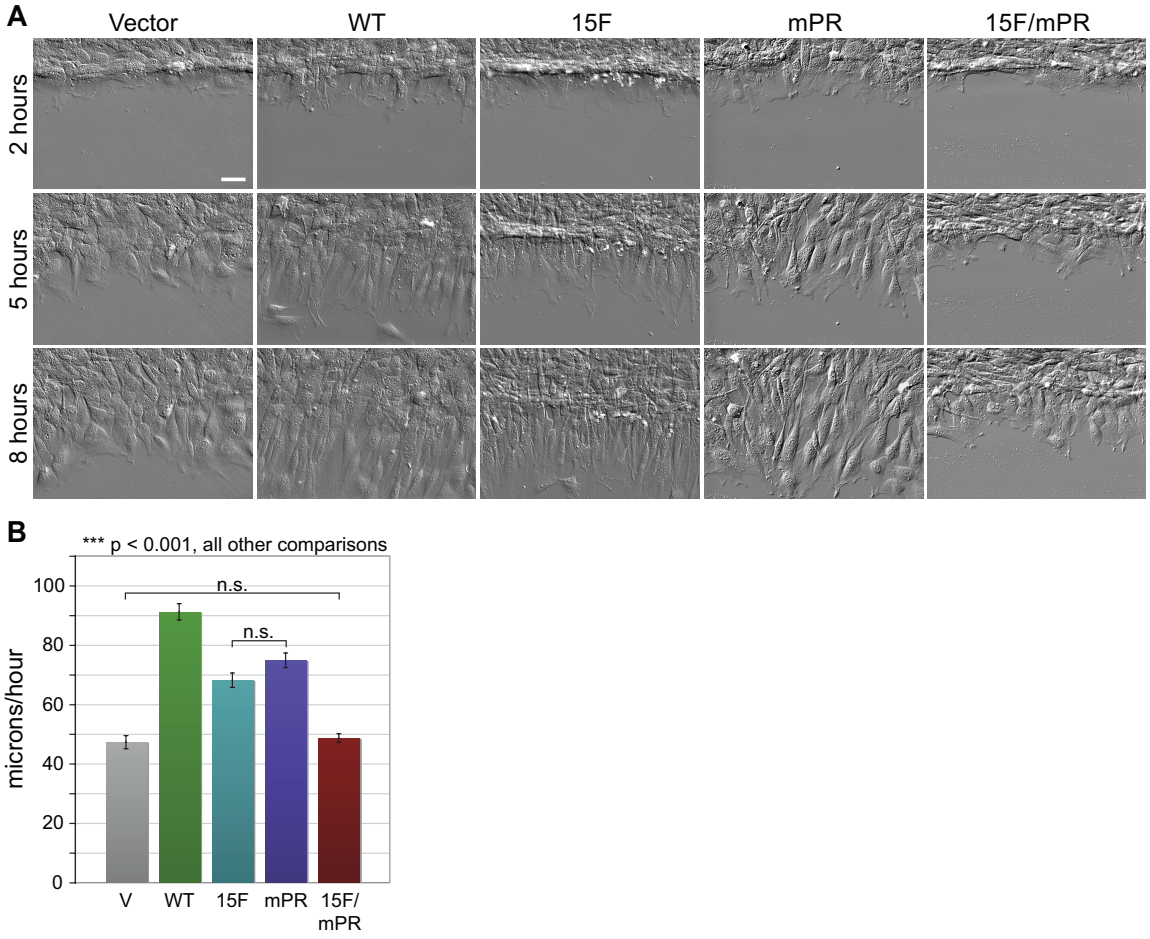

Figure 6. p130Cas SD and SBD signaling stimulate wound healing migration. Monolayer scratch wounds were generated and cells were imaged over 8 hours by live DIC microscopy. (A) Representative images of cells expressing either p130Cas WT, 15F, mPR, or 15F/mPR variants at 2, 5, and 8 hours post wounding. Vector only control cells are also shown. Scale bar is 50 µm. (B) Migration rates were quantified by tracking nuclei of 75 individual cells (25 each from 3 separate wounds) for each cell type. Mean migration rate was calculated as the total distance traveled over the 2 to 8 hour period after wounding. Bars indicate s.e.m. Significance values were determined by one-way ANOVA followed by Tukey-Kramer post hoc testing; n.s. (not significant), ***p < 0.001.

migration that is distinct from its ability to promote SD tyrosine phosphorylation. I also evaluated individual cells in a replating assay in order to determine if p130Cas SD and SBD signaling facilitated cell spreading. These studies indicated that both p130Cas SD and SBD signaling facilitate the initiation of cell spreading, but do not have obvious effects in the final spread cell area (Figure 7). Thus, in addition to promoting cell migration, both p130Cas SD and SBD signaling are implicated in regulating cell adhesion. To gain a better understanding of how the p130Cas signaling domains promote cell migration and adhesion I analyzed the component steps of actin-driven leading edge protrusion and FA dynamics.

P130Cas SBD-mediated SD signaling is implicated in promoting actin flux at the leading edge lamellipodium

I evaluated how p130Cas signaling impacts plasma membrane protrusion and actin flux at the leading edge of cells migrating at a wound edge using kymography of high temporal resolution DIC images. Figure 8A shows representative kymographs. Quantitative analysis indicated that cells expressing WT p130Cas have increased protrusion velocities relative to Vector cells and to all three p130Cas signaling variants (Figure 8B). Thus, mutation of the SD is sufficient to reduce the protrusion rate to the levels seen in Vector cells. Since mutation of the SBD also results in impaired SD tyrosine phosphorylation (Figure 5B) (Fonseca et al., 2004, Ruest et al., 2001), the finding that 15F and mPR cells have similar protrusion rates implicates the primary role of the SBD in protrusion as mediating SD tyrosine phosphorylation.

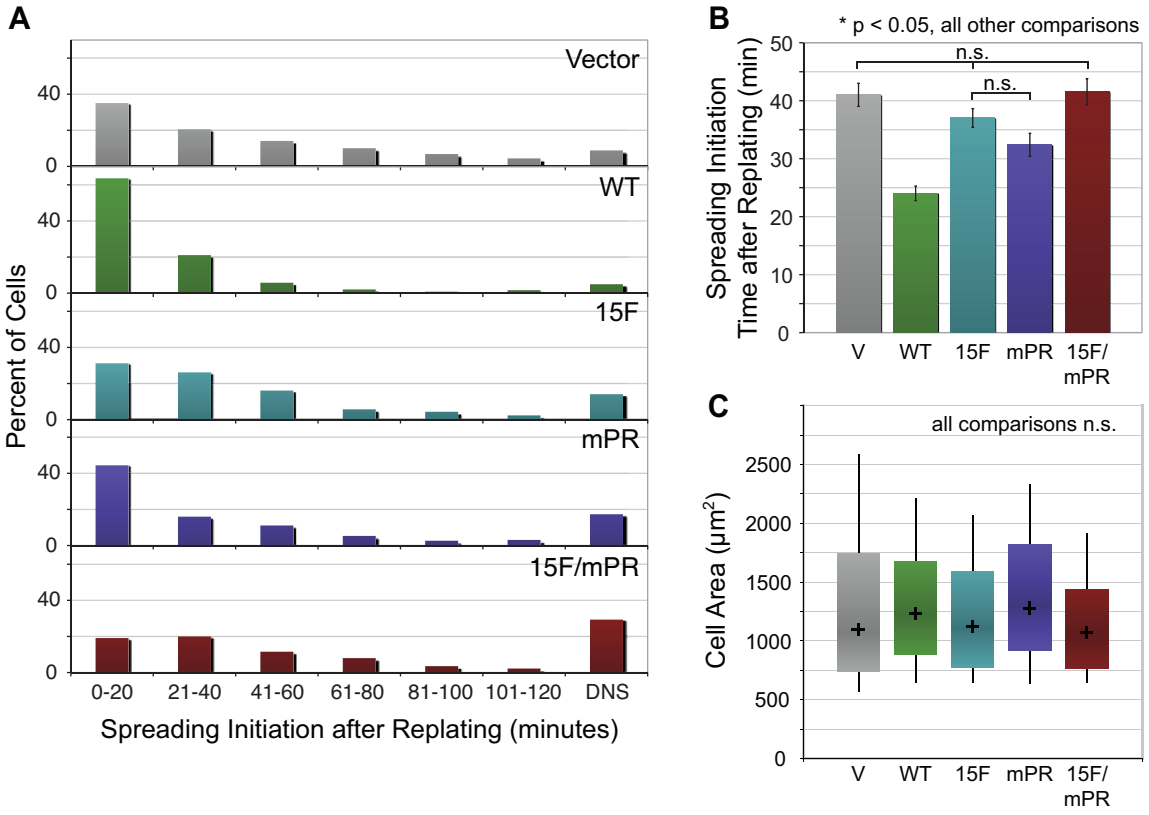

Figure 7. p130Cas SD and SBD signaling facilitate the initiation of cell spreading but have no effect on the final spread cell area. Cells were plated onto glass coverslips coated with 1 μg/ml fibronectin and imaged for 2 hours by live DIC microscopy as they attached and spread. (A) Histogram distributions of the time at which cells initiated spreading after replating, and the number of cells that did not spread (DNS) at the 2-hour time point. A total of 211-298 cells for each cell type from 3 separate replating assays were analyzed. Cells that divided during the two-hour period were excluded from the analysis. (B) The mean time of spreading initiation was quantified from the cells that spread within the first two hours. Data shown represent the mean spreading initiation times determined from 145-256 cells for each cell type. Bars indicate s.e.m. (C) Box and whisker plots of spread cell area for cells that were fully spread at two hours after replating. The area of 74-93 cells for each cell type from 3 separate replating assays was measured. The (+) indicates the median, the bottom and top of the box indicate the 25th and 75th percentiles, and the lower and upper whiskers indicate the 10th and 90th percentiles. Significance values were determined by one-way ANOVA followed by Tukey-Kramer post hoc testing; n.s. (not significant), *$p < 0.05$.

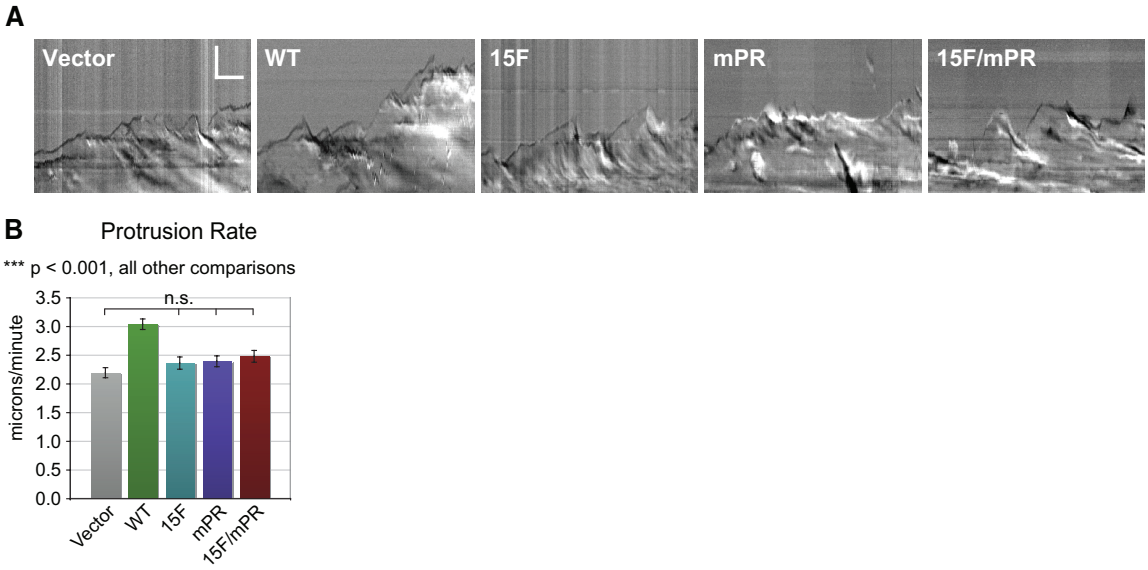

Figure 8. p130Cas SD signaling stimulates leading edge protrusion. Monolayer scratch wounds were generated and DIC images of cells migrating at the wound edge were captured every 3 seconds for 15 minutes and used to evaluate leading edge dynamics using kymography. (A) Sample kymographs representative of mean protrusion values. Vertical scale bar is 5 μm, horizontal scale bar is 2 minutes. (B) Rates of protrusion representing the mean of 60-90 individual cells for each cell type. Leading edge protrusion velocity was quantified by measuring the distance and duration of individual protrusions from 3 kymographs per cell. Bars indicate s.e.m. Significance values were determined by one-way ANOVA followed by Tukey-Kramer post hoc testing; n.s. (not significant), ***$p < 0.001$.

To further study the impact of p130Cas SD signaling on leading edge protrusion, Vector, WT, and 15F cells were transiently transfected to express mCherry-actin and photobleaching of the fluorophore was used to assess actin dynamics. Cells migrating at the wound edge and expressing low levels of mCherry-actin were selected, then a region of the leading edge lamellipodium with active protrusion was bleached to create a reference mark. A kymograph through the bleach region was used to measure actin protrusion velocity and retrograde flow rate, and these values were used to calculate the actin assembly rate (Figure 9A shows representative examples and Figure 9C shows a schematic of the rate calculation). Cells expressing WT p130Cas display higher values for all three rates in comparison to Vector cells (Figure 9B). The cells expressing the p130Cas 15F mutant have protrusion, retrograde flow, and actin assembly rates similar to those in Vector cells. The failure of the 15F mutant to stimulate actin flux implicates SD tyrosine phosphorylation as the primary mechanism by which p130Cas promotes actin assembly at the leading edge. Note that the protrusion rate values shown in Figure 8B are somewhat lower than those shown in Figure 9B, which is due to the fact that only a subpopulation of actively protruding cells were selected for bleaching in the latter analysis.

Discussion

I used live cell imaging techniques to investigate the extent to which p130Cas signaling domains contribute to the dynamic membrane protrusion events that drive cell motility. These properties were examined in a monolayer wound healing response,

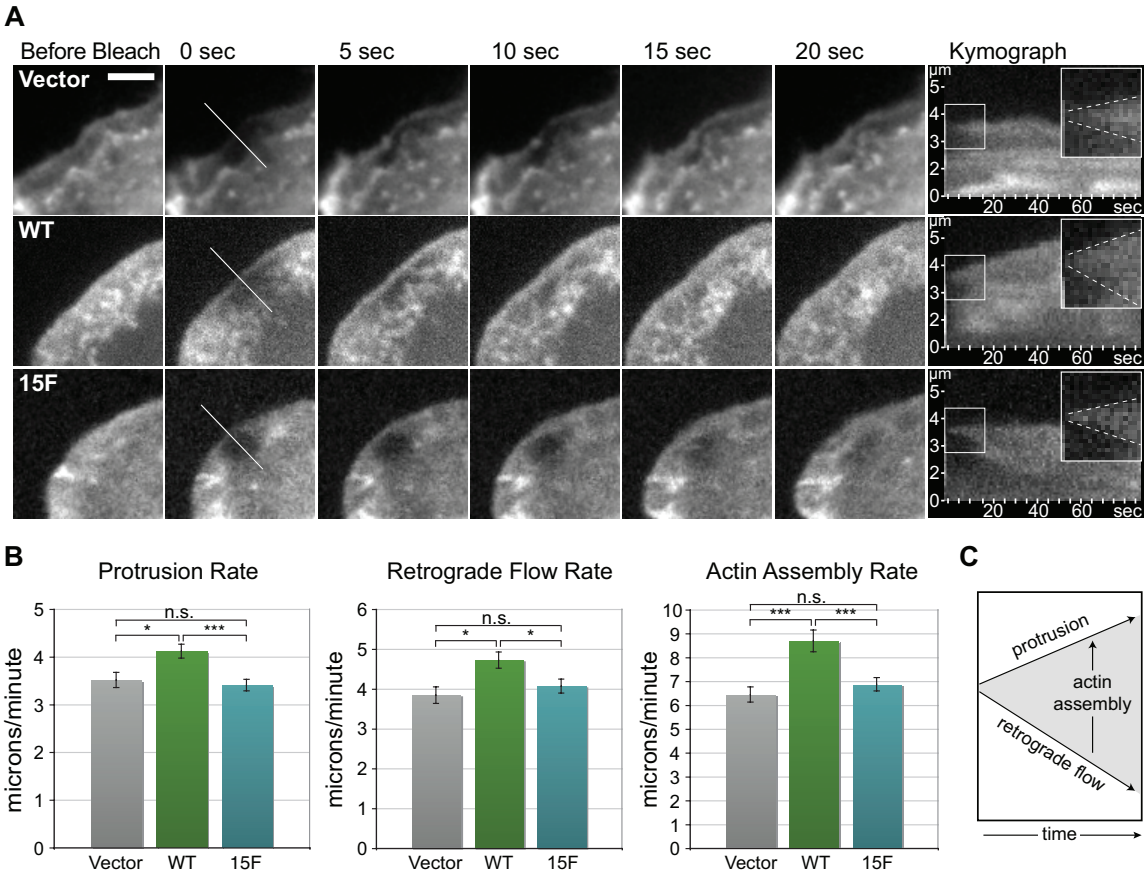

Figure 9. p130Cas SD signaling stimulates actin flux through the leading edge lamellipodium. p130Cas WT, 15F, and Vector only cells expressing a low level of mCherry-actin and migrating at the wound edge were viewed by wide field fluorescence microscopy. The leading edge was photobleached for 15 seconds then images were captured at one-second intervals and analyzed using kymography. (A) Time-lapse images and kymographs (far right) of mCherry-actin representative of mean values for actin assembly. Kymograph inset is a 2x magnification of the boxed area with upper and lower dotted lines marking protrusion and retrograde flow, respectively. Nascent actin assembly is characterized by the area between the dotted lines. Scale bar is 5μm. (B) Rates of protrusion, retrograde flow, and actin assembly representing the mean of 57 to 92 individual cells for each cell type. Bars indicate s.e.m. Significance values were determined by one-way ANOVA followed by Tukey-Kramer post hoc testing; *$p < 0.05$, ***$p < 0.001$. (C) Schematic of protrusion, retrograde flow, and actin assembly rate calculations.

comparing MEFs expressing WT p130Cas versus variants in which the signaling capacities of the SD and/or the SBD were disrupted by point mutations. Our results indicate that both the tyrosine phosphorylation sites in the SD and the Src SH3 binding site in the SBD contribute significantly to the ability of p130Cas to stimulate cell migration through enhancing actin dynamics. Loss of either signaling function fully impaired p130Cas-enhanced rates of plasma membrane protrusion. However, the ability of p130Cas to enhance cell migration rate was fully abolished only when the SD and SBD functions were simultaneously impaired. These findings indicate that the p130Cas SBD has a function in promoting cell migration that is distinct from its capacity to recruit and activate Src to promote SD tyrosine phosphorylation.

Neither the 15F mutation (loss of tyrosine phosphorylation sites) in the SD nor the mPR mutation (disruption of the Src SH3-binding motif) in the SBD fully impaired the ability of p130Cas to promote cell migration. But combining both mutations (15F/mPR) fully abolished the migration-promoting activity of p130Cas (Figure 6). In contrast to our results, another study reported that mutation of either the SD or the SH3 binding motif of the SBD was sufficient to fully impair p130Cas-enhanced cell migration (Huang et al., 2002) and thus a distinct role for the SBD could not be attributed. Our finding of a distinct role for the SBD in cell migration is consistent with the multiple biochemical functions attributed to this domain (Burnham et al., 2000, Donaldson et al., 2000, Li et al., 2000).

Upon tyrosine phosphorylation, the p130Cas SD interacts with the SH2/SH3 adapter proteins, Crk and Nck, and thus may recruit these activators of actin assembly to stimulate plasma membrane protrusion (Cho and Klemke, 2002, Klemke et al., 1998,

Rivera et al., 2006). Therefore I addressed whether p130Cas-enhanced cell migration could be attributed to an enhanced rate of membrane protrusion at the leading edge. I found that both the SD and SBD are required to promote leading edge protrusion. Cells expressing p130Cas WT had approximately 30% higher protrusion rates relative to Vector control cells and to all three p130Cas mutant cells (15F, mPR, and 15F/mPR). Thus tyrosine phosphorylation, likely mediated by Src recruited to the SBD, is the key p130Cas signaling event driving enhanced protrusion. The data do not indicate a distinct role for the SBD in driving protrusion and thus, do not fully account for the p130Cas mediated cell migration response. In extending this analysis I demonstrated that WT p130Cas stimulated actin assembly and retrograde flow at the leading edge lamellipodium and that these effects were fully blocked by the SD 15F mutation. Thus new experimental evidence linking p130Cas signaling to leading edge actin dynamics was provided.

Chapter III

THE ROLE OF P130CAS SIGNALING IN FOCAL ADHESION DYNAMICS

Introduction

P130Cas has been implicated in regulating the dynamics of two structures essential to cell migration: the lamellipodium and adhesion sites. A previous study evaluating the impact of several adhesion signaling components on adhesion dynamics implicated p130Cas in the regulation of adhesion disassembly (Webb et al., 2004), but no studies have evaluated the p130Cas signaling domains involved. To determine the contributions of the p130Cas SD and SBD signaling to this processes, I used live-cell imaging techniques to visualize adhesion dynamics in cells expressing a fluorescently-tagged paxillin to mark adhesion sites. I generated temporal intensity profiles in order to determine not only the rates of adhesion assembly and disassembly, but also to characerize adhesion behavior from initial assembly through disassembly. The data support distinct roles for the p130Cas SD and SBD in shortening adhesion lifetimes and sustaining uninterrupted adhesion disassembly, but a cooperative role in regulating the rates of initial adhesion formation and final disassembly.

Materials and Methods

Cells and cell culture

Cas -/- MEFs (Honda et al., 1998) were kindly provided by Hisamaru Hirai (University of Tokyo). MEFs were maintained in Dulbecco's Modified Eagle's Medium (Mediatech, Manassas, VA) supplemented with 10% fetal bovine serum (Atlanta Biologicals, Lawrenceville, GA), 1% antibiotic/antimicotic (Mediatech, Manassas, VA), and 1% non-essential amino acids (Invitrogen, Carlsbad, CA). The retroviral packaging cell line Phoenix Ectotropic (E) kindly provided by Gary Nolan (Stanford University), was maintained as previously described (Brabek et al., 2004).

Plasmids and protein expression

The LZRS-MS-IRES-GFP retroviral vector (Ireton et al., 2002) was used to express p130Cas variants in conjunction with cytoplasmic GFP from a bicistronic transcript as described in Chapter II. The same cell populations of Cas -/- MEFs stably expressing p130Cas WT, 15F, mPR, or 15F/mPR and the empty Vector control MEFs described in Chapter II were used in these studies.

Two plasmids were used for transient expression. mCherry-C1-paxillin (previously described (Efimov et al., 2008, Donato et al., 2010)) and mCherry-Actin. Actin was subcloned from Clontech pEGFP-actin using NheI and BglII restriction sites into the mCherry-C1 plasmid (provided by Maria Nemethova, Vienna, Austria). The resulting product is expressed with an N-terminal mCherry tag. Cells were transfected for transient expression using Lipofectamine 2000 (Invitrogen, Carlsbad, CA).

Live cell fluorescence imaging

Cells were transiently transfected with mCherry-C1-paxillin or using Lipofectamine 2000, then grown to confluence (48 hours) on 1 μg/ml fibronectin-coated coverslips. Wounds were generated and cells mounted as in the wound healing migration assay, see Chapter II. Cells migrating at the wound edge and expressing a low, but detectable level of fluorescently-tagged protein were selected for imaging. Cells expressing mCherry-tagged protein were visualized using a Pinkel triple filter set (Semrock, Rochester, NY) and a TIRF 100x 1.49 NA oil-immersion lens. Images were captured on a back-illuminated EM-CCD camera, Cascade 512B (Photometrics). Wide field fluorescence images of FA dynamics were captured every 60 seconds for 4 hours starting at an average of 2.5 hours post wounding (s.d. +/- 0.5 hours) for all cells.

FA lifetime quantification

The lifetimes of individual FAs forming at the leading edge (50-100 FAs, 10-20 each from 5 cells) of cells migrating at a wound edge were quantified by tracking FAs from assembly through disassembly and counting the number of sequential frames in which individual FAs had signal greater than background levels.

Antibodies

Monoclonal antibody against paxillin was obtained from BD Transduction Laboratories (San Jose, CA). Cy3-conjugated AffiniPure donkey anti-mouse IgG secondary antibody was obtained from Jackson ImmunoResearch Laboratories Inc. (West Grove, PA).

Immunostaining

Cells growing at low density were plated and allowed to attach and spread for 4 hours. Cells were fixed for 30 minutes in 2% paraformaldehyde (in a buffer containing 20 mM PIPES (pH 7.1), 127 mM NaCl, 5 mM KCl, 1.1 mM NaH_2PO_4, 0.4 mM KH_2PO_4, 2 mM $MgCl_2$, 5.5 mM glucose, 1 mM EGTA), then permeabilized in 0.4% Triton X in phosphate-buffered saline (PBS). Cells were blocked for 1 hour in 1% bovine serum albumin in PBS, then immunostained for paxillin with detection by Cy3-conjugated secondary antibody. The coverslips were mounted in Prolong Gold Mounting Media (Invitrogen). Images were acquired using a Nikon Eclipse 80i microscope equipped with a CoolSNAP ES camera (Photometrics) and Plan Apo 60x objective lens.

FA area quantification

Single cells with a clear polarized morphology were selected for analysis. Background in the nuclear region was eliminated to facilitate maximal FA detection, then initial FA masks were generated using the Moments filter in the ImageJ Segmentation, Multithresholder plugin. To eliminate noise and cellular background, particles in the mask were filtered to remove particles less than 15 pixels (0.344 μm^2) and greater than 10000 pixels. The remaining particles in the mask were then compared to the original image. To produce the final mask, the particles were subdivided if multiple adhesions were clearly represented within a single particle, or they were deleted if they did not correlate with a clearly visible FA. Finally the area of all particles in the mask was measured using ImageJ particle analysis.

FA temporal intensity profiles

Using ImageJ, FAs were outlined in each frame of the FA time-course. Background subtracted total pixel intensity was measured from each frame, using immediately adjacent pixels (not in the FA) to measure background intensity. To reduce noise, a moving average of either five or three consecutive intensity data points of background-subtracted FA intensity measurements was plotted (used for curve-fitting and local maxima quantification, respectively).

FA assembly and disassembly rate calculations

To reduce noise and facilitate curve fitting, temporal intensity profiles with a moving average of five consecutive intensity data points of background subtracted FA intensity measurements were used. Each data set was fit for six parameters using a least squares fitting routine in Matlab, three parameters for FA assembly, initial growth to maximum signal (r_{rise}, I_0, I_{lim}) and three for FA disassembly, final decay (r_{decay}, A, I_∞). The assembly was fit to a logistic function:

$$I(t) = \frac{I_{\lim} I_0 e^{r_{rise} t}}{I_{\lim} + I_0\left(e^{r_{rise} t} - 1\right)},$$

where I = signal intensity, t = time, I_0 = signal intensity at t = 0, r_{rise} = rate of exponential growth during the initial rise at small I values, and I_{lim} = signal as $t \to \infty$, also called the limiting value. This function is fit using a portion of the data, from the first non-zero point to one point beyond the maximum. Three additional parameters are determined by fitting the final disassembly to a simple exponential decay plus offset:

$$I(t) = Ae^{-r_{decay} t} + I_\infty,$$

where A is the amplitude of the decay, r_{decay} is the rate of decay, and P_∞ is the offset from zero signal. The range of data employed in this fitting was selected in order to capture only the final decay, while fitting to as much signal as possible for each intensity data set. This range of data varies with each data set, but begins at a point with an average value of 51% (s.d. ± 22%) of the fitted limiting value (I_{lim}) and continues until the FA intensity is indistinguishable from the background. For statistical analysis of FA assembly, poor fits (extreme values greater than two standard deviations above the mean or fits that used fewer than five data points in the exponential rise phase to approximate FA growth) were eliminated from the analysis.

FA local intensity maxima quantification

To reduce noise, a moving average three consecutive intensity data points of background-subtracted FA intensity measurements was plotted. The data were normalized so that the maximum intensity value for each FA equaled 100 (arbitrary units), and the number of local maxima in each intensity profile was quantified. A local maximum was defined as at least three consecutive rising points or an increase of ~10% of the maximum intensity value followed by at least three consecutive falling points or a decrease of ~10% of the maximum intensity value.

Statistical analysis

To compare the means of the numerous groups, one-way analysis of variance (ANOVA) followed by the Tukey-Kramer post hoc test was used to determine significance for pair-wise comparisons of all samples. Values were considered not significant (n.s.) when $p \geq 0.05$.

Results

P130Cas SD and SBD signaling domains have distinct roles in shortening FA lifetimes

To evaluate how p130Cas signaling domains impact FA dynamics, mCherry-paxillin was transiently expressed in the various cell populations in order to mark FAs with a fluorophore, and then cells were visualized by time-lapse wide field fluorescence microscopy. Individual FAs forming at the leading edge of cells migrating into a wound were tracked from assembly through disassembly and their lifetimes were determined by counting sequential frames in which the adhesion signal was above background. From inspection of representative time-lapse images (Figure 10), it is apparent that most FAs in Vector cells are present throughout the 90-minute time-course whereas in WT cells many FAs are seen to form and fully disassemble after 30-40 minutes (Figure 10, arrowheads). FAs in the 15F/mPR cells also appear to persist throughout the 90-minute time-course, while FAs in both the 15F and mPR cells appear to have intermediate lifetimes. Quantitative analysis confirms that WT cells have the shortest mean FA lifetimes, Vector and 15F/mPR cells have the longest lifetimes, and 15F and mPR single mutant cells have intermediate lifetimes (Figure 11A). The significant differences in mean FA lifetime among these groups reflect distinct distribution patterns such that the majority of FA lifetimes in WT cells fall under 40 minutes, those of 15F and mPR single mutant cells cluster between 20 and 80 minutes, and the FA lifetimes in Vector and 15F/mPR cells distribute even more broadly with no dominant peak (Figure 11B). Similar to what I

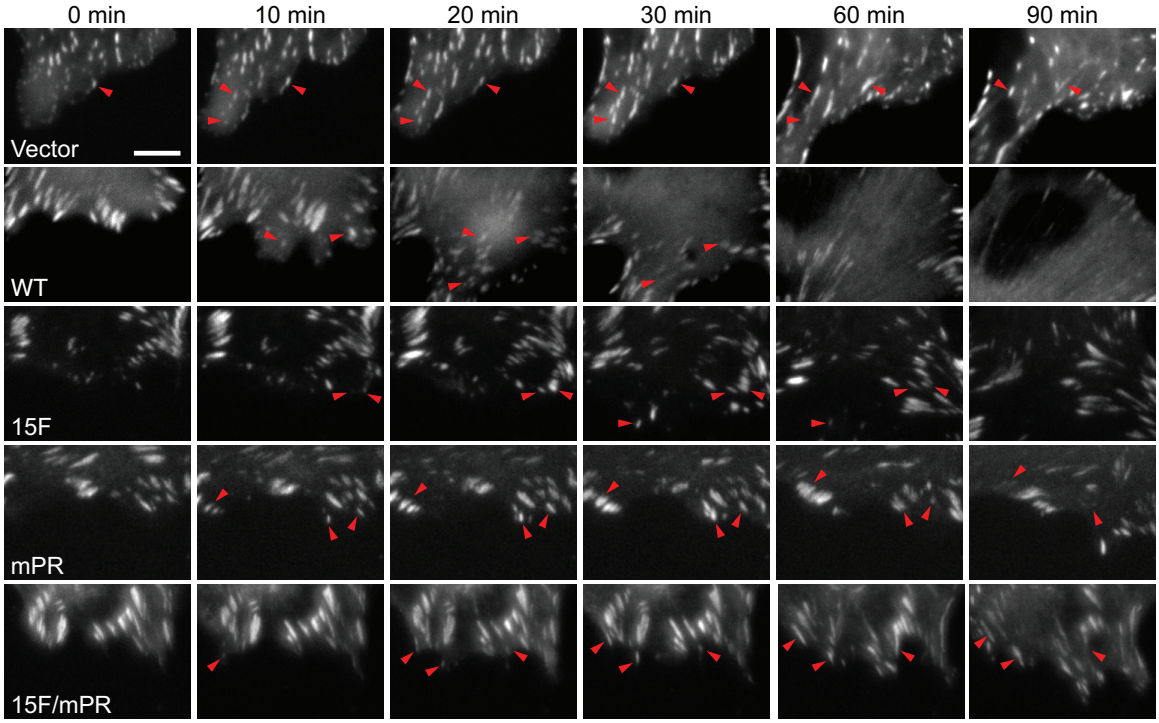

Figure 10. p130Cas SD and SBD signaling cooperate to shorten FA lifetimes, timelapse images. p130Cas WT and signaling deficient cells expressing a low level of mCherry-paxillin and migrating at the wound edge were viewed by wide field fluorescence microscopy with images captured at one-minute intervals. Representative images at 0, 10, 20, 30, 60, and 90 minutes are shown. Arrowheads indicate FAs representative of mean values. Scale bar is 10 μm.

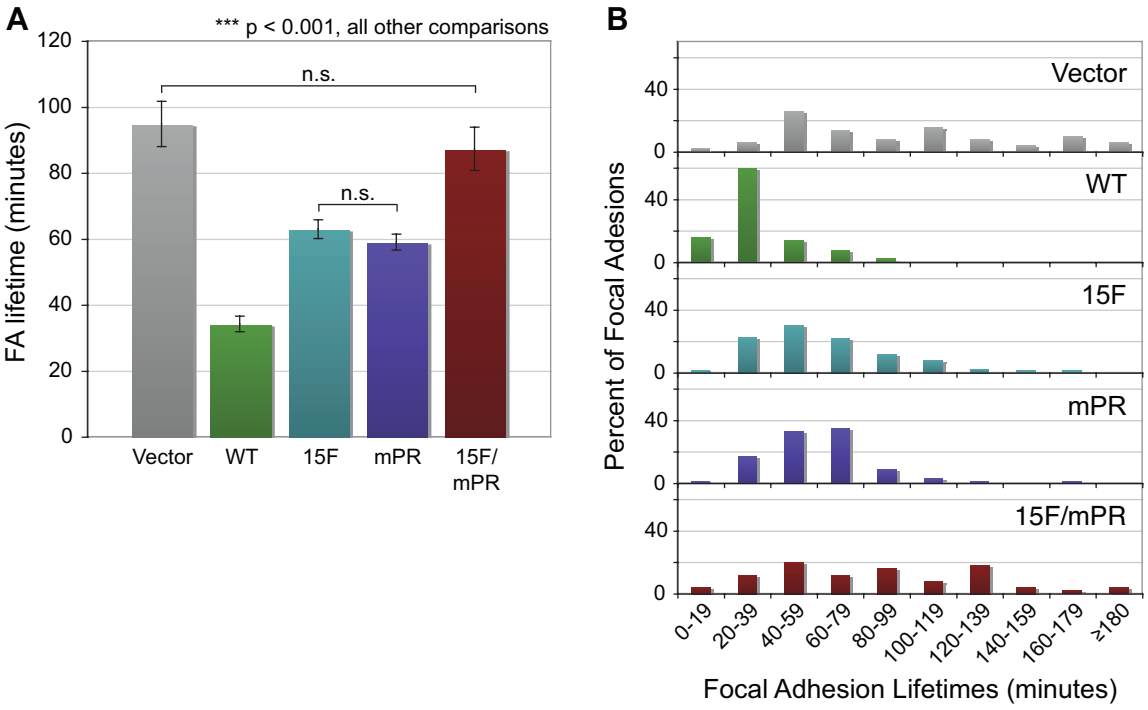

Figure 11. p130Cas SD and SBD signaling cooperate to shorten FA lifetimes, quantification. p130Cas WT and signaling deficient cells expressing a low level of mCherry-paxillin and migrating at the wound edge were viewed by wide field fluorescence microscopy with images captured at one-minute intervals. (A) FA lifetimes determined by counting the number of sequential frames with mCherry-paxillin FA fluorescence intensity above background levels. Data shown represent the mean FA lifetimes of 50-100 FAs (10-20 FAs from five cells) for each cell type. Bars indicate s.e.m. Significance values were determined by one-way ANOVA followed by Tukey-Kramer post hoc testing; n.s. (not significant), ***$p < 0.001$. (B) Histogram distributions of FA lifetimes, shown in 20-minute intervals. Note that the majority of WT FA lifetimes are less than 40 minutes while for all other cell types the majority of FAs lifetimes are greater than 40 minutes. Note also that the single mutants (15F and mPR) have similar distributions and that the Vector only control and 15F/mPR double mutant cells have similar distributions.

observed for cell migration rate, this additive defect indicates distinct roles for the SD and SBD in shortening FA lifetimes. To complement the analysis of FA dynamics, FA size distribution was determined from isolated cells stained for paxillin. Consistent with their shorter FA lifetimes, cells expressing WT p130Cas have a greater percentage of smaller FAs relative to cells expressing p130Cas signaling mutants (Figure 12).

P130Cas SBD-mediated SD signaling is implicated in enhancing rates of FA assembly and disassembly

To better understand how p130Cas impacts FA dynamics, temporal fluorescence intensity profiles of the individual FAs evaluated in Figures 10 and 11 were generated using a moving average of five data points to facilitate curve fitting. In the temporal profiles, increasing fluorescence intensity reflects FAs undergoing assembly, while decreasing intensity indicates disassembly. These profiles were then used to determine the rates of FA assembly and disassembly. Two representative fits of FA assembly and disassembly for each cell type are presented in Figure 13. FA assembly rate was modeled using a logistic function (exponential growth at early time points which plateaus to a maximum) and the final continuous phase of FA disassembly was modeled as simple exponential decay. This approach to determine apparent rate constants for FA assembly (r_{rise}) and FA disassembly (r_{decay}) follows on methodology for rate constant determination established by Webb et al. (2004), while using a greater percentage of the observed data to generate the rate constants.

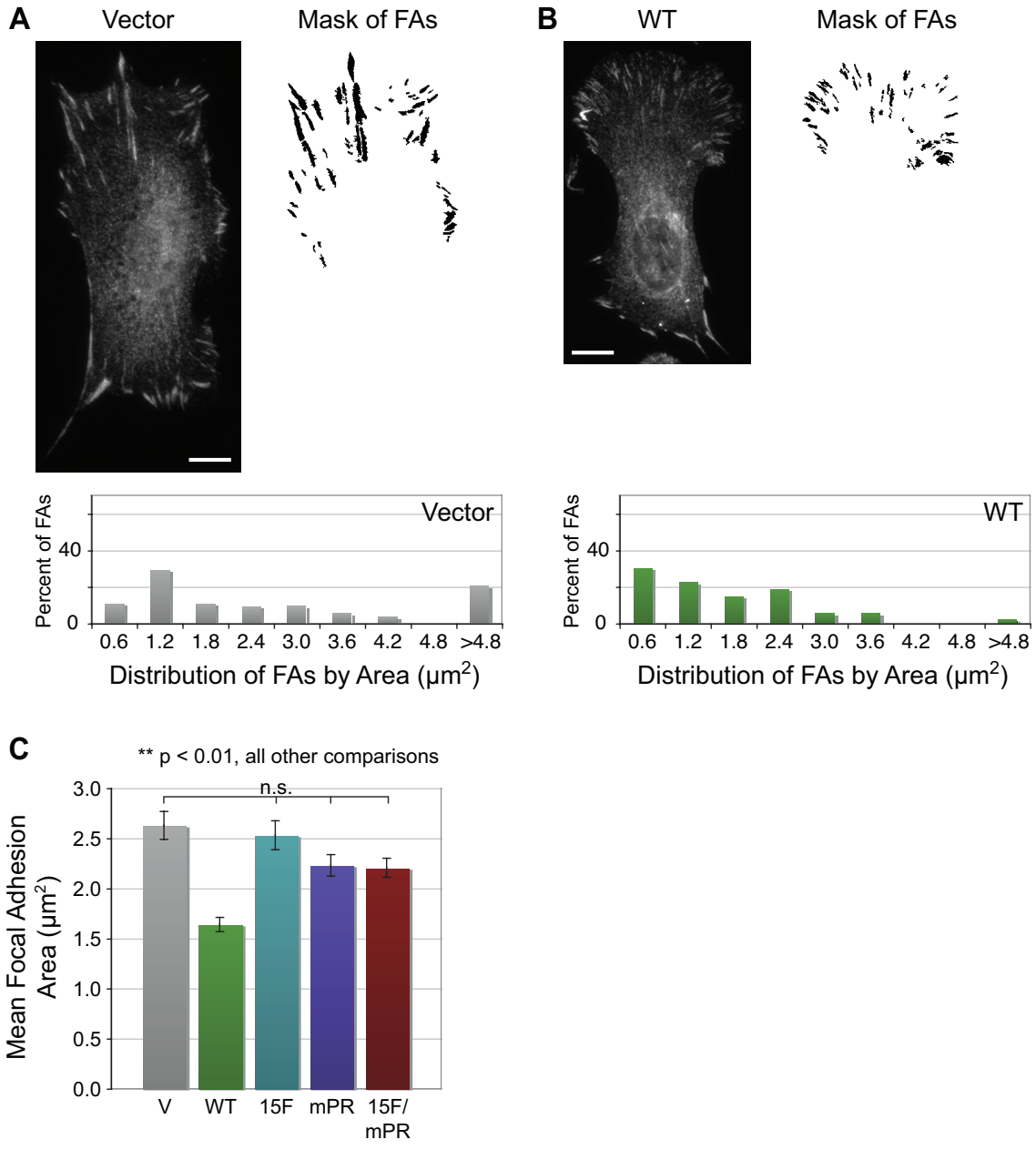

Figure 12. Defects in p130Cas SD and SBD signaling give rise to larger FAs in the front of polarized cells. FA size was assessed by wide field fluorescence imaging of fixed cells immunostained for paxillin to mark FAs. Single cells with a clear polarized morphology were selected and a mask of the front FAs was generated from the paxillin image. (A-B) Representative fixed images stained for paxillin, FA masks, and FA distribution pattern are shown for a Vector and WT cell. Scale bars are 10 μm. (C) Mean front FA size was quantified by evaluating FAs from 10-11 cells for each cell type. Bars indicate s.e.m. Significance values were determined by one-way ANOVA followed by Tukey-Kramer post hoc testing; n.s. (not significant), **$p < 0.01$.

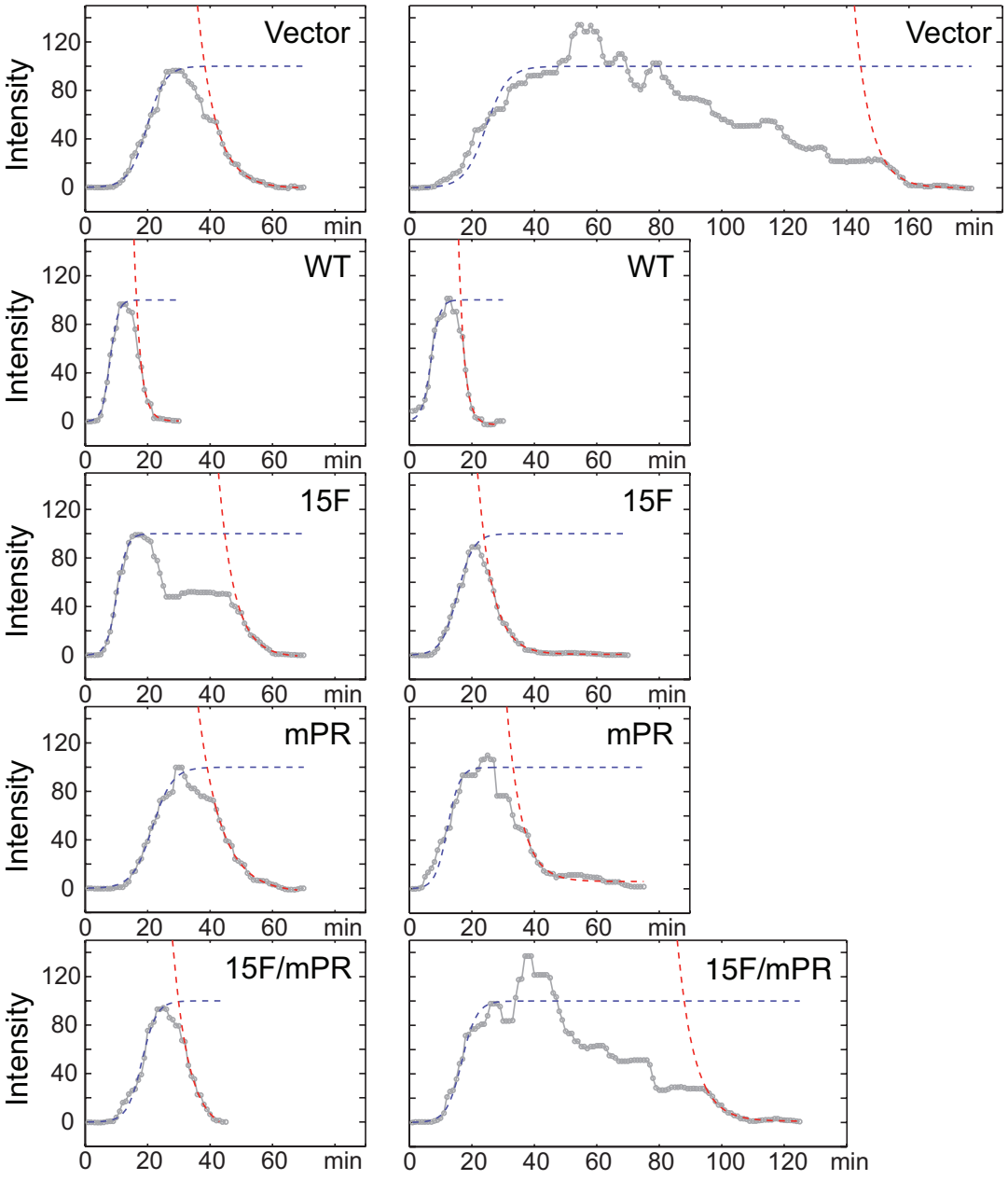

Figure 13. SBD-mediated SD signaling is implicated in stimulating both FA assembly and disassembly rates, sample curve fits. Apparent rate constants of FA assembly (r_{rise}) and disassembly (r_{decay}) were determined by fitting FA assembly to a logistic function and the final FA disassembly to exponential decay. Two examples of curve fits to FA intensity data (grey line) for assembly (purple dotted line) and disassembly (red dotted line) representative of the mean r_{rise} and r_{decay} are shown for each cell type. The graphs are normalized so that the modeled logistic function plateau equals 100.

Quantitative analysis showed that the mean FA assembly rate is significantly higher in p130Cas WT cells (1.5-1.8 fold) than for all other cell types (Figure 14A). The mean FA assembly rates of Vector, 15F, mPR, and 15F/mPR cells were not significantly different from one another. Reflective of the mean differences, the majority of WT r_{rise} values are greater than 1.00×10^{-2} Hz, whereas the majority of r_{rise} values for all other cell types fall below this value (Figure 15A). Similar results were obtained for measurements of FA disassembly. The mean FA disassembly rate is significantly higher in p130Cas WT cells (1.9-2.0 fold) than for all other cell types, and the mean FA disassembly rates are not significantly different between the other cells (Figure 14B). Reflective of the mean differences, the majority of WT r_{decay} values are greater than 0.50×10^{-2} Hz, whereas the majority of r_{decay} values for all other cells fall below this value (Figure 15B).

Similar to the results for leading edge protrusion, this analysis shows that the SD 15F mutation alone is sufficient to reduce both the FA assembly and disassembly rates to the levels seen in Vector cells. Once again, as SD tyrosine phosphorylation is impaired by the mPR mutation (Figure 5) (Fonseca et al., 2004, Ruest et al., 2001), the finding that 15F and mPR cells have similar r_{rise} and r_{decay} values indicates that the primary signaling role of the SBD in enhancing the rates of FA assembly/disassembly is by mediating SD tyrosine phosphorylation.

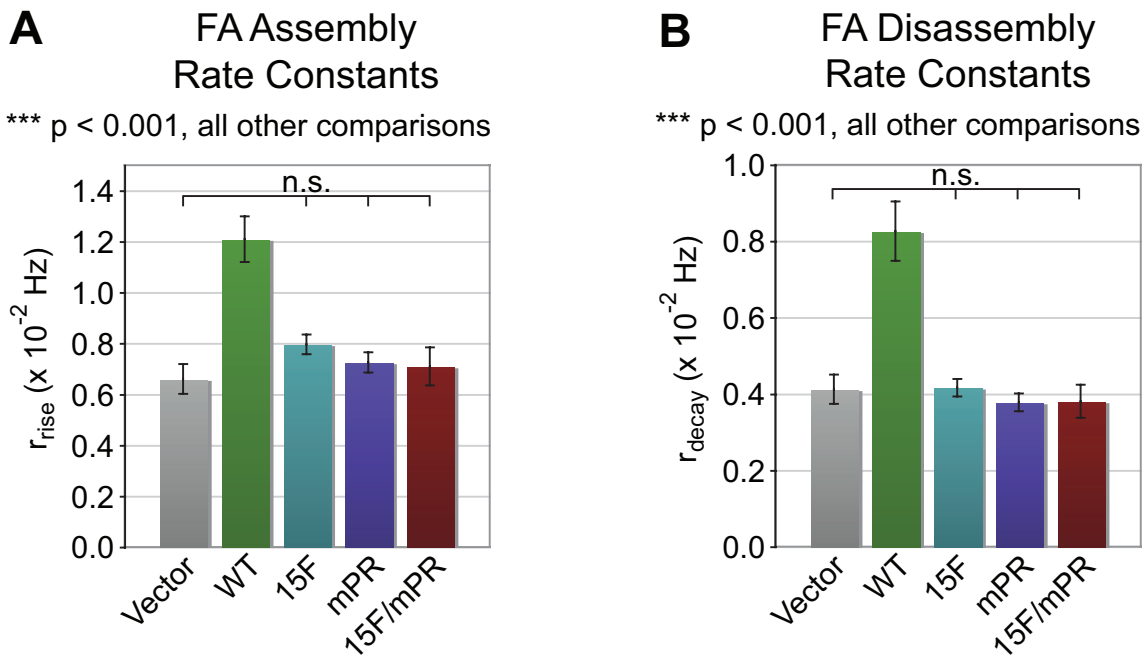

Figure 14. SBD-mediated SD signaling is implicated in stimulating both FA assembly and disassembly rates, mean values. Apparent rate constants of FA assembly (r_{rise}) and disassembly (r_{decay}) were determined by fitting FA assembly to a logistic function and the final FA disassembly to exponential decay. (A and B) Mean r_{rise} and r_{decay} values for each cell type are shown. Data represent the mean of 45-100 FAs from 5 cells. Bars indicate s.e.m. Significance values were determined by one-way ANOVA followed by Tukey-Kramer post hoc testing; n.s. (not significant), where all other comparisons are significant at ***$p < 0.001$.

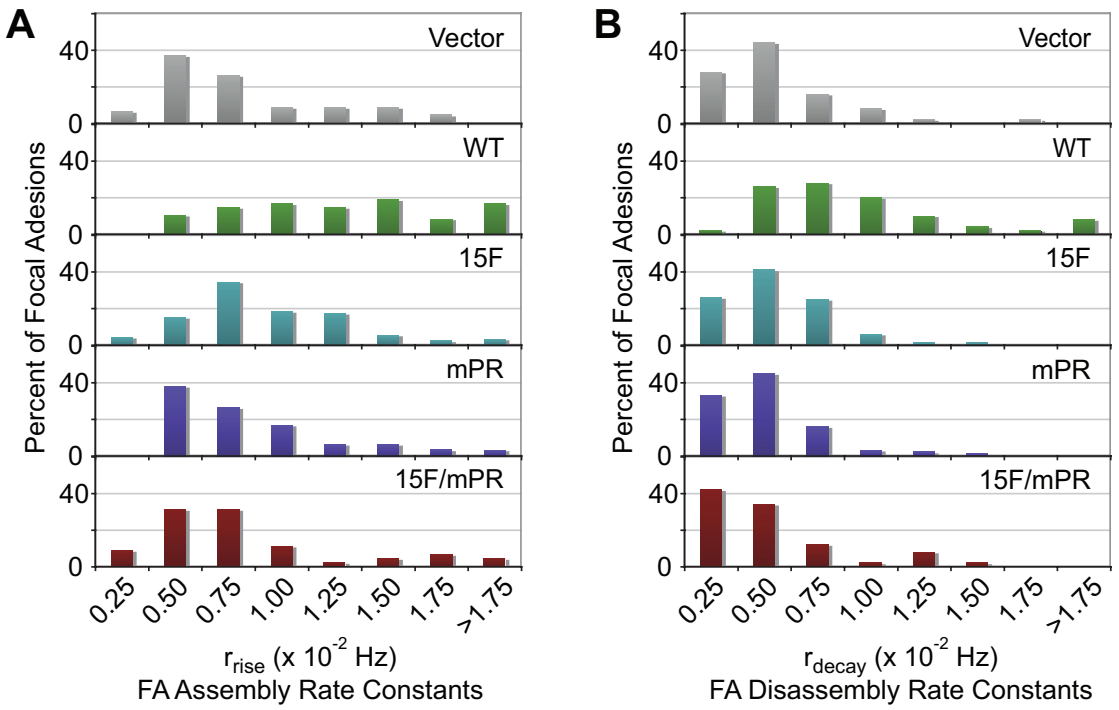

Figure 15. SBD-mediated SD signaling is implicated in stimulating both FA assembly and disassembly rates, histogram distrobutions. Apparent rate constants of FA assembly (r_{rise}) and disassembly (r_{decay}) were determined by fitting FA assembly to a logistic function and the final FA disassembly to exponential decay. (A and B) Histogram distributions of the r_{rise} and r_{decay} values for each cell type are shown in intervals of 0.25 x 10^{-2} Hz. In panel D, note that the majority of WT r_{rise} values are greater than 1.00 x 10^{-2} Hz while for all other cell types the majority of r_{rise} values are less than 1.00 x 10^{-2} Hz and have similar distributions. In panel E, note that the majority of WT r_{decay} values are greater than 0.50 x 10^{-2} Hz while for all other cell types the majority of r_{rise} values are less than 0.50 x 10^{-2} Hz and have similar distributions.

P130Cas SD and SBD signaling domains have distinct roles in sustaining FA disassembly

In modeling FA disassembly rates, I noted prominent discontinuous FA disassembly, particularly in the p130Cas signaling deficient cells. In order to quantify this phenomenon, I re-plotted the temporal intensity profiles using a moving average of 3 data points to highlight the numerous intensity peaks. From representative profiles (Figure 16), it can be seen that FAs with shorter lifetimes have simple bell-shaped profiles with a single peak of intensity while longer-lived FAs have more complex profiles with numerous local intensity maxima (arrowheads). The multiple local intensity maxima are indicative of abortive disassembly attempts. Quantitative analysis (Figure 17A and B) showed that FAs in p130Cas WT cells mostly have a single intensity maximum while FAs from the cells deficient in p130Cas signaling tend to have more complex profiles. For 15F and mPR cells, 2-3 local intensity maxima are most common. For Vector and 15F/mPR cells, there is an even broader distribution of FA local intensity maxima number with >5 often observed (Figure 17A). I noted that FAs with multiple intensity maxima typically exhibit sliding behavior. This can be readily seen from a representative kymograph shown in Figure 18B. The mean FA local intensity maxima number is significantly lower in the WT cells compared to all other cell types, while 15F and mPR cells have significantly fewer local intensity maxima than the Vector and 15F/mPR cells. These results indicate that signaling deficiencies in the SD and SBD of p130Cas extend FA lifetimes primarily due to a failure to sustain FA disassembly.

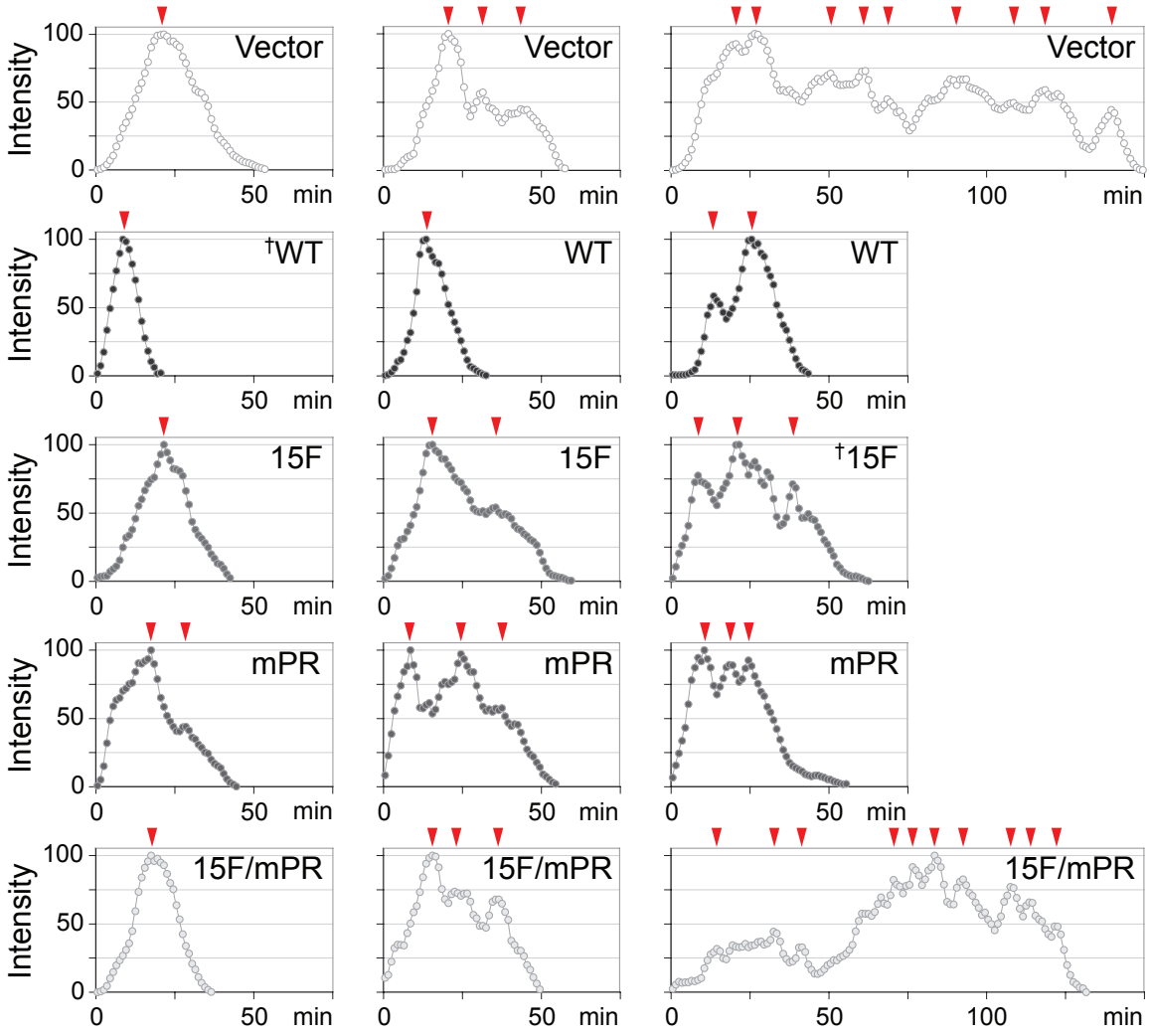

Figure 16. FA profile complexity is increased in the absence of p130Cas SD and SBD signaling. FA intensity profiles were created from time-lapse images, intensity profiles. Three FA intensity profiles representative of each cell type are shown, normalized with the maximum intensity at 100. Arrowheads indicate local intensity maxima. † indicates intensity profiles shown in Figure 18 with corresponding kymographs.

As was observed for cell migration rate, the additive effect of the 15F and mPR signaling variants indicates that sustained FA disassembly is regulated by distinct p130Cas signaling functions of the SD and SBD.

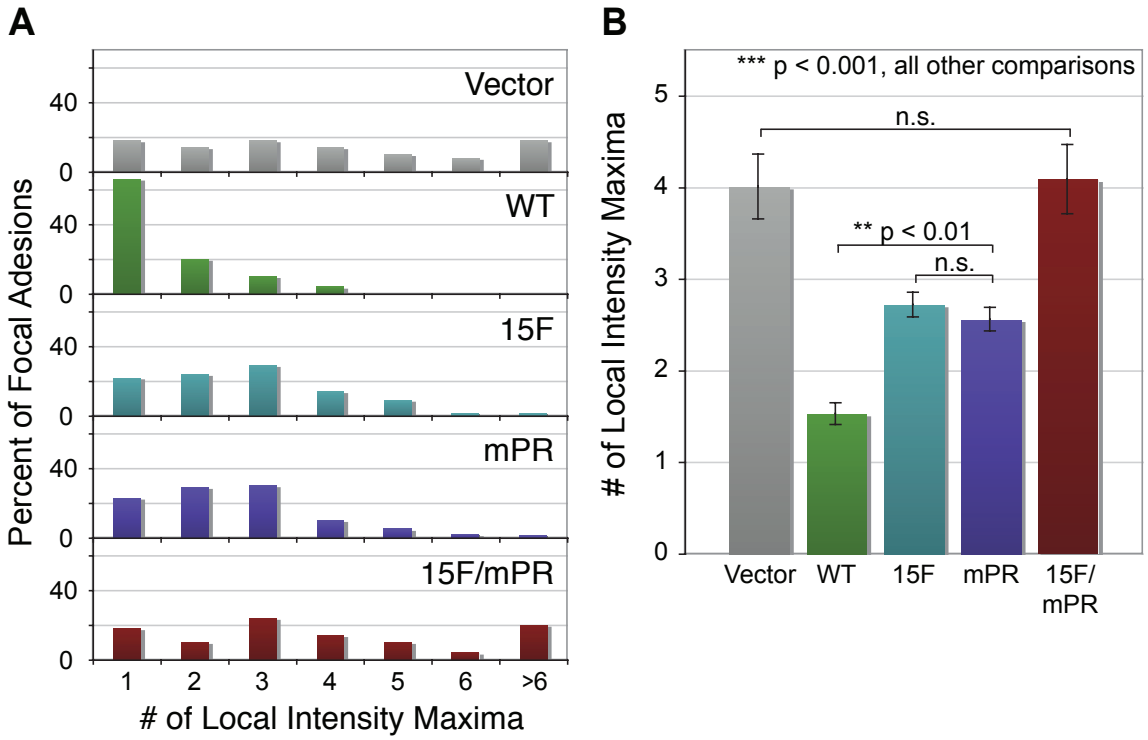

Figure 17. FA profile complexity is increased in the absence of p130Cas SD and SBD signaling. FA intensity profiles were created from time-lapse images, quantification. (A) Histogram distributions of the number of local maxima per FA intensity profile for each cell type. The majority (66%) of WT FAs have a single maximum. The single mutants are evenly distributed between 1-3 local maxima. The Vector and the 15F/mPR mutant cells show a broad distribution with a substantial number of FAs with > 5 local intensity maxima. (B) FA profile complexities for each cell type were quantified by counting the number of local intensity maxima. Data shown represent the mean number of local maxima for 50-100 FAs (10-20 FAs from each of five cells). Bars indicate s.e.m. Significance values were determined by one-way ANOVA followed by Tukey-Kramer post hoc testing; n.s. (not significant), **p < 0.01, ***p < 0.001.

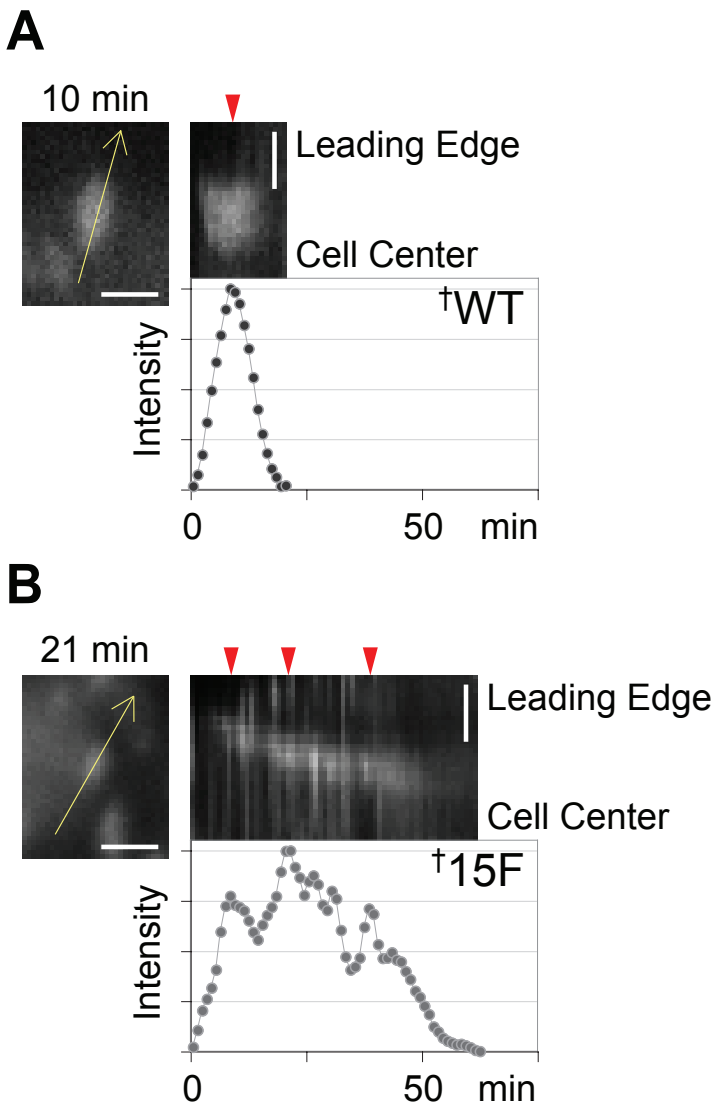

Figure 18. Kymographs of representative FAs showing single versus multiple intensity peaks. To visually illustrate the FA dynamics represented by peaks in the intensity profiles, two representative FA kymographs were generated corresponding to intensity profiles in Fig 7A, (marked with a †) that have either a single peak (A) or multiple peaks (B). The images on the left show the FAs at the indicated time point with arrows designating both the region used for the kymograph and the direction of migration. Kymographs are shown on the right, presented above the corresponding intensity profiles. Red arrowheads indicate local intensity maxima, as in Fig 7A. Scale bars are 2 μm.

Discussion

I used live cell imaging techniques to investigate the extent to which p130Cas signaling domains contribute to the dynamic regulation of cell-ECM adhesion during cell motility. As in the evaluation of actin dynamics in Chapter II, these properties were examined in a monolayer wound healing response, comparing MEFs expressing WT p130Cas versus variants in which the signaling capacities of the SD and/or the SBD were disrupted by point mutations. Our results indicate that both the tyrosine phosphorylation sites in the SD and the Src SH3 binding site in the SBD contribute significantly to the ability of p130Cas to stimulate cell migration through enhancing FA dynamics. Loss of either signaling function fully impaired p130Cas-enhanced rates of FA assembly/disassembly. In contrast, the ability of p130Cas to enhance cell migration rate and to maintain uninterrupted FA disassembly were fully abolished only when the SD and SBD functions were simultaneously impaired. These findings indicate that the p130Cas SBD has a function in maintaining FA disassembly and promoting cell migration that is distinct from its capacity to recruit and activate Src to promote SD tyrosine phosphorylation.

Observations that p130Cas SD tyrosine phosphorylation occurs primarily within mature FAs located away from the leading edge (Ballestrem et al., 2006, Fonseca et al., 2004) suggest p130Cas signaling may act to regulate FA dynamics during cell migration. Indeed, Cas -/- MEFs are reported to have a lower rate of FA disassembly compared to cells expressing p130Cas (Webb et al., 2004) but which, if any, of the p130Cas signaling functions are involved in this process was not previously addressed. I found that both the SD tyrosine phosphorylation sites and the SBD Src SH3-binding motif have important

roles in regulating FA dynamics. Approximately 2-fold higher rates of FA assembly and disassembly were observed in p130Cas WT cells relative to Vector control cells and to all p130Cas mutant cells (15F, mPR, and 15F/mPR). The similar defects observed in all p130Cas mutants implicate SD tyrosine phosphorylation mediated by Src recruited to the SBD as the key signaling function of p130Cas in stimulating FA assembly and disassembly rates, similar to leading edge protrusion. That these two processes show similar dependencies on p130Cas signaling domains suggests they may be coupled as has been speculated (Ridley et al., 2003).

I found that FAs from cells deficient in p130Cas SD and SBD signaling functions (15F/mPR and Vector) have ~3-fold longer lifetimes in comparison to p130Cas WT cells (Figure 11). This cannot be fully attributed to the differences in assembly/disassembly rate constants. Rather, the defect of extended FA lifetimes was linked to unusual FA temporal fluorescence intensity profiles containing multiple peaks (Figure 16). Such profiles are indicative of a defect in sustaining FA disassembly. FAs with multiple intensity maxima typically exhibit sliding behavior as is evident from the kymography data (Figure 18). It is notable that the full defects of extended FA lifetime and abortive FA disassembly were achieved only when both the SD and SBD mutations were combined, similar to our findings on cell migration rate. Thus we conclude that a major function of p130Cas in promoting cell migration is to sustain FA disassembly, with SD tyrosine phosphorylation and SBD SH3-binding motifs having distinct roles in this process.

It is interesting to speculate that p130Cas signaling may sustain FA disassembly as a consequence of its capacity to stimulate localized actin flux, in this case originating

from mature FAs under high contractile tension. The coupled retrograde movement of actin and FA components has been likened to a 'slippage clutch" whereby cells transduce mechanical signals and transmit force to the ECM (Brown et al., 2006, Hu et al., 2007, Wang, 2007). Moreover p130Cas in FAs may act as a "mechanotransducer" whereby stress-fiber generated tension triggers a conformational change that enhances Src-mediated SD tyrosine phosphorylation (Sawada et al., 2006). The resultant signaling by p130Cas may thus act to stimulate local actin assembly at the stress fiber/FA interface, thereby disengaging the slippage clutch to release tension and allow FA disassembly to occur. In this model, the aborted FA disassemblies observed in p130Cas signaling deficient cells would be due to repeated failures to fully disengage the clutch. A possible role for p130Cas SD signaling promoting actin assembly in mature FAs was suggested by another recent study from our group where Src activity was specifically elevated in FAs through expression of a FAK-Src chimeric protein (Siesser et al., 2008). This resulted in greatly elevated p130Cas SD tyrosine phosphorylation and a striking display of transient actin assembly in mature FAs. Results from our present study further indicate that the p130Cas SBD has a role in sustaining FA disassembly that is distinct from that of the SD. In this regard, I note that SBD-activated Src can phosphorylate other substrates including paxillin and cortactin (Burnham et al., 2000), both of which have been implicated in regulating FA dynamics (Bryce et al., 2005, Kruchten et al., 2008, Webb et al., 2004, Zaidel-Bar et al., 2007b). Interestingly, a cortactin mutant that cannot undergo Src phosphorylation extends FA disassembly time and appears to give rise to FA profiles with multiple intensity peaks (Kruchten et al., 2008), similar to what I observed in

p130Cas signaling deficient cells. It will be of interest for future studies to evaluate the role of p130Cas-activated Src substrates in FA dynamics.

Chapter IV

CONCLUDING REMARKS AND FUTURE DIRECTIONS

Concluding Remarks

It has long been known that p130Cas plays a major role in integrin-mediated signaling, particularly in enhancing cell migration. P130Cas has also been implicated in disease processes, particularly in promoting disease progression and metastasis in cancer. It is important to understand how p130Cas initiates signaling cascades in order to better understand the fundamental process of cell migration, and also because understanding how p130Cas signals may provide targets to intervene in disease processes.

While numerous studies hypothesized that the well-characterized p130Cas/Crk/Rac pathway functioned to drive leading edge protrusion, no direct quantitative measurements of leading edge dynamics downstream of p130Cas were made. Because the leading edge actin dynamics are considered the main driving force behind cell migration, migration rates are often used as a proxy for direct measurements of lamellipodial dynamics. While the observation that p130Cas SD signaling drives increased rates of protrusion and actin flux in the lamellipodium was not surprising, these studies provide the first direct measurements of the rates of lamellipodial activity downstream of p130Cas signaling. Furthermore, using measurements of cell migration as a proxy would have yielded a different result.

P130Cas had also been implicated in regulating adhesion disassembly (Webb et al., 2004), but no studies had evaluated the mechanism of this process or the p130Cas signaling domains involved. In evaluating adhesion dynamics of p130Cas signaling variants, the use of temporal intensity profiles for the entire lifetime of all adhesions analyzed revealed complex adhesion behavior between the initial formation and final disassembly consisting of fluctuations in adhesion intensity often correlated with sliding behavior. Such aborted adhesion disassembly attempts had not previously been noted.

Furthermore, the use of a logistic function, rather than exponential growth, to model the apparent rate constant of assembly allowed a greater percentage of data points to be used in the rate approximation, by including points outside the purely exponential growth. This was especially useful for rapidly dynamic adhesions that did not have as many data points at the chosen sampling interval.

The activity of the two main p130Cas signaling domains is linked but not exclusive. The p130Cas Src-binding domain (SBD) recruits and activates Src, which can in turn phosphorylate the p130Cas substrate domain (SD). However Src activated by binding the SBD is also capable of phosphorylating other targets, which is facilitated by the highly interconnected binding relationships within adhesion sites. Furthermore, the p130Cas SD can also be phosphorylated by Src that is bound to the FAK Y397 autophosphorylation site. Therefore, while the signaling of the p130Cas SD and SBD are intimately related, it is possible that they have distinct signaling functions as was shown. The conclusions from Chapters II and III are summarized in Figure 19.

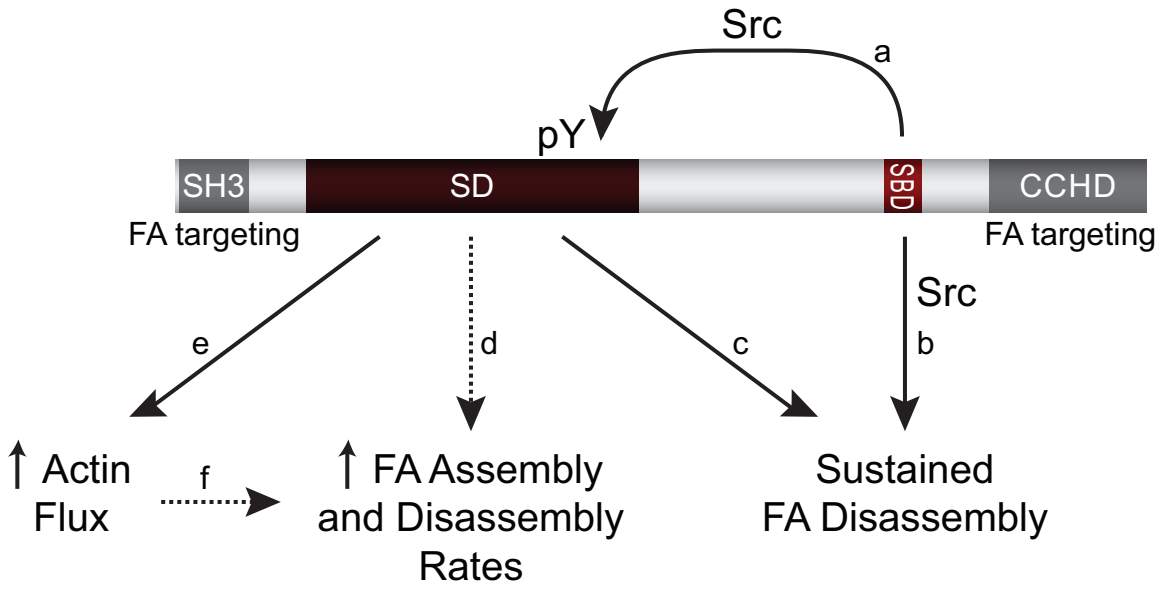

Figure 19. Summary of p130Cas SD and SBD signaling in the regulation of FA and actin dynamics. The SBD activates Src to promote SD tyrosine phosphorylation (a) and also promotes sustained FA disassembly through a distinct pathway (b). SD tyrosine phosphorylation acts to sustain FA disassembly (c), stimulate the rates of FA assembly and disassembly (d), and promote leading edge actin flux (e). Increased FA assembly/disassembly rates may be a direct effect of SD signaling on adhesion dynamics (d) or an indirect effect resulting from leading edge protrusion driving more rapid FA assembly/disassembly (e, f). Dotted lines indicated that the effect of SD on FA assembly and disassembly rates could be either direct or indirect.

Future Directions

Evaluate p130Cas-mediated Actin Assembly in a Biochemical Assay using Xenopus *Egg Extracts*

An approach to better characterize the effect of p130Cas SD signaling on actin assembly is to use a biochemical *Xenopus* egg extract assay. Beads loaded with tyrosine-phosphorylated p130Cas SD would be added to *Xenopus* extracts containing fluorescent actin. If the SD stimulates actin assembly, a halo of fluorescence would appear around the bead. This assay has been used to study fundament characteristics of the actin nucleation machinery and facilitates biochemical perturbation of the system (Ma et al., 1998, Rohatgi et al., 1999).

Significant preparatory work has been completed for these experiments. Initial results were potentially interesting but inconsistent. Purified p130Cas SD has been expressed, purified, and Src-phosphorylated to high levels through an *in vitro* kinase reation. However, the phosphorylation is rapidly removed in *Xenopus* extracts in the absence of high levels of phosphatase inhibitors. The addition of sufficient levels of phosphatase inhibitor to block p130Cas dephosphorylation has global effects on the actin *in vitro*, leading to F-actin clumping.

One alternative approach includes preloading phosphorylated p130Cas SD with the anticipated second messengers Crk and/or Nck which would remove one assembly step required once in the extract and may also serve to partially protect the SD tyrosines from dephosphorylation. Epitope-tagged Crk and Nck have been bacterially expressed,

affinity purified, and eluted from beads for this purpose. A second alternative approach entails using ATPγ-S for the *in vitro* kinase assay, which is partially resistant to phosphatases and should be removed more slowly. A third alternative includes the used of pyrene actin assay to evaluate actin assembly. Preliminary experiments indicate possible differences in actin assembly using the bead assay, but the actin does not always appear around the bead as a halo. Actin sedimentation assays may show differences in the F-actin/G-actin ratio that are hard to quantify in the bead assay.

Evaluate the Formation of p130Cas/Crk and p130Cas/Nck Complexes in Live Cells using FRET

P130Cas is clearly phosphorylated in both focal complexes and mature focal adhesions. P130Cas activity regulating lamellipodial dynamics would be expected preferentially in the nascent adhesions forming at the front of the cell, whereas p130Cas signaling regulating adhesion disassembly would be expected in mature adhesions behind the leading edge. The localization of p130Cas/Crk or p130Cas/Nck coupling could reveal different roles for these two adapters. Because p130Cas is not the only binding partner for the SH2-SH3 adapter proteins in adhesions, simple localization by immunofluorescence does not reveal information about specific signaling pathways. In contrast, FRET between Venus-tagged p130Cas and Cerulean-tagged SH2-SH3 would likely indicate complex formation. The Venus-tagged p130Cas 15F mutant would be a good negative control where complex formation would not be expected and any FRET signal could be attributed to background. In addition to localization information, live-cell FRET would also reveal how p130Cas coupling to adapter proteins changes over time, for example during the lifetime of an adhesion.

Evaluate Actin Dynamics at Stress Fiber Termini

As mentioned in the Discussion of Chapter III, it is interesting to speculate that p130Cas may drive increased rates of actin assembly at adhesion sites in addition to its role in driving an increased rate of actin assembly at the leading edge. A FAK-Src gain of function chimera showed increased p130Cas phosphorylation and dramatic bursts of actin assembly at adhesion sites that was dependent on Src kinase activity (Siesser et al., 2008). The ability to control tension at stress fibers by regulating the rate of actin assembly is a potential mechanism whereby p130Cas signaling could regulate focal adhesion disassembly. Thus, future experiments should address the dynamics of actin not only in the leading edge of cells expressing p130Cas signaling variants but also in stress fibers near the interface with adhesion sites. This would require transient expression of two fluorescently-tagged proteins, one to mark actin, and one to mark adhesion sites. Stress fibers incorporate new actin assembly at their adhesion-anchored termini (Hotulainen and Lappalainen, 2006). Similar to experiments evaluating actin dynamics in the lamellipodium (Figure 9), the rate of actin assembly could be determined by tracking incorporation of fluorescent actin after photobleaching at the stress fiber terminus. Preliminary studies have already demonstrated the feasibility of this approach.

Evalutate the FRAP Exchange Rate of p130Cas Signaling Variants at Adhesion Sites

Recent FRAP (fluorescence recovery after photobleaching) studies showed that P130Cas exchanges rapidly at adhesion sites with a high mobile fraction compared to paxillin (Donato et al., 2010). The work presented in this thesis demonstrates p130Cas regulates adhesion dynamics, both the rates of adhesion assembly/disassembly and the ability of adhesions to sustain continuous adhesion disassembly. These parameters could

be altered by changes in the dynamic localization of p130Cas itself. Extension of FRAP studies to p130Cas signaling variants would demonstrate whether the dynamic exchange and high mobile fraction of p130Cas is dependent on the p130Cas signaling domains or is an intrinsic property of the targeting domains. It would be important to complete these studies in both a wild type p130Cas background and a Cas -/- background to differentiate if potential differences in exchange rates are due to global adhesion changes due to changes in p130Cas signaling or the affinity of the individual fluorescently-tagged p130Cas molecules.

The FRAP exchange rates for adhesion components have been shown to differ at the proximal (near the stress fiber) and distal (away from the stress fiber) ends of mature adhesions (Wolfenson et al., 2009b). Thus it would also be important to evaluate exchange in both early and late adhesions, and within proximal and distal ends of mature adhesions.

Evaluate the Impact of p130Cas Signaling on Focal Adhesion Maturation and Molecular Composition

The longer-lived adhesions in the p130Cas signaling variants with numerous intensity peaks, which often exhibit sliding behavior, need to be molecularly characterized. Quantitative analysis of the localization of adhesion components including the maturation markers zyxin and alpha-actinin (Zaidel-Bar et al., 2003, Laukaitis et al., 2001, Webb et al., 2004) may reveal information about the molecular nature mature/immature of these adhesions that distinguishes them from adhesion in cells expressing p130Cas WT. In addition, two-color adhesion dynamics studies simultaneously evaluating both early and late adhesion markers could illuminate whether

other components enter and leave adhesions at the same rate. In addition to the proposed FRAP studies evaluating the mobile fraction and exchange rate of fluorophore-tagged p130Cas, creating two-color temporal intensity profiles for several adhesion protein pairs, including paxillin and p130Cas may lend insight into the mechanism of p130Cas regulation of adhesion disassembly. It is possible that p130Cas signaling variants disassemble from adhesions at a slower rate relative to other adhesion markers, or that defects in p130Cas signaling result in defective removal of other adhesion components.

The Role of Substrates of SBD-activated Src in Addition to p130Cas

Several Src substrates are already known to have decreased levels of tyrosine phosphorylation in the absence of a functional p130Cas SBD, including paxillin and cortactin (Burnham et al., 1999). These need to be evaluated in the p130Cas signaling variants. If differences are observed, particularly in the p130Cas SBD mutant, these proteins should be evaluated in p130Cas-mediated adhesion disassembly. Src-mediated paxillin and cortactin signaling have already been implicated in regulating adhesion dynamics (Webb et al., 2004, Kruchten et al., 2008).

Evaluate Cellular Traction Forces in p130Cas Signaling Variants

Initial data gathered in collaboration with Yuli Wang revealed no differences in cellular traction forces between Vector and WT p130Cas re-expressing cells plated on micropatterned flexible polyacrylamide substrates that control for cell area. However it is possible that polarized migrating cells that lack p130Cas signaling may have differences in the distribution or dynamics of traction forces, or the ability to respond to externally applied forces as compared to cells expressing WT p130Cas. These questions

could be addressed using flexible polyacrylamide substrates cross-linked to fibronectin and embedded with fluorescent beads to track gel displacement and calculate traction forces.

In addition, a recent paper (Fraley et al., 2010), demonstrated a lack of detectable adhesion sites in cells fully embedded in a 3D matrix, as compared to 2D glass, 2D flexible substrates, or cells plated on a 3D matrix but not fully embedded. However adhesion proteins, including p130Cas, still regulate migration (Fraley et al., 2010). These studies emphasize the need to evaluate cell migration in 3D environments in addition to the traditional 2D environment.

REFERENCES

ALEXANDROPOULOS, K., DONLIN, L. T., XING, L. & REGELMANN, A. G. 2003. Sin: good or bad? A T lymphocyte perspective. *Immunol Rev,* 192**,** 181-95.

ALEXANDROPOULOS, K. & REGELMANN, A. G. 2009. Regulation of T-lymphocyte physiology by the Chat-H/CasL adapter complex. *Immunol Rev,* 232**,** 160-74.

ALEXANDROVA, A. Y., ARNOLD, K., SCHAUB, S., VASILIEV, J. M., MEISTER, J. J., BERSHADSKY, A. D. & VERKHOVSKY, A. B. 2008. Comparative dynamics of retrograde actin flow and focal adhesions: formation of nascent adhesions triggers transition from fast to slow flow. *PLoS One,* 3**,** e3234.

ANDERSON, T. W., VAUGHAN, A. N. & CRAMER, L. P. 2008. Retrograde flow and myosin II activity within the leading cell edge deliver F-actin to the lamella to seed the formation of graded polarity actomyosin II filament bundles in migrating fibroblasts. *Mol Biol Cell,* 19**,** 5006-18.

AROLD, S. T., HOELLERER, M. K. & NOBLE, M. E. 2002. The structural basis of localization and signaling by the focal adhesion targeting domain. *Structure,* 10**,** 319-27.

ASSOIAN, R. K. & KLEIN, E. A. 2008. Growth control by intracellular tension and extracellular stiffness. *Trends Cell Biol,* 18**,** 347-52.

ASTIER, A., MANIE, S. N., LAW, S. F., CANTY, T., HAGHAYGHI, N., DRUKER, B. J., SALGIA, R., GOLEMIS, E. A. & FREEDMAN, A. S. 1997. Association of the Cas-like molecule HEF1 with CrkL following integrin and antigen receptor signaling in human B-cells: potential relevance to neoplastic lymphohematopoietic cells. *Leuk Lymphoma,* 28**,** 65-72.

BALLESTREM, C., EREZ, N., KIRCHNER, J., KAM, Z., BERSHADSKY, A. & GEIGER, B. 2006. Molecular mapping of tyrosine-phosphorylated proteins in focal adhesions using fluorescence resonance energy transfer. *J Cell Sci,* 119**,** 866-75.

BECKERLE, M. C., BURRIDGE, K., DEMARTINO, G. N. & CROALL, D. E. 1987. Colocalization of calcium-dependent protease II and one of its substrates at sites of cell adhesion. *Cell,* 51**,** 569-77.

BERG, J. S., DERFLER, B. H., PENNISI, C. M., COREY, D. P. & CHENEY, R. E. 2000. Myosin-X, a novel myosin with pleckstrin homology domains, associates with regions of dynamic actin. *J Cell Sci,* 113 Pt 19**,** 3439-51.

BERSHADSKY, A., CHAUSOVSKY, A., BECKER, E., LYUBIMOVA, A. & GEIGER, B. 1996. Involvement of microtubules in the control of adhesion-dependent signal transduction. *Curr Biol,* 6**,** 1279-89.

BERTOLUCCI, C. M., GUIBAO, C. D. & ZHENG, J. 2005. Structural features of the focal adhesion kinase-paxillin complex give insight into the dynamics of focal adhesion assembly. *Protein Sci,* 14**,** 644-52.

BETTENCOURT-DIAS, M. & GLOVER, D. M. 2007. Centrosome biogenesis and function: centrosomics brings new understanding. *Nat Rev Mol Cell Biol,* 8**,** 451-63.

BHATT, A., KAVERINA, I., OTEY, C. & HUTTENLOCHER, A. 2002. Regulation of focal complex composition and disassembly by the calcium-dependent protease calpain. *J Cell Sci,* 115**,** 3415-25.

BIYASHEVA, A., SVITKINA, T., KUNDA, P., BAUM, B. & BORISY, G. 2004. Cascade pathway of filopodia formation downstream of SCAR. *J Cell Sci,* 117**,** 837-48.

BLACK, D. S. & BLISKA, J. B. 1997. Identification of p130Cas as a substrate of Yersinia YopH (Yop51), a bacterial protein tyrosine phosphatase that translocates into mammalian cells and targets focal adhesions. *EMBO J,* 16**,** 2730-44.

BORISY, G. G. & SVITKINA, T. M. 2000. Actin machinery: pushing the envelope. *Curr Opin Cell Biol,* 12**,** 104-12.

BOUTON, A. H., RIGGINS, R. B. & BRUCE-STASKAL, P. J. 2001. Functions of the adapter protein Cas: signal convergence and the determination of cellular responses. *Oncogene,* 20**,** 6448-58.

BRABEK, J., CONSTANCIO, S. S., SHIN, N. Y., POZZI, A., WEAVER, A. M. & HANKS, S. K. 2004. CAS promotes invasiveness of Src-transformed cells. *Oncogene,* 23**,** 7406-15.

BRABEK, J., CONSTANCIO, S. S., SIESSER, P. F., SHIN, N. Y., POZZI, A. & HANKS, S. K. 2005. Crk-associated substrate tyrosine phosphorylation sites are critical for invasion and metastasis of SRC-transformed cells. *Mol Cancer Res,* 3**,** 307-15.

BRIKNAROVA, K., NASERTORABI, F., HAVERT, M. L., EGGLESTON, E., HOYT, D. W., LI, C., OLSON, A. J., VUORI, K. & ELY, K. R. 2005. The serine-rich domain from Crk-associated substrate (p130cas) is a four-helix bundle. *J Biol Chem,* 280**,** 21908-14.

BRINKMAN, A., VAN DER FLIER, S., KOK, E. M. & DORSSERS, L. C. 2000. BCAR1, a human homologue of the adapter protein p130Cas, and antiestrogen resistance in breast cancer cells. *J Natl Cancer Inst,* 92**,** 112-20.

BROUSSARD, J. A., WEBB, D. J. & KAVERINA, I. 2008. Asymmetric focal adhesion disassembly in motile cells. *Curr Opin Cell Biol,* 20**,** 85-90.

BROWN, C. M., HEBERT, B., KOLIN, D. L., ZARENO, J., WHITMORE, L., HORWITZ, A. R. & WISEMAN, P. W. 2006. Probing the integrin-actin linkage using high-resolution protein velocity mapping. *J Cell Sci,* 119**,** 5204-14.

BRYCE, N. S., CLARK, E. S., LEYSATH, J. L., CURRIE, J. D., WEBB, D. J. & WEAVER, A. M. 2005. Cortactin promotes cell motility by enhancing lamellipodial persistence. *Curr Biol,* 15**,** 1276-85.

BUDAY, L., WUNDERLICH, L. & TAMAS, P. 2002. The Nck family of adapter proteins: regulators of actin cytoskeleton. *Cell Signal,* 14**,** 723-31.

BUGYI, B. & CARLIER, M. F. 2010. Control of actin filament treadmilling in cell motility. *Annu Rev Biophys,* 39**,** 449-70.

BURNHAM, M. R., BRUCE-STASKAL, P. J., HARTE, M. T., WEIDOW, C. L., MA, A., WEED, S. A. & BOUTON, A. H. 2000. Regulation of c-SRC activity and function by the adapter protein CAS. *Mol Cell Biol,* 20**,** 5865-78.

BURNHAM, M. R., HARTE, M. T. & BOUTON, A. H. 1999. The role of SRC-CAS interactions in cellular transformation: ectopic expression of the carboxy terminus of CAS inhibits SRC-CAS interaction but has no effect on cellular transformation. *Mol Carcinog,* 26**,** 20-31.

BUTLER, B., GAO, C., MERSICH, A. T. & BLYSTONE, S. D. 2006. Purified integrin adhesion complexes exhibit actin-polymerization activity. *Curr Biol,* 16**,** 242-51.

CABODI, S., MORO, L., BAJ, G., SMERIGLIO, M., DI STEFANO, P., GIPPONE, S., SURICO, N., SILENGO, L., TURCO, E., TARONE, G. & DEFILIPPI, P. 2004. p130Cas interacts with estrogen receptor alpha and modulates non-genomic estrogen signaling in breast cancer cells. *J Cell Sci,* 117**,** 1603-11.

CABODI, S., TINNIRELLO, A., DI STEFANO, P., BISARO, B., AMBROSINO, E., CASTELLANO, I., SAPINO, A., ARISIO, R., CAVALLO, F., FORNI, G., GLUKHOVA, M., SILENGO, L., ALTRUDA, F., TURCO, E., TARONE, G. & DEFILIPPI, P. 2006. p130Cas as a new regulator of mammary epithelial cell proliferation, survival, and HER2-neu oncogene-dependent breast tumorigenesis. *Cancer Res,* 66**,** 4672-80.

CARY, L. A., HAN, D. C., POLTE, T. R., HANKS, S. K. & GUAN, J. L. 1998. Identification of p130Cas as a mediator of focal adhesion kinase-promoted cell migration. *J Cell Biol,* 140**,** 211-21.

CASAMASSIMA, A. & ROZENGURT, E. 1997. Tyrosine phosphorylation of p130(cas) by bombesin, lysophosphatidic acid, phorbol esters, and platelet-derived growth

factor. Signaling pathways and formation of a p130(cas)-Crk complex. *J Biol Chem,* 272**,** 9363-70.

CASAMASSIMA, A. & ROZENGURT, E. 1998. Insulin-like growth factor I stimulates tyrosine phosphorylation of p130(Cas), focal adhesion kinase, and paxillin. Role of phosphatidylinositol 3'-kinase and formation of a p130(Cas).Crk complex. *J Biol Chem,* 273**,** 26149-56.

CHAN, Y. R. & GALLO, R. L. 1998. PR-39, a syndecan-inducing antimicrobial peptide, binds and affects p130(Cas). *J Biol Chem,* 273**,** 28978-85.

CHAO, W. T. & KUNZ, J. 2009. Focal adhesion disassembly requires clathrin-dependent endocytosis of integrins. *FEBS Lett,* 583**,** 1337-43.

CHEN, H. C., APPEDDU, P. A., PARSONS, J. T., HILDEBRAND, J. D., SCHALLER, M. D. & GUAN, J. L. 1995. Interaction of focal adhesion kinase with cytoskeletal protein talin. *J Biol Chem,* 270**,** 16995-9.

CHO, S. Y. & KLEMKE, R. L. 2002. Purification of pseudopodia from polarized cells reveals redistribution and activation of Rac through assembly of a CAS/Crk scaffold. *J Cell Biol,* 156**,** 725-36.

CHODNIEWICZ, D. & KLEMKE, R. L. 2004. Regulation of integrin-mediated cellular responses through assembly of a CAS/Crk scaffold. *Biochim Biophys Acta,* 1692**,** 63-76.

CHOI, C. K., VICENTE-MANZANARES, M., ZARENO, J., WHITMORE, L. A., MOGILNER, A. & HORWITZ, A. R. 2008. Actin and alpha-actinin orchestrate the assembly and maturation of nascent adhesions in a myosin II motor-independent manner. *Nat Cell Biol,* 10**,** 1039-50.

COWELL, L. N., GRAHAM, J. D., BOUTON, A. H., CLARKE, C. L. & O'NEILL, G. M. 2006. Tamoxifen treatment promotes phosphorylation of the adhesion molecules, p130Cas/BCAR1, FAK and Src, via an adhesion-dependent pathway. *Oncogene,* 25**,** 7597-607.

CRAMER, L. P., SIEBERT, M. & MITCHISON, T. J. 1997. Identification of novel graded polarity actin filament bundles in locomoting heart fibroblasts: implications for the generation of motile force. *J Cell Biol,* 136**,** 1287-305.

CROWLEY, E. & HORWITZ, A. F. 1995. Tyrosine phosphorylation and cytoskeletal tension regulate the release of fibroblast adhesions. *J Cell Biol,* 131**,** 525-37.

CUNNINGHAM-EDMONDSON, A. C. & HANKS, S. K. 2009. p130Cas substrate domain signaling promotes migration, invasion, and survival or estrogen receptro-negative breast cancer cells. *Breast Cancer: Targets and Therapy,* 1**,** 39-52.

DEFILIPPI, P., DI STEFANO, P. & CABODI, S. 2006. p130Cas: a versatile scaffold in signaling networks. *Trends Cell Biol,* 16**,** 257-63.

DEMALI, K. A., BARLOW, C. A. & BURRIDGE, K. 2002. Recruitment of the Arp2/3 complex to vinculin: coupling membrane protrusion to matrix adhesion. *J Cell Biol,* 159**,** 881-91.

DONALDSON, J. C., DEMPSEY, P. J., REDDY, S., BOUTON, A. H., COFFEY, R. J. & HANKS, S. K. 2000. Crk-associated substrate p130(Cas) interacts with nephrocystin and both proteins localize to cell-cell contacts of polarized epithelial cells. *Exp Cell Res,* 256**,** 168-78.

DONATO, D. M., RYZHOVA, L. M., MEENDERINK, L. M., KAVERINA, I. & HANKS, S. K. 2010. Dynamics and mechanism of p130Cas localization to focal adhesions. *J Biol Chem,* 285**,** 20769-79.

DORSSERS, L. C., VAN AGTHOVEN, T., BRINKMAN, A., VELDSCHOLTE, J., SMID, M. & DECHERING, K. J. 2005. Breast cancer oestrogen independence mediated by BCAR1 or BCAR3 genes is transmitted through mechanisms distinct from the oestrogen receptor signalling pathway or the epidermal growth factor receptor signalling pathway. *Breast Cancer Res,* 7**,** R82-92.

DORSSERS, L. C., VAN DER FLIER, S., BRINKMAN, A., VAN AGTHOVEN, T., VELDSCHOLTE, J., BERNS, E. M., KLIJN, J. G., BEEX, L. V. & FOEKENS, J. A. 2001. Tamoxifen resistance in breast cancer: elucidating mechanisms. *Drugs,* 61**,** 1721-33.

DOURDIN, N., BHATT, A. K., DUTT, P., GREER, P. A., ARTHUR, J. S., ELCE, J. S. & HUTTENLOCHER, A. 2001. Reduced cell migration and disruption of the actin cytoskeleton in calpain-deficient embryonic fibroblasts. *J Biol Chem,* 276**,** 48382-8.

DUBASH, A. D., MENOLD, M. M., SAMSON, T., BOULTER, E., GARCIA-MATA, R., DOUGHMAN, R. & BURRIDGE, K. 2009. Chapter 1. Focal adhesions: new angles on an old structure. *Int Rev Cell Mol Biol,* 277**,** 1-65.

EFIMOV, A., KHARITONOV, A., EFIMOVA, N., LONCAREK, J., MILLER, P. M., ANDREYEVA, N., GLEESON, P., GALJART, N., MAIA, A. R., MCLEOD, I. X., YATES, J. R., 3RD, MAIATO, H., KHODJAKOV, A., AKHMANOVA, A. & KAVERINA, I. 2007. Asymmetric CLASP-dependent nucleation of noncentrosomal microtubules at the trans-Golgi network. *Dev Cell,* 12**,** 917-30.

EFIMOV, A., SCHIEFERMEIER, N., GRIGORIEV, I., OHI, R., BROWN, M. C., TURNER, C. E., SMALL, J. V. & KAVERINA, I. 2008. Paxillin-dependent stimulation of microtubule catastrophes at focal adhesion sites. *J Cell Sci,* 121**,** 196-204.

ETIENNE-MANNEVILLE, S. 2004. Actin and microtubules in cell motility: which one is in control? *Traffic,* 5**,** 470-7.

EUTENEUER, U. & SCHLIWA, M. 1984. Persistent, directional motility of cells and cytoplasmic fragments in the absence of microtubules. *Nature,* 310**,** 58-61.

EZRATTY, E. J., BERTAUX, C., MARCANTONIO, E. E. & GUNDERSEN, G. G. 2009. Clathrin mediates integrin endocytosis for focal adhesion disassembly in migrating cells. *J Cell Biol,* 187**,** 733-47.

EZRATTY, E. J., PARTRIDGE, M. A. & GUNDERSEN, G. G. 2005. Microtubule-induced focal adhesion disassembly is mediated by dynamin and focal adhesion kinase. *Nat Cell Biol,* 7**,** 581-90.

FAIX, J., BREITSPRECHER, D., STRADAL, T. E. & ROTTNER, K. 2009. Filopodia: Complex models for simple rods. *Int J Biochem Cell Biol,* 41**,** 1656-64.

FELLER, S. M. 2001. Crk family adaptors-signalling complex formation and biological roles. *Oncogene,* 20**,** 6348-71.

FONSECA, P. M., SHIN, N. Y., BRABEK, J., RYZHOVA, L., WU, J. & HANKS, S. K. 2004. Regulation and localization of CAS substrate domain tyrosine phosphorylation. *Cell Signal,* 16**,** 621-9.

FRALEY, S. I., FENG, Y., KRISHNAMURTHY, R., KIM, D. H., CELEDON, A., LONGMORE, G. D. & WIRTZ, D. 2010. A distinctive role for focal adhesion proteins in three-dimensional cell motility. *Nat Cell Biol,* 12**,** 598-604.

FRANCO, S. J., RODGERS, M. A., PERRIN, B. J., HAN, J., BENNIN, D. A., CRITCHLEY, D. R. & HUTTENLOCHER, A. 2004. Calpain-mediated proteolysis of talin regulates adhesion dynamics. *Nat Cell Biol,* 6**,** 977-83.

GALBRAITH, C. G., YAMADA, K. M. & SHEETZ, M. P. 2002. The relationship between force and focal complex development. *J Cell Biol,* 159**,** 695-705.

GARCIA-GUZMAN, M., DOLFI, F., RUSSELLO, M. & VUORI, K. 1999. Cell adhesion regulates the interaction between the docking protein p130(Cas) and the 14-3-3 proteins. *J Biol Chem,* 274**,** 5762-8.

GARTON, A. J., BURNHAM, M. R., BOUTON, A. H. & TONKS, N. K. 1997. Association of PTP-PEST with the SH3 domain of p130cas; a novel mechanism of protein tyrosine phosphatase substrate recognition. *Oncogene,* 15**,** 877-85.

GARTON, A. J., FLINT, A. J. & TONKS, N. K. 1996. Identification of p130(cas) as a substrate for the cytosolic protein tyrosine phosphatase PTP-PEST. *Mol Cell Biol,* 16**,** 6408-18.

GEIGER, B., SPATZ, J. P. & BERSHADSKY, A. D. 2009. Environmental sensing through focal adhesions. *Nat Rev Mol Cell Biol,* 10**,** 21-33.

GINGRAS, A. R., VOGEL, K. P., STEINHOFF, H. J., ZIEGLER, W. H., PATEL, B., EMSLEY, J., CRITCHLEY, D. R., ROBERTS, G. C. & BARSUKOV, I. L. 2006. Structural and dynamic characterization of a vinculin binding site in the talin rod. *Biochemistry,* 45**,** 1805-17.

GOTOH, T., CAI, D., TIAN, X., FEIG, L. A. & LERNER, A. 2000. p130Cas regulates the activity of AND-34, a novel Ral, Rap1, and R-Ras guanine nucleotide exchange factor. *J Biol Chem,* 275**,** 30118-23.

GOTOH, T., HATTORI, S., NAKAMURA, S., KITAYAMA, H., NODA, M., TAKAI, Y., KAIBUCHI, K., MATSUI, H., HATASE, O., TAKAHASHI, H. & ET AL. 1995. Identification of Rap1 as a target for the Crk SH3 domain-binding guanine nucleotide-releasing factor C3G. *Mol Cell Biol,* 15**,** 6746-53.

GOTOH, T., NIINO, Y., TOKUDA, M., HATASE, O., NAKAMURA, S., MATSUDA, M. & HATTORI, S. 1997. Activation of R-Ras by Ras-guanine nucleotide-releasing factor. *J Biol Chem,* 272**,** 18602-7.

GUPTON, S. L. & GERTLER, F. B. 2007. Filopodia: the fingers that do the walking. *Sci STKE,* 2007**,** re5.

HALL, A. 2009. The cytoskeleton and cancer. *Cancer Metastasis Rev,* 28**,** 5-14.

HAMID, N., GUSTAVSSON, A., ANDERSSON, K., MCGEE, K., PERSSON, C., RUDD, C. E. & FALLMAN, M. 1999. YopH dephosphorylates Cas and Fyn-binding protein in macrophages. *Microb Pathog,* 27**,** 231-42.

HANKS, S. K., RYZHOVA, L., SHIN, N. Y. & BRABEK, J. 2003. Focal adhesion kinase signaling activities and their implications in the control of cell survival and motility. *Front Biosci,* 8**,** d982-96.

HARTE, M. T., HILDEBRAND, J. D., BURNHAM, M. R., BOUTON, A. H. & PARSONS, J. T. 1996. p130Cas, a substrate associated with v-Src and v-Crk, localizes to focal adhesions and binds to focal adhesion kinase. *J Biol Chem,* 271**,** 13649-55.

HARTE, M. T., MACKLEM, M., WEIDOW, C. L., PARSONS, J. T. & BOUTON, A. H. 2000. Identification of two focal adhesion targeting sequences in the adapter molecule p130(Cas). *Biochim Biophys Acta,* 1499**,** 34-48.

HELFMAN, D. M., LEVY, E. T., BERTHIER, C., SHTUTMAN, M., RIVELINE, D., GROSHEVA, I., LACHISH-ZALAIT, A., ELBAUM, M. & BERSHADSKY, A. D. 1999. Caldesmon inhibits nonmuscle cell contractility and interferes with the formation of focal adhesions. *Mol Biol Cell,* 10**,** 3097-112.

HONDA, H., NAKAMOTO, T., SAKAI, R. & HIRAI, H. 1999. p130(Cas), an assembling molecule of actin filaments, promotes cell movement, cell migration, and cell spreading in fibroblasts. *Biochem Biophys Res Commun,* 262**,** 25-30.

HONDA, H., ODA, H., NAKAMOTO, T., HONDA, Z., SAKAI, R., SUZUKI, T., SAITO, T., NAKAMURA, K., NAKAO, K., ISHIKAWA, T., KATSUKI, M., YAZAKI, Y. & HIRAI, H. 1998. Cardiovascular anomaly, impaired actin bundling and resistance to Src-induced transformation in mice lacking p130Cas. *Nat Genet,* 19**,** 361-5.

HORWITZ, R. & WEBB, D. 2003. Cell migration. *Curr Biol,* 13**,** R756-9.

HOTULAINEN, P. & LAPPALAINEN, P. 2006. Stress fibers are generated by two distinct actin assembly mechanisms in motile cells. *J Cell Biol,* 173**,** 383-94.

HU, K., JI, L., APPLEGATE, K. T., DANUSER, G. & WATERMAN-STORER, C. M. 2007. Differential transmission of actin motion within focal adhesions. *Science,* 315**,** 111-5.

HUANG, J., HAMASAKI, H., NAKAMOTO, T., HONDA, H., HIRAI, H., SAITO, M., TAKATO, T. & SAKAI, R. 2002. Differential regulation of cell migration, actin stress fiber organization, and cell transformation by functional domains of Crk-associated substrate. *J Biol Chem,* 277**,** 27265-72.

HUANG, J., SAKAI, R. & FURUICHI, T. 2006. The docking protein Cas links tyrosine phosphorylation signaling to elongation of cerebellar granule cell axons. *Mol Biol Cell,* 17**,** 3187-96.

HUANG, Z., YAZDANI, U., THOMPSON-PEER, K. L., KOLODKIN, A. L. & TERMAN, J. R. 2007. Crk-associated substrate (Cas) signaling protein functions with integrins to specify axon guidance during development. *Development,* 134**,** 2337-47.

HUMPHRIES, J. D., WANG, P., STREULI, C., GEIGER, B., HUMPHRIES, M. J. & BALLESTREM, C. 2007. Vinculin controls focal adhesion formation by direct interactions with talin and actin. *J Cell Biol,* 179**,** 1043-57.

HUTTENLOCHER, A., PALECEK, S. P., LU, Q., ZHANG, W., MELLGREN, R. L., LAUFFENBURGER, D. A., GINSBERG, M. H. & HORWITZ, A. F. 1997. Regulation of cell migration by the calcium-dependent protease calpain. *J Biol Chem,* 272**,** 32719-22.

HUVENEERS, S. & DANEN, E. H. 2009. Adhesion signaling - crosstalk between integrins, Src and Rho. *J Cell Sci,* 122**,** 1059-69.

ILIC, D., FURUTA, Y., KANAZAWA, S., TAKEDA, N., SOBUE, K., NAKATSUJI, N., NOMURA, S., FUJIMOTO, J., OKADA, M. & YAMAMOTO, T. 1995.

Reduced cell motility and enhanced focal adhesion contact formation in cells from FAK-deficient mice. *Nature,* 377**,** 539-44.

IRETON, R. C., DAVIS, M. A., VAN HENGEL, J., MARINER, D. J., BARNES, K., THORESON, M. A., ANASTASIADIS, P. Z., MATRISIAN, L., BUNDY, L. M., SEALY, L., GILBERT, B., VAN ROY, F. & REYNOLDS, A. B. 2002. A novel role for p120 catenin in E-cadherin function. *J Cell Biol,* 159**,** 465-76.

JIANG, G., GIANNONE, G., CRITCHLEY, D. R., FUKUMOTO, E. & SHEETZ, M. P. 2003. Two-piconewton slip bond between fibronectin and the cytoskeleton depends on talin. *Nature,* 424**,** 334-7.

KATOH, K., KANO, Y., AMANO, M., ONISHI, H., KAIBUCHI, K. & FUJIWARA, K. 2001. Rho-kinase--mediated contraction of isolated stress fibers. *J Cell Biol,* 153**,** 569-84.

KAVERINA, I., KRYLYSHKINA, O., BENINGO, K., ANDERSON, K., WANG, Y. L. & SMALL, J. V. 2002. Tensile stress stimulates microtubule outgrowth in living cells. *J Cell Sci,* 115**,** 2283-91.

KAVERINA, I., KRYLYSHKINA, O., GIMONA, M., BENINGO, K., WANG, Y. L. & SMALL, J. V. 2000. Enforced polarisation and locomotion of fibroblasts lacking microtubules. *Curr Biol,* 10**,** 739-42.

KAVERINA, I., KRYLYSHKINA, O. & SMALL, J. V. 1999. Microtubule targeting of substrate contacts promotes their relaxation and dissociation. *J Cell Biol,* 146**,** 1033-44.

KIRSCH, K. H., GEORGESCU, M. M. & HANAFUSA, H. 1998. Direct binding of p130(Cas) to the guanine nucleotide exchange factor C3G. *J Biol Chem,* 273**,** 25673-9.

KIRSCH, K. H., GEORGESCU, M. M., ISHIMARU, S. & HANAFUSA, H. 1999. CMS: an adapter molecule involved in cytoskeletal rearrangements. *Proc Natl Acad Sci U S A,* 96**,** 6211-6.

KLEMKE, R. L., LENG, J., MOLANDER, R., BROOKS, P. C., VUORI, K. & CHERESH, D. A. 1998. CAS/Crk coupling serves as a "molecular switch" for induction of cell migration. *J Cell Biol,* 140**,** 961-72.

KLINGHOFFER, R. A., SACHSENMAIER, C., COOPER, J. A. & SORIANO, P. 1999. Src family kinases are required for integrin but not PDGFR signal transduction. *EMBO J,* 18**,** 2459-71.

KOVACIC-MILIVOJEVIC, B., DAMSKY, C. C., GARDNER, D. G. & ILIC, D. 2002. Requirements for the localization of p130 Cas to Z-lines in cardiac myocytes. *Cell Mol Biol Lett,* 7**,** 323-9.

KOVACIC-MILIVOJEVIC, B., ROEDIGER, F., ALMEIDA, E. A., DAMSKY, C. H., GARDNER, D. G. & ILIC, D. 2001. Focal adhesion kinase and p130Cas mediate both sarcomeric organization and activation of genes associated with cardiac myocyte hypertrophy. *Mol Biol Cell,* 12**,** 2290-307.

KRUCHTEN, A. E., KRUEGER, E. W., WANG, Y. & MCNIVEN, M. A. 2008. Distinct phospho-forms of cortactin differentially regulate actin polymerization and focal adhesions. *Am J Physiol Cell Physiol,* 295**,** C1113-22.

KUMAR, S., MAXWELL, I. Z., HEISTERKAMP, A., POLTE, T. R., LELE, T. P., SALANGA, M., MAZUR, E. & INGBER, D. E. 2006. Viscoelastic retraction of single living stress fibers and its impact on cell shape, cytoskeletal organization, and extracellular matrix mechanics. *Biophys J,* 90**,** 3762-73.

LAFLAMME, S. E., NIEVES, B., COLELLO, D. & REVERTE, C. G. 2008. Integrins as regulators of the mitotic machinery. *Curr Opin Cell Biol,* 20**,** 576-82.

LAI, F. P., SZCZODRAK, M., BLOCK, J., FAIX, J., BREITSPRECHER, D., MANNHERZ, H. G., STRADAL, T. E., DUNN, G. A., SMALL, J. V. & ROTTNER, K. 2008. Arp2/3 complex interactions and actin network turnover in lamellipodia. *EMBO J,* 27**,** 982-92.

LAUFFENBURGER, D. A. & HORWITZ, A. F. 1996. Cell migration: a physically integrated molecular process. *Cell,* 84**,** 359-69.

LAUKAITIS, C. M., WEBB, D. J., DONAIS, K. & HORWITZ, A. F. 2001. Differential dynamics of alpha 5 integrin, paxillin, and alpha-actinin during formation and disassembly of adhesions in migrating cells. *J Cell Biol,* 153**,** 1427-40.

LE CLAINCHE, C. & CARLIER, M. F. 2008. Regulation of actin assembly associated with protrusion and adhesion in cell migration. *Physiol Rev,* 88**,** 489-513.

LEE, T. N., GOLD, G., WORKMAN, R., COOK, C. A. & KONRAD, R. J. 2004. Glucose stimulates the association of Crk with p130Cas in pancreatic beta cells. *Pancreas,* 29**,** e100-5.

LEGATE, K. R., WICKSTROM, S. A. & FASSLER, R. 2009. Genetic and cell biological analysis of integrin outside-in signaling. *Genes Dev,* 23**,** 397-418.

LI, E., STUPACK, D. G., BROWN, S. L., KLEMKE, R., SCHLAEPFER, D. D. & NEMEROW, G. R. 2000. Association of p130CAS with phosphatidylinositol-3-OH kinase mediates adenovirus cell entry. *J Biol Chem,* 275**,** 14729-35.

LIU, F., HILL, D. E. & CHERNOFF, J. 1996. Direct binding of the proline-rich region of protein tyrosine phosphatase 1B to the Src homology 3 domain of p130(Cas). *J Biol Chem,* 271**,** 31290-5.

LOCK, J. G., WEHRLE-HALLER, B. & STROMBLAD, S. 2008. Cell-matrix adhesion complexes: master control machinery of cell migration. *Semin Cancer Biol,* 18**,** 65-76.

LU, Y., BRUSH, J. & STEWART, T. A. 1999. NSP1 defines a novel family of adaptor proteins linking integrin and tyrosine kinase receptors to the c-Jun N-terminal kinase/stress-activated protein kinase signaling pathway. *J Biol Chem,* 274**,** 10047-52.

LUO, W., SLEBOS, R. J., HILL, S., LI, M., BRABEK, J., AMANCHY, R., CHAERKADY, R., PANDEY, A., HAM, A. J. & HANKS, S. K. 2008. Global impact of oncogenic Src on a phosphotyrosine proteome. *J Proteome Res,* 7**,** 3447-60.

MA, L., ROHATGI, R. & KIRSCHNER, M. W. 1998. The Arp2/3 complex mediates actin polymerization induced by the small GTP-binding protein Cdc42. *Proc Natl Acad Sci U S A,* 95**,** 15362-7.

MAKKINJE, A., NEAR, R. I., INFUSINI, G., VANDEN BORRE, P., BLOOM, A., CAI, D., COSTELLO, C. E. & LERNER, A. 2009. AND-34/BCAR3 regulates adhesion-dependent p130Cas serine phosphorylation and breast cancer cell growth pattern. *Cell Signal,* 21**,** 1423-35.

MATSUDA, M., MAYER, B. J., FUKUI, Y. & HANAFUSA, H. 1990. Binding of transforming protein, P47gag-crk, to a broad range of phosphotyrosine-containing proteins. *Science,* 248**,** 1537-9.

MAYER, B. J., HAMAGUCHI, M. & HANAFUSA, H. 1988. Characterization of p47gag-crk, a novel oncogene product with sequence similarity to a putative modulatory domain of protein-tyrosine kinases and phospholipase C. *Cold Spring Harb Symp Quant Biol,* 53 Pt 2**,** 907-14.

MELLOR, H. 2010. The role of formins in filopodia formation. *Biochim Biophys Acta,* 1803**,** 191-200.

MILLER, P. M., FOLKMANN, A. W., MAIA, A. R., EFIMOVA, N., EFIMOV, A. & KAVERINA, I. 2009. Golgi-derived CLASP-dependent microtubules control Golgi organization and polarized trafficking in motile cells. *Nat Cell Biol,* 11**,** 1069-80.

MIRANTI, C. K. & BRUGGE, J. S. 2002. Sensing the environment: a historical perspective on integrin signal transduction. *Nat Cell Biol,* 4**,** E83-90.

MITRA, S. K. & SCHLAEPFER, D. D. 2006. Integrin-regulated FAK-Src signaling in normal and cancer cells. *Curr Opin Cell Biol,* 18**,** 516-23.

NAKAMOTO, T., SAKAI, R., HONDA, H., OGAWA, S., UENO, H., SUZUKI, T., AIZAWA, S., YAZAKI, Y. & HIRAI, H. 1997. Requirements for localization of p130cas to focal adhesions. *Mol Cell Biol,* 17**,** 3884-97.

NAKAMOTO, T., SAKAI, R., OZAWA, K., YAZAKI, Y. & HIRAI, H. 1995. Direct binding of C-terminal region of p130Cas to SH2 and SH3 domains of Src kinase. *J Biol Chem,* 271**,** 8959-65.

NOBES, C. D. & HALL, A. 1995. Rho, rac, and cdc42 GTPases regulate the assembly of multimolecular focal complexes associated with actin stress fibers, lamellipodia, and filopodia. *Cell,* 81**,** 53-62.

NOBES, C. D. & HALL, A. 1999. Rho GTPases control polarity, protrusion, and adhesion during cell movement. *J Cell Biol,* 144**,** 1235-44.

NOJIMA, Y., TACHIBANA, K., SATO, T., SCHLOSSMAN, S. F. & MORIMOTO, C. 1995. Focal adhesion kinase (pp125FAK) is tyrosine phosphorylated after engagement of alpha 4 beta 1 and alpha 5 beta 1 integrins on human T-lymphoblastic cells. *Cell Immunol,* 161**,** 8-13.

O'NEILL, G. M., FASHENA, S. J. & GOLEMIS, E. A. 2000. Integrin signalling: a new Cas(t) of characters enters the stage. *Trends Cell Biol,* 10**,** 111-9.

PALECEK, S. P., HUTTENLOCHER, A., HORWITZ, A. F. & LAUFFENBURGER, D. A. 1998. Physical and biochemical regulation of integrin release during rear detachment of migrating cells. *J Cell Sci,* 111 (Pt 7)**,** 929-40.

PANKOV, R., CUKIERMAN, E., KATZ, B. Z., MATSUMOTO, K., LIN, D. C., LIN, S., HAHN, C. & YAMADA, K. M. 2000. Integrin dynamics and matrix assembly: tensin-dependent translocation of alpha(5)beta(1) integrins promotes early fibronectin fibrillogenesis. *J Cell Biol,* 148**,** 1075-90.

PAPAGRIGORIOU, E., GINGRAS, A. R., BARSUKOV, I. L., BATE, N., FILLINGHAM, I. J., PATEL, B., FRANK, R., ZIEGLER, W. H., ROBERTS, G. C., CRITCHLEY, D. R. & EMSLEY, J. 2004. Activation of a vinculin-binding site in the talin rod involves rearrangement of a five-helix bundle. *EMBO J,* 23**,** 2942-51.

PEACOCK, J. G., MILLER, A. L., BRADLEY, W. D., RODRIGUEZ, O. C., WEBB, D. J. & KOLESKE, A. J. 2007. The Abl-related gene tyrosine kinase acts through p190RhoGAP to inhibit actomyosin contractility and regulate focal adhesion dynamics upon adhesion to fibronectin. *Mol Biol Cell,* 18**,** 3860-72.

PELLEGRIN, S. & MELLOR, H. 2007. Actin stress fibres. *J Cell Sci,* 120**,** 3491-9.

PELLICENA, P. & MILLER, W. T. 2001. Processive phosphorylation of p130Cas by Src depends on SH3-polyproline interactions. *J Biol Chem,* 276**,** 28190-6.

PERRIN, B. J. & HUTTENLOCHER, A. 2002. Calpain. *Int J Biochem Cell Biol,* 34**,** 722-5.

PERSSON, C., CARBALLEIRA, N., WOLF-WATZ, H. & FALLMAN, M. 1997. The PTPase YopH inhibits uptake of Yersinia, tyrosine phosphorylation of p130Cas and FAK, and the associated accumulation of these proteins in peripheral focal adhesions. *EMBO J,* 16**,** 2307-18.

PETCH, L. A., BOCKHOLT, S. M., BOUTON, A., PARSONS, J. T. & BURRIDGE, K. 1995. Adhesion-induced tyrosine phosphorylation of the p130 src substrate. *J Cell Sci,* 108 (Pt 4)**,** 1371-9.

PETERSON, L. J., RAJFUR, Z., MADDOX, A. S., FREEL, C. D., CHEN, Y., EDLUND, M., OTEY, C. & BURRIDGE, K. 2004. Simultaneous stretching and contraction of stress fibers in vivo. *Mol Biol Cell,* 15**,** 3497-508.

PETRUZZELLI, L., TAKAMI, M. & HERRERA, R. 1996. Adhesion through the interaction of lymphocyte function-associated antigen-1 with intracellular adhesion molecule-1 induces tyrosine phosphorylation of p130cas and its association with c-CrkII. *J Biol Chem,* 271**,** 7796-801.

POLLARD, T. D. & BORISY, G. G. 2003. Cellular motility driven by assembly and disassembly of actin filaments. *Cell,* 112**,** 453-65.

POLTE, T. R. & HANKS, S. K. 1995. Interaction between focal adhesion kinase and Crk-associated tyrosine kinase substrate p130Cas. *Proc Natl Acad Sci U S A,* 92**,** 10678-82.

POLTE, T. R. & HANKS, S. K. 1997. Complexes of focal adhesion kinase (FAK) and Crk-associated substrate (p130(Cas)) are elevated in cytoskeleton-associated fractions following adhesion and Src transformation. Requirements for Src kinase activity and FAK proline-rich motifs. *J Biol Chem,* 272**,** 5501-9.

PONTI, A., MACHACEK, M., GUPTON, S. L., WATERMAN-STORER, C. M. & DANUSER, G. 2004. Two distinct actin networks drive the protrusion of migrating cells. *Science,* 305**,** 1782-6.

POZZI, A. & ZENT, R. 2003. Integrins: sensors of extracellular matrix and modulators of cell function. *Nephron Exp Nephrol,* 94**,** e77-84.

PRASAD, N., TOPPING, R. S. & DECKER, S. J. 2001. SH2-containing inositol 5'-phosphatase SHIP2 associates with the p130(Cas) adapter protein and regulates cellular adhesion and spreading. *Mol Cell Biol,* 21**,** 1416-28.

PRATT, S. J., EPPLE, H., WARD, M., FENG, Y., BRAGA, V. M. & LONGMORE, G. D. 2005. The LIM protein Ajuba influences p130Cas localization and Rac1 activity during cell migration. *J Cell Biol,* 168**,** 813-24.

PUKLIN-FAUCHER, E., GAO, M., SCHULTEN, K. & VOGEL, V. 2006. How the headpiece hinge angle is opened: New insights into the dynamics of integrin activation. *J Cell Biol,* 175**,** 349-60.

REDDIG, P. J. & JULIANO, R. L. 2005. Clinging to life: cell to matrix adhesion and cell survival. *Cancer Metastasis Rev,* 24**,** 425-39.

REYNOLDS, A. B., KANNER, S. B., WANG, H. C. & PARSONS, J. T. 1989. Stable association of activated pp60src with two tyrosine-phosphorylated cellular proteins. *Mol Cell Biol,* 9**,** 3951-8.

RID, R., SCHIEFERMEIER, N., GRIGORIEV, I., SMALL, J. V. & KAVERINA, I. 2005. The last but not the least: the origin and significance of trailing adhesions in fibroblastic cells. *Cell Motil Cytoskeleton,* 61**,** 161-71.

RIDLEY, A. J., SCHWARTZ, M. A., BURRIDGE, K., FIRTEL, R. A., GINSBERG, M. H., BORISY, G., PARSONS, J. T. & HORWITZ, A. R. 2003. Cell migration: integrating signals from front to back. *Science,* 302**,** 1704-9.

RIGGINS, R. B., QUILLIAM, L. A. & BOUTON, A. H. 2003. Synergistic promotion of c-Src activation and cell migration by Cas and AND-34/BCAR3. *J Biol Chem,* 278**,** 28264-73.

RIGGINS, R. B., THOMAS, K. S., TA, H. Q., WEN, J., DAVIS, R. J., SCHUH, N. R., DONELAN, S. S., OWEN, K. A., GIBSON, M. A., SHUPNIK, M. A., SILVA, C. M., PARSONS, S. J., CLARKE, R. & BOUTON, A. H. 2006. Physical and functional interactions between Cas and c-Src induce tamoxifen resistance of breast cancer cells through pathways involving epidermal growth factor receptor and signal transducer and activator of transcription 5b. *Cancer Res,* 66**,** 7007-15.

RIVELINE, D., ZAMIR, E., BALABAN, N. Q., SCHWARZ, U. S., ISHIZAKI, T., NARUMIYA, S., KAM, Z., GEIGER, B. & BERSHADSKY, A. D. 2001. Focal contacts as mechanosensors: externally applied local mechanical force induces growth of focal contacts by an mDia1-dependent and ROCK-independent mechanism. *J Cell Biol,* 153**,** 1175-86.

RIVERA, G. M., ANTOKU, S., GELKOP, S., SHIN, N. Y., HANKS, S. K., PAWSON, T. & MAYER, B. J. 2006. Requirement of Nck adaptors for actin dynamics and cell migration stimulated by platelet-derived growth factor B. *Proc Natl Acad Sci U S A,* 103**,** 9536-41.

RODRIGUEZ, O. C., SCHAEFER, A. W., MANDATO, C. A., FORSCHER, P., BEMENT, W. M. & WATERMAN-STORER, C. M. 2003. Conserved microtubule-actin interactions in cell movement and morphogenesis. *Nat Cell Biol,* 5**,** 599-609.

ROHATGI, R., MA, L., MIKI, H., LOPEZ, M., KIRCHHAUSEN, T., TAKENAWA, T. & KIRSCHNER, M. W. 1999. The interaction between N-WASP and the Arp2/3 complex links Cdc42-dependent signals to actin assembly. *Cell,* 97**,** 221-31.

ROZENGURT, E. 1998. Signal transduction pathways in the mitogenic response to G protein-coupled neuropeptide receptor agonists. *J Cell Physiol,* 177**,** 507-17.

RUEST, P. J., SHIN, N. Y., POLTE, T. R., ZHANG, X. & HANKS, S. K. 2001. Mechanisms of CAS substrate domain tyrosine phosphorylation by FAK and Src. *Mol Cell Biol,* 21**,** 7641-52.

RUSH, J., MORITZ, A., LEE, K. A., GUO, A., GOSS, V. L., SPEK, E. J., ZHANG, H., ZHA, X. M., POLAKIEWICZ, R. D. & COMB, M. J. 2005. Immunoaffinity profiling of tyrosine phosphorylation in cancer cells. *Nat Biotechnol,* 23**,** 94-101.

SAKAI, R., IWAMATSU, A., HIRANO, N., OGAWA, S., TANAKA, T., MANO, H., YAZAKI, Y. & HIRAI, H. 1994. A novel signaling molecule, p130, forms stable complexes in vivo with v-Crk and v-Src in a tyrosine phosphorylation-dependent manner. *EMBO J,* 13**,** 3748-56.

SAKAKIBARA, A. & HATTORI, S. 2000. Chat, a Cas/HEF1-associated adaptor protein that integrates multiple signaling pathways. *J Biol Chem,* 275**,** 6404-10.

SAWADA, Y. & SHEETZ, M. P. 2002. Force transduction by Triton cytoskeletons. *J Cell Biol,* 156**,** 609-15.

SAWADA, Y., TAMADA, M., DUBIN-THALER, B. J., CHERNIAVSKAYA, O., SAKAI, R., TANAKA, S. & SHEETZ, M. P. 2006. Force sensing by mechanical extension of the Src family kinase substrate p130Cas. *Cell,* 127**,** 1015-26.

SCHALLER, M. D., HILDEBRAND, J. D. & PARSONS, J. T. 1999. Complex formation with focal adhesion kinase: A mechanism to regulate activity and subcellular localization of Src kinases. *Mol Biol Cell,* 10**,** 3489-505.

SCHALLER, M. D., HILDEBRAND, J. D., SHANNON, J. D., FOX, J. W., VINES, R. R. & PARSONS, J. T. 1994. Autophosphorylation of the focal adhesion kinase, pp125FAK, directs SH2-dependent binding of pp60src. *Mol Cell Biol,* 14**,** 1680-8.

SCHALLER, M. D., OTEY, C. A., HILDEBRAND, J. D. & PARSONS, J. T. 1995. Focal adhesion kinase and paxillin bind to peptides mimicking beta integrin cytoplasmic domains. *J Cell Biol,* 130**,** 1181-7.

SCHLAEPFER, D. D., BROOME, M. A. & HUNTER, T. 1997. Fibronectin-stimulated signaling from a focal adhesion kinase-c-Src complex: involvement of the Grb2, p130cas, and Nck adaptor proteins. *Mol Cell Biol,* 17**,** 1702-13.

SCLIWA, M. & HONER, B. 1993. Microtubules, centrosomes and intermediate filaments in directed cell movement. *Trends Cell Biol,* 3**,** 377-80.

SHIN, N. Y., DISE, R. S., SCHNEIDER-MERGENER, J., RITCHIE, M. D., KILKENNY, D. M. & HANKS, S. K. 2004. Subsets of the major tyrosine phosphorylation sites in Crk-associated substrate (CAS) are sufficient to promote cell migration. *J Biol Chem,* 279**,** 38331-7.

SHROFF, H., GALBRAITH, C. G., GALBRAITH, J. A. & BETZIG, E. 2008. Live-cell photoactivated localization microscopy of nanoscale adhesion dynamics. *Nat Methods,* 5**,** 417-23.

SHROFF, H., GALBRAITH, C. G., GALBRAITH, J. A., WHITE, H., GILLETTE, J., OLENYCH, S., DAVIDSON, M. W. & BETZIG, E. 2007. Dual-color superresolution imaging of genetically expressed probes within individual adhesion complexes. *Proc Natl Acad Sci U S A,* 104**,** 20308-13.

SIEGRIST, S. E. & DOE, C. Q. 2007. Microtubule-induced cortical cell polarity. *Genes Dev,* 21**,** 483-96.

SIESSER, P. M., MEENDERINK, L. M., RYZHOVA, L., MICHAEL, K. E., DUMBAULD, D. W., GARCIA, A. J., KAVERINA, I. & HANKS, S. K. 2008. A FAK/Src chimera with gain-of-function properties promotes formation of large peripheral adhesions associated with dynamic actin assembly. *Cell Motil Cytoskeleton,* 65**,** 25-39.

SINGH, M. K., DADKE, D., NICOLAS, E., SEREBRIISKII, I. G., APOSTOLOU, S., CANUTESCU, A., EGLESTON, B. L. & GOLEMIS, E. A. 2008. A novel Cas family member, HEPL, regulates FAK and cell spreading. *Mol Biol Cell,* 19**,** 1627-36.

SMALL, J. V., ROTTNER, K., KAVERINA, I. & ANDERSON, K. I. 1998. Assembling an actin cytoskeleton for cell attachment and movement. *Biochim Biophys Acta,* 1404**,** 271-81.

SMALL, J. V., STRADAL, T., VIGNAL, E. & ROTTNER, K. 2002. The lamellipodium: where motility begins. *Trends Cell Biol,* 12**,** 112-20.

SMITH, H. W., MARRA, P. & MARSHALL, C. J. 2008. uPAR promotes formation of the p130Cas-Crk complex to activate Rac through DOCK180. *J Cell Biol,* 182**,** 777-90.

SNIADECKI, N. J., ANGUELOUCH, A., YANG, M. T., LAMB, C. M., LIU, Z., KIRSCHNER, S. B., LIU, Y., REICH, D. H. & CHEN, C. S. 2007. Magnetic microposts as an approach to apply forces to living cells. *Proc Natl Acad Sci U S A,* 104**,** 14553-8.

SONGYANG, Z. & CANTLEY, L. C. 1995. Recognition and specificity in protein tyrosine kinase-mediated signalling. *Trends Biochem Sci,* 20**,** 470-5.

SUTTERLIN, C. & COLANZI, A. 2010. The Golgi and the centrosome: building a functional partnership. *J Cell Biol,* 188**,** 621-8.

SVITKINA, T. M., BULANOVA, E. A., CHAGA, O. Y., VIGNJEVIC, D. M., KOJIMA, S., VASILIEV, J. M. & BORISY, G. G. 2003. Mechanism of filopodia initiation by reorganization of a dendritic network. *J Cell Biol,* 160**,** 409-21.

TACHIBANA, K., SATO, T., D'AVIRRO, N. & MORIMOTO, C. 1995. Direct association of pp125FAK with paxillin, the focal adhesion-targeting mechanism of pp125FAK. *J Exp Med,* 182**,** 1089-99.

TANG, D. D. 2009. p130 Crk-associated substrate (CAS) in vascular smooth muscle. *J Cardiovasc Pharmacol Ther,* 14**,** 89-98.

TIKHMYANOVA, N., LITTLE, J. L. & GOLEMIS, E. A. 2010a. CAS proteins in normal and pathological cell growth control. *Cell Mol Life Sci,* 67**,** 1025-48.

TIKHMYANOVA, N., TULIN, A. V., ROEGIERS, F. & GOLEMIS, E. A. 2010b. Dcas supports cell polarization and cell-cell adhesion complexes in development. *PLoS One,* 5.

URBAN, E., JACOB, S., NEMETHOVA, M., RESCH, G. P. & SMALL, J. V. 2010. Electron tomography reveals unbranched networks of actin filaments in lamellipodia. *Nat Cell Biol,* 12**,** 429-35.

VAN DER FLIER, S., BRINKMAN, A., LOOK, M. P., KOK, E. M., MEIJER-VAN GELDER, M. E., KLIJN, J. G., DORSSERS, L. C. & FOEKENS, J. A. 2000. Bcar1/p130Cas protein and primary breast cancer: prognosis and response to tamoxifen treatment. *J Natl Cancer Inst,* 92**,** 120-7.

VASILIEV, J. M., GELFAND, I. M., DOMNINA, L. V., IVANOVA, O. Y., KOMM, S. G. & OLSHEVSKAJA, L. V. 1970. Effect of colcemid on the locomotory behaviour of fibroblasts. *J Embryol Exp Morphol,* 24**,** 625-40.

VERKHOVSKY, A. B., SVITKINA, T. M. & BORISY, G. G. 1995. Myosin II filament assemblies in the active lamella of fibroblasts: their morphogenesis and role in the formation of actin filament bundles. *J Cell Biol,* 131**,** 989-1002.

VERKHOVSKY, A. B., SVITKINA, T. M. & BORISY, G. G. 1999a. Network contraction model for cell translocation and retrograde flow. *Biochem Soc Symp,* 65**,** 207-22.

VERKHOVSKY, A. B., SVITKINA, T. M. & BORISY, G. G. 1999b. Self-polarization and directional motility of cytoplasm. *Curr Biol,* 9**,** 11-20.

VIBOUD, G. I. & BLISKA, J. B. 2005. Yersinia outer proteins: role in modulation of host cell signaling responses and pathogenesis. *Annu Rev Microbiol,* 59**,** 69-89.

VICENTE-MANZANARES, M., MA, X., ADELSTEIN, R. S. & HORWITZ, A. R. 2009. Non-muscle myosin II takes centre stage in cell adhesion and migration. *Nat Rev Mol Cell Biol,* 10**,** 778-90.

VUORI, K., HIRAI, H., AIZAWA, S. & RUOSLAHTI, E. 1996. Introduction of p130cas signaling complex formation upon integrin-mediated cell adhesion: a role for Src family kinases. *Mol Cell Biol,* 16**,** 2606-13.

VUORI, K. & RUOSLAHTI, E. 1995. Tyrosine phosphorylation of p130Cas and cortactin accompanies integrin-mediated cell adhesion to extracellular matrix. *J Biol Chem,* 270**,** 22259-62.

WANG, X., WENG, L. P. & YU, Q. 2000. Specific inhibition of FGF-induced MAPK activation by the receptor-like protein tyrosine phosphatase LAR. *Oncogene,* 19**,** 2346-53.

WANG, Y. L. 1985. Exchange of actin subunits at the leading edge of living fibroblasts: possible role of treadmilling. *J Cell Biol,* 101**,** 597-602.

WANG, Y. L. 2007. Flux at focal adhesions: slippage clutch, mechanical gauge, or signal depot. *Sci STKE,* 2007**,** pe10.

WATANABE, N., KATO, T., FUJITA, A., ISHIZAKI, T. & NARUMIYA, S. 1999. Cooperation between mDia1 and ROCK in Rho-induced actin reorganization. *Nat Cell Biol,* 1**,** 136-43.

WEBB, D. J., DONAIS, K., WHITMORE, L. A., THOMAS, S. M., TURNER, C. E., PARSONS, J. T. & HORWITZ, A. F. 2004. FAK-Src signalling through paxillin, ERK and MLCK regulates adhesion disassembly. *Nat Cell Biol,* 6**,** 154-61.

WEHRLE-HALLER, B. & IMHOF, B. A. 2003. Actin, microtubules and focal adhesion dynamics during cell migration. *Int J Biochem Cell Biol,* 35**,** 39-50.

WEIDOW, C. L., BLACK, D. S., BLISKA, J. B. & BOUTON, A. H. 2000. CAS/Crk signalling mediates uptake of Yersinia into human epithelial cells. *Cell Microbiol,* 2**,** 549-60.

WITTMANN, T. & WATERMAN-STORER, C. M. 2001. Cell motility: can Rho GTPases and microtubules point the way? *J Cell Sci,* 114**,** 3795-803.

WOLFENSON, H., HENIS, Y. I., GEIGER, B. & BERSHADSKY, A. D. 2009a. The heel and toe of the cell's foot: a multifaceted approach for understanding the structure and dynamics of focal adhesions. *Cell Motil Cytoskeleton,* 66**,** 1017-29.

WOLFENSON, H., LUBELSKI, A., REGEV, T., KLAFTER, J., HENIS, Y. I. & GEIGER, B. 2009b. A role for the juxtamembrane cytoplasm in the molecular dynamics of focal adhesions. *PLoS One,* 4**,** e4304.

WOZNIAK, M. A., MODZELEWSKA, K., KWONG, L. & KEELY, P. J. 2004. Focal adhesion regulation of cell behavior. *Biochim Biophys Acta,* 1692**,** 103-19.

YAMAKITA, Y., TOTSUKAWA, G., YAMASHIRO, S., FRY, D., ZHANG, X., HANKS, S. K. & MATSUMURA, F. 1999. Dissociation of FAK/p130(CAS)/c-Src complex during mitosis: role of mitosis-specific serine phosphorylation of FAK. *J Cell Biol,* 144**,** 315-24.

ZAIDEL-BAR, R. 2009. Evolution of complexity in the integrin adhesome. *J Cell Biol,* 186**,** 317-21.

ZAIDEL-BAR, R., BALLESTREM, C., KAM, Z. & GEIGER, B. 2003. Early molecular events in the assembly of matrix adhesions at the leading edge of migrating cells. *J Cell Sci,* 116**,** 4605-13.

ZAIDEL-BAR, R., ITZKOVITZ, S., MA'AYAN, A., IYENGAR, R. & GEIGER, B. 2007a. Functional atlas of the integrin adhesome. *Nat Cell Biol,* 9**,** 858-67.

ZAIDEL-BAR, R., MILO, R., KAM, Z. & GEIGER, B. 2007b. A paxillin tyrosine phosphorylation switch regulates the assembly and form of cell-matrix adhesions. *J Cell Sci,* 120**,** 137-48.

ZAMIR, E. & GEIGER, B. 2001. Molecular complexity and dynamics of cell-matrix adhesions. *J Cell Sci,* 114**,** 3583-90.

ZAMIR, E., GEIGER, B. & KAM, Z. 2008. Quantitative multicolor compositional imaging resolves molecular domains in cell-matrix adhesions. *PLoS One,* 3**,** e1901.

ZAMIR, E., KATZ, B. Z., AOTA, S., YAMADA, K. M., GEIGER, B. & KAM, Z. 1999. Molecular diversity of cell-matrix adhesions. *J Cell Sci,* 112 (Pt 11)**,** 1655-69.

ZHANG, H., BERG, J. S., LI, Z., WANG, Y., LANG, P., SOUSA, A. D., BHASKAR, A., CHENEY, R. E. & STROMBLAD, S. 2004. Myosin-X provides a motor-based link between integrins and the cytoskeleton. *Nat Cell Biol,* 6**,** 523-31.

ZHANG, X., JIANG, G., CAI, Y., MONKLEY, S. J., CRITCHLEY, D. R. & SHEETZ, M. P. 2008. Talin depletion reveals independence of initial cell spreading from integrin activation and traction. *Nat Cell Biol,* 10**,** 1062-8.